THESIS APPROVAL

GRADUATE SCHOOL, KASETSART UNIVERSITY

Master of Science (Chemistry)
DEGREE

Chemistry
FIELD

Chemistry
DEPARTMENT

TITLE: Adsorption of Water Vapor and Pollutants on Chars and Soil Minerals

NAME: Mr. Ratchapol Batmart

THIS THESIS HAS BEEN ACCEPTED BY

THESIS ADVISOR
(Associate Professor Apisit Songsasen, Ph.D.)

THESIS CO-ADVISOR
(Associate Professor Veerasak Udomchoke, D.Tech.Sc.)

DEPARTMENT HEAD
(Associate Professor Supa Hannongbua, Dr.rer.nat.)

APPROVED BY THE GRADUATE SCHOOL ON _____

DEAN
(Associate Professor Gunjana Theeragool, D.Agr.)

THESIS

ADSORPTION OF WATER VAPOR AND POLLUTANTS ON CHARS AND SOIL MINERALS

RATCHAPOL BATMART

A Thesis Submitted in Partial Fulfillment of
the Requirements for the Degree of
Master of Science (Chemistry)
Graduate School, Kasetsart University
2012

Ratchapol Batmart 2012: Adsorption of Water Vapor and Pollutants on Chars and Soil Minerals. Master of Science (Chemistry), Major Field: Chemistry, Department of Chemistry. Thesis Advisor: Associate Professor Apisit Songsasen, Ph.D. 222 pages.

The adsorption of water vapor and pollutants by soil minerals and chars from agricultural waste (AW), which studied in term of adsorption isotherm and thermodynamics of adsorption. The pore structure, surface character and functional group on surface of chars and soil minerals were characterized by SEM and FT-IR. The specific surface areas of adsorbents were calculated from the phenol and chromium (VI) adsorption. The results showed that the adsorption capacities of adsorbents depended on type of adsorbates and temperature. For adsorption of water vapor, montmorillonite had the highest adsorption capacity (0.4201 g/g). The phenol and chromium (VI) adsorption found that char from oil palm shell had the highest adsorption capacity. The specific surface areas of char from oil palm shell for phenol and chromium (VI) adsorption are 129.42 m^2/g and 1.05 m^2/g, respectively.

The adsorption isotherm of water vapor, phenol and chromium (VI) were studied. Adsorption isotherm of water vapor was fitted to Freundlich model as considered from the correlation coefficient (R^2) of plot between log q_e versus log C_e. The adsorption isotherm of phenol and chromium (VI) were fitted to both Langmuir and Freundlich isotherm. Adsorption isotherm of phenol was also well fitted with Freundlich model when increasing temperature. In addition, the thermodynamic parameters of water vapor adsorption indicated that the positive values of ΔH^o and negatives values of ΔG^o were endothermic process and spontaneous by nature. Moreover, the thermodynamic parameters indicated that the phenol adsorptions on char from oil palm shell was exothermic process and spontaneous by nature. However, chars from bamboo and coconut shell are endothermic but spontaneous by nature.

_____ _____ __ / __ / __

Student's signature Thesis Advisor's signature

ACKNOWLEDGEMENTS

I would like to express my profound appreciation to my supervisor, Associate Professor Dr. Apisit Songsasen for introducing me to an interesting research theme. I wish appreciate his valuable guidance and encouragement throughout the span of my study and research. I also wish to express my sincere gratitude to advisory committee, Associate Professor Dr. Veerasak Udomchoke, for his worthy suggestion and constructive criticism, and Mr. Suchat Suwannatus, inventing the instruments to generate water vapor from used in my research.

I would like to thank the Center of Excellent for Innovation in Chemistry: Postgraduate Education and Research Program in Chemistry (PERCH-CIC) for financial support and the Department of Chemistry, Faculty of Science, Kasetsart University for all research facilities.

Finally, I am specially appreciated my parents for continuously boosting my morale and giving me financial assistance. I would like to thank all my colleagues and my friends for devoting their valuable time to helping me during my graduate study.

Ratchapol Batmart

March, 2012

TEBLE OF CONTENTS

Page

TEBLE OF CONTENTS (Continued)

Page

LIST OF TABLES

LIST OF TABLES (Continued)

LIST OF TABLES (Continued)

LIST OF TABLES (Continued)

Appendix Table **Page**

LIST OF TABLES (Continued)

Appendix Table **Page**

LIST OF TABLES (Continued)

LIST OF TABLES (Continued)

LIST OF FIGURES

LIST OF FIGURES (Continued)

LIST OF FIGURES (Continued)

LIST OF FIGURES (Continued)

LIST OF FIGURES (Continued)

LIST OF FIGURES (Continued)

LIST OF FIGURES (Continued)

LIST OF FIGURES (Continued)

LIST OF FIGURES (Continued)

LIST OF FIGURES (Continued)

LIST OF ABBEVIATIONS

SEM	=	Scanning Electron Microscopy
FT-IR	=	Fourier Transform Infrared Spectroscopy
UV-Vis	=	UV-Vis Spectrophotometry
AW	=	Agricultural Waste
IGA	=	Intelligent Gravimetric Analyzer
XRD	=	X-ray Diffraction
AC	=	Activated Carbon
RH	=	Relative Humidity
AA	=	Atomic Adsorption Spectroscopy
ICP	=	Inductively Coupled Plasma Technique
SE	=	Specific Surface Area

ADSORPTION OF WATER VAPOR AND POLLUTANTS ON CHARS AND SOIL MINERALS

INTRODUCTION

Soil minerals and chars have known as natural materials and waste from agricultural operation, respectively. Chars such as palm shell, coconut shell and bamboo, have a high specific surface area, high pore volume, and high porosity. They have excellent adsorption capability for organic pollutants. The surface of chars such as commercial activated carbon (CAC), granular activated carbon (GAC) and powder activated carbon (PAC) were modified by various methods (Amphol *et al.,* 2009*).* Soil minerals are composed mainly of the montmorillonite clay. The montmorillonite is 2:1 clay type. Structure of montmorillonite is shown in Figure 1. The ideal montmorillonite composition is HSi_2AlO_6, particles are thin (thickness ~1 to 3 nm and width ~500 nm), flat disks shape. The crystal structure is one Al-octahedral sheet sandwiched between two Si-tetrahedral sheets. Montmorillonite is characterized by pronounced swelling when wet and shrinkage on drying.

Soil minerals and chars are used in different fields of science, environment and engineering due to its favorable properties such as good adsorbent, low materials, represent unused resources, widely available and are environment friendly. The chars used as an adsorbent in the purification, separation of liquids and gases, an adsorbent in the soils, and an adsorbent organic pollutant of industrial factory (Dubey, 2007). In the past, soil minerals have a very large specific surface area, giving them a tremendous capacity to absorb water and other substances (Fabrice *et al.,* 2009).

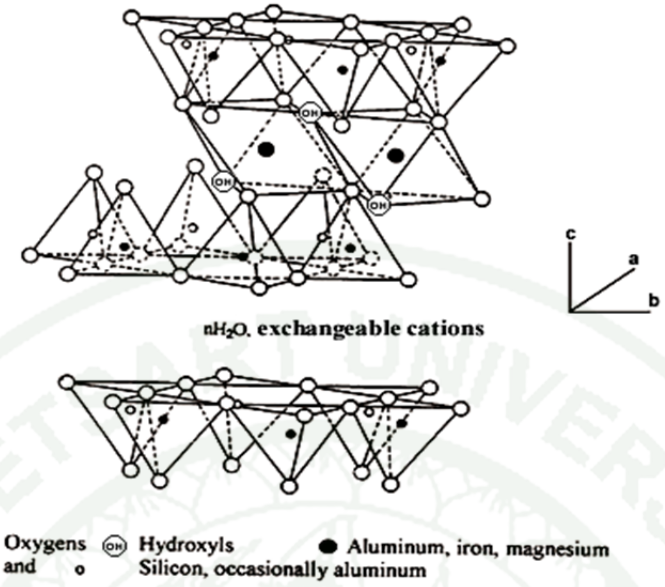

Figure 1 The clay structure of montmorillonite.

Source: Brack (1998)

Adsorption of water vapor on chars and soil minerals have attracted much attention in pay to the structure of water in a confined space, especially in carbon pores, shape and pore size distribution, and chemical potential corresponding to vapor pressure of adsorbent (Qingrong *et al.,* 2008). The adsorption of water vapor on chars and soil minerals in the atmosphere is exothermic reaction. Which exothermic reaction has importantly in the rain making process, humidity in the atmosphere are adsorb by adsorbents and occurring exothermic reaction, it is process produced rain clouds. Rain-making involves a process of precipitate water vapor in the atmosphere, condensed into minute water particles as rain clouds. Further precipitation brought about by cooling brings rainfall, Rainmaking refers to the act of attempting to artificially induce or increase precipitation, usually to stave off drought (Royal rainmaking, 1998).

1. Adsorption

Adsorption is a process that occurs when a gas or liquid solute accumulates on the surface of a solid or a liquid (adsorbent), forming a film of molecules or atoms (adsobate). It is different from absorption, in which a substance diffuses into a liquid or solid to form a solution (Bansal and Goyal, 2005).

1.1 Adsorption process

Adsorption arises as a result of the unsaturated and unbalanced molecular forces that are present on every solid surface. Thus, when a solid surface is brought into contact with a liquid or gas, there is an interaction between the field of forces of the surface and that of the liquid or gas. The solid surface tends to satisfy these residual forces by attracting and retaining on its surface the molecules, atom, or ion of the gas or liquid. This results in a greater concentration of the gas or liquid in the near vicinity of solid surface than in the bulk gas or vapor phase, despite the nature of gas or vapor. The adsorption characteristic into pores of adsorbent is shown in Figure 2.

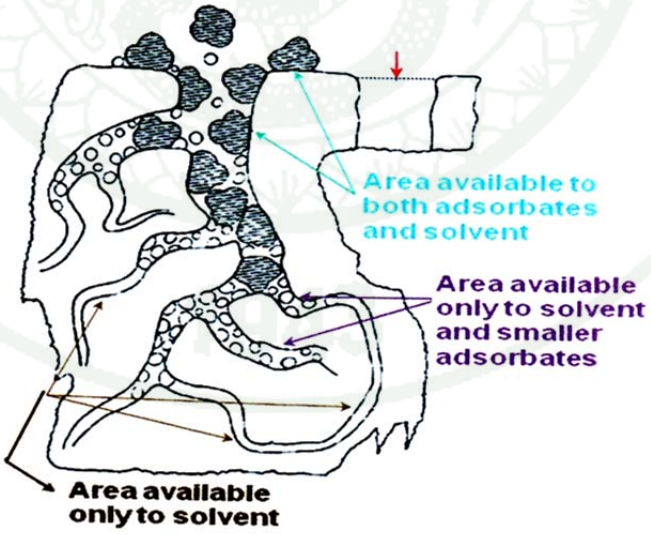

Figure 2 The adsorption characteristic into pores of adsorbent.

Source: Culp and Culp (1974)

The adsorption involves two types of forces as physisorption (characteristic of weak Van der Waals forces) or chemisorptions (characteristic of covalent bonding).

1.1 Physical adsorption: The adsorbate is bound to the surface by relatively weak Van der Waals forces, which are similar to the molecular force of cohesion and are involved in the condensation of vapors into liquids.

1.2 Chemical adsorption: Chemisorption involves exchange or sharing of electrons between the adsorbent molecules and the surface of the adsorbent resulting in a chemical reaction. The bond and is thus much stronger than in the physisorption.

Both physical and chemical adsorption may occur on the surface at the same time; a layer of molecules may be physically adsorbed on top of an underlying chemisorbed layer. For example, at liquid nitrogen temperature (77 K) nitrogen gas is adsorbed physically on iron but at 800 K, an energy level too high for physical adsorption bonds, nitrogen is adsorbed chemically to form iron nitride (Webb, 2003).

2.2 Adsorption isotherm

To measure total surface area, the physical adsorption is non-specific and required, but even with physical adsorption the isotherm varies somewhat the nature of the adsorbent. Most physical adsorption isotherm may be grouped into six types, which are frequently referred to as the Brunauer, Deming, Deming and Teller (BDDT) classification (Figure 3). In all cases the amount of vapor adsorbed gradually increases as its partial pressure is increases, becoming at some point equivalent to a monolayer, but then increasing to a multilayer. This eventually merges into a condensed phase. Types of adsorption isotherm are shown in Figure 3.

Type I is frequently called the Langmuir type. The asymptotic value was originally ascribed to a monolayer, as derived from the Langmuir equation.

However, this isotherm is seldom encountered on nonporous materials. It is fairly common with certain activated carbon, silica gels, and zeolites that contain only very fine pores, and it is now generally believed that in these cases the asymptotic value represents the complete filling of microspores at a relative pressure substantially less than unity, rather than monolayer adsorption. This type of isotherm would also be expected for reversible chemisorption.

Type II, sometimes termed the sigmoid or S-shaped isotherm, is commonly encountered on nonporous structure. Point B occurs at "knee" and is the stage at which monolayer coverage is complete.

Type III isotherm is convex over the entire range and dose not exhibit a point B. It is relatively rare and is typical of a system where the forces of adsorption are relatively weak, as when the adsorbate is not wetted by the surface, e.g., water vapor on graphite.

Type IV is encountered with porous material. At low values of P/P^o the isotherm is similar to type II, but adsorption increases markedly at higher values of P/P^o where pore (capillary) condensation takes place. A hysteresis effect associated with this pore condensation is frequently, but not always, observed. Isotherms of this type are often encountered with industrial catalysts, and the capillary condensation curve may be used to determine a pore size distribution.

Type V is similar to type III, but with pore condensation taking place at higher values of P/P^o. It is also relatively rare.

Type VI is the stepped isotherm which is rarely found. This system involves the step-by-step adsorption on surface, like uniform adsorption. The isotherm shape depends on the system and temperature for adsorption.

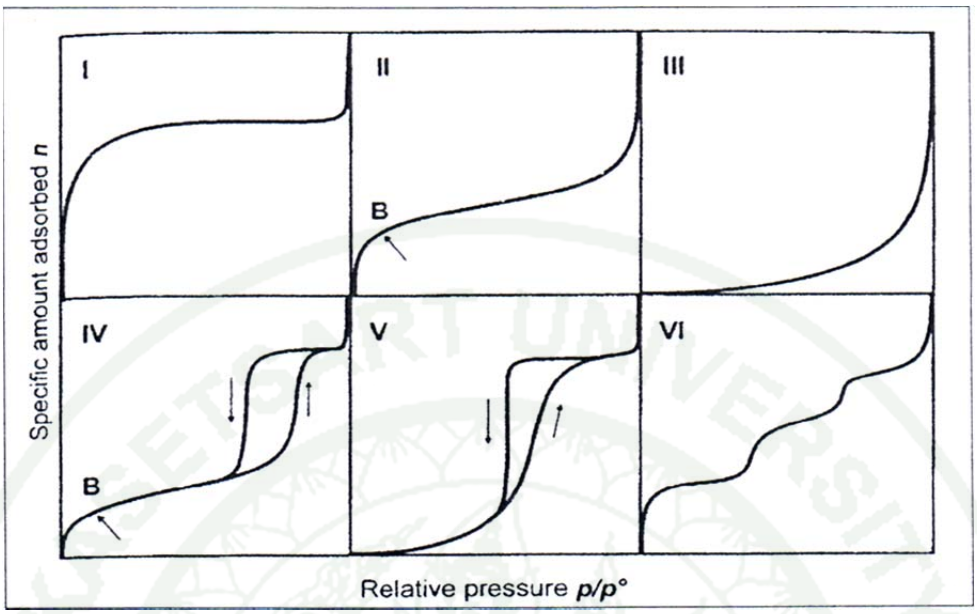

Figure 3 Types of adsorption isotherm

Source: Masel (1996)

The adsorption isotherm indicates how the adsorption molecules distribute between the liquid phase and the solid phase when the adsorption process reaches an equilibrium state. The analysis of the isotherm data by fitting them to different isotherm models is an important step to find the suitable models that can be used for design purpose.

The procedures for the kinetic experiments were basically identical to those for the equilibrium test. The solution samples were taken at regular time interval and the concentration of sample were measured. The plots of X/M versus C_e for adsorption are shown in Figure 4 and the amount of adsorption (q_t, mg/g) at time (t) was calculated by the following equation.

$$q_t = \frac{X}{m} = \frac{(C_o - C_t)V}{m} \qquad \text{.....(8)}$$

where q_t is the amount of adsorption at the time (mg/g)

X is the amount of adsorbate (mg)

m is the mass of adsorbent used (g)

C_o is the liquid-phase concentration of adsorbate at the initial (mg/L)

C_t is liquid-phase concentration of samples at the time (mg/L)

V is the volume of solution (L)

For equilibrium

$$q_e = \frac{X}{m} = \frac{(C_0 - C_e)V}{m} \quad \text{..... (9)}$$

where q_e is the amount of adsorption at equilibrium (mg/g)

C_e is the liquid-phase concentration of adsorbate at the time (mg/L)

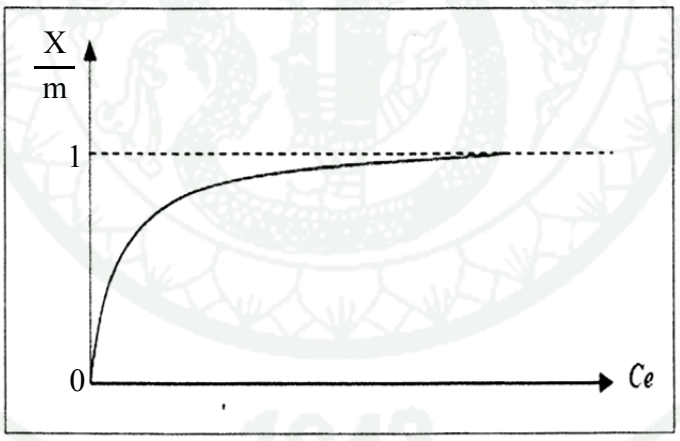

Figure 4 The plots of X/M versus C_e for adsorption.

Source: Cheremisinoff and Morresi (1987)

2.2.1 Langmuir isotherm

Langmuir isotherm assumes monolayer adsorption onto a surface containing a finite number of adsorption sites of uniform strategies of adsorption with transmigration of adsorbate in the plane of surface. The linear form of the Langmuir isotherm equation is represented by the following equation;

$$q_e = \frac{Q_o b C_e}{1+bC_e} \qquad \text{.....…….. (10)}$$

$$\frac{C_e}{q_e} = \frac{1}{Q_o b} + \frac{C_e}{Q_o} \qquad \text{.....…….. (11)}$$

where C_e is the equilibrium concentration of the adsorbate (mg/L)

q_e is the amount of adsorbate per unit mass of adsorbent (mg/g)

Q_o is the maximum surface coverage (formation of monolayer) of sorbent (mg/g)

b is the adsorption energy constant of Langmuir adsorption isotherm (L/mg)

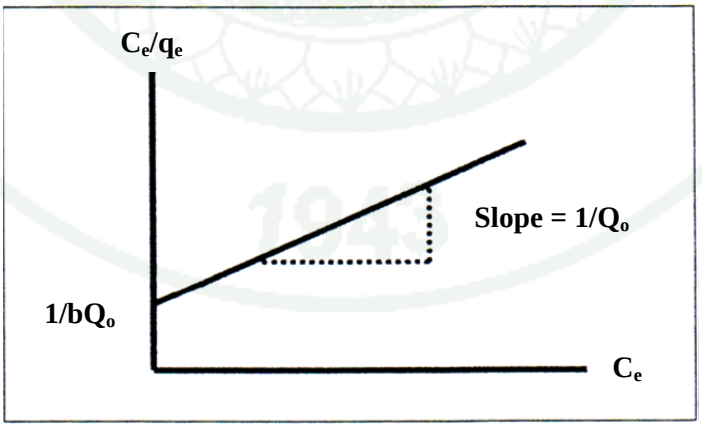

Figure 5 The Langmuir isotherm plots of C_e/q_e versus C_e for adsorption.

Source: Cheremisinoff and Morresi (1987)

Langmuir isotherm plot of C_e/q_e versus C_e for adsorption is shown in Figure 5. Furthermore, the plot of C_e/q_e versus C_e gives straight line with slope $1/Q_o$ is obtained. The Langmuir constant b and Q_o are calculated from this isotherm. When the molecule adsorbs on the surface of activated carbon based on the Langmuir isotherm, the specific surface area can be calculated as follows;

$$S = \frac{Q_o}{MW} \times N \times a \quad \text{.....…….. (12)}$$

where S is the specific surface area (m^2/g)

Q_o is the maximum surface coverage (formation of monolayer) of sorbent (mg/g)

MW is the molecular weight (g/mol)

N is the Avogadro number (6.02×10^{23} molecule/mol)

a is the cross sectional area of adsorbate ($Å^2$)

2.2.2 Freundlich isotherm

Freundlich isotherm assumes heterogeneous surface energies, in which the energy term in Langmuir equation varies as a function of the surface coverage. The well-known logarithmic form of Freundlich model is given by the following equation.

$$q_e = K_F C_e^{1/n} \quad \text{..... (13)}$$

$$\log q_e = \log K_F + \frac{1}{n} \log C_e \quad \text{..... (14)}$$

where q_e is the amount adsorbed at equilibrium (mg/g)

C_e is the equilibrium concentration of the adsorbate (mg/L)

K_F is the Freundlich isotherm constant related to adsorption capacity $((mg^{-1})(mg^{-1})^{1/n})$

n is the Freundlich isotherm constant related to adsorption intensity

The slope 1/n ranging between 0 and 1 is a measure of adsorption intensity or surface heterogeneity, becoming more heterogeneous as its value gets closer to zero. A value for 1/n below one indicates a normal Langmuir isotherm while 1/n above one is indicative of cooperative adsorption. The Freundlich isotherm plot of log q_e versus log C_e for the adsorption is shown in Figure 6. Moreover, the plot of log q_e versus log C_e gives straight line with slop 1/n is obtained.

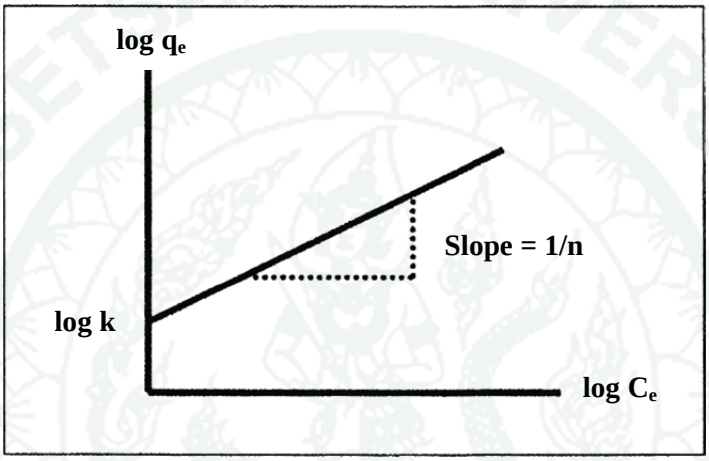

Figure 6 The Freundlich isotherm plots of log q_e versus log C_e for adsorption.

Source: Cheremisinoff and Morresi (1987)

2. Heat of adsorptions consideration

The adsorption mechanism was physical adsorption, in contrast to chemical adsorption in which the amount of adsorbate adsorbed on an adsorbent increases with increasing adsorption temperature (Uchida *et al.,* 2000). The heat of adsorption was calculated by applying the Clausius- Clapeyron equation to the adsorption isotherm as follows (Alberty and Silbey, 1992; Tanada *et al.*, 2000)

$$\frac{dP}{dT} = \frac{P\Delta H_{vap}}{RT^2} \quad \text{..... (15)}$$

Where P is the equilibrium pressure of gas, T is the absolute temperature, ΔH_{vap} is the heat of vaporization, and R is the gas constant. On rearrangement equation (15) becomes;

$$\frac{dP}{P} = \frac{\Delta H_{vap}}{RT^2} dT \quad \text{..... (16)}$$

The equation (16) can be rewritten as follows;

$$d \ln \frac{P}{P^o} = \frac{\Delta H_{vap}}{RT^2} dT \quad \text{..... (17)}$$

Where P^o is the standard pressure used. Replacement of P by C_eRT and P^o by C^oRT from ideal gas law where C_e is the molar concentration and C^o is the standard value of the molar concentration (1 mol/L), equation (17) becomes;

$$d \ln \frac{C_e}{C^o} = \frac{\Delta H_{vap}}{RT^2} dT \quad \text{..... (18)}$$

For adsorption in solution the ΔH_{vap} is replaced by ΔH_{ads} which is the heat of adsorption. Integrating on the assumption that the ΔH_{ads} is independent of temperature and concentration and since the term ln C^o is equal to zero, equation (18) yields;

$$\int d \ln C_e = \frac{\Delta H_{ads}}{R} \int T^{-2} dT$$

$$\ln C_e = -\frac{\Delta H_{ads}}{R} \frac{1}{T} + c \quad \text{..... (19)}$$

where C_e is the equilibrium concentration (mmol/L), ΔH_{ads} is the isosteric heat of adsorption (kJ/mol), R is the universal gas constant (8.314 J/mol.K) and c is the integration constant. Plot of $\ln C_e$ versus 1/T should give a straight line of slope is $-(\Delta H_{ads}/R)$. The plots of applied Clausius-Clapeyron equation to adsorption isotherm in equation (19) as $\ln C_e$ versus 1/T.

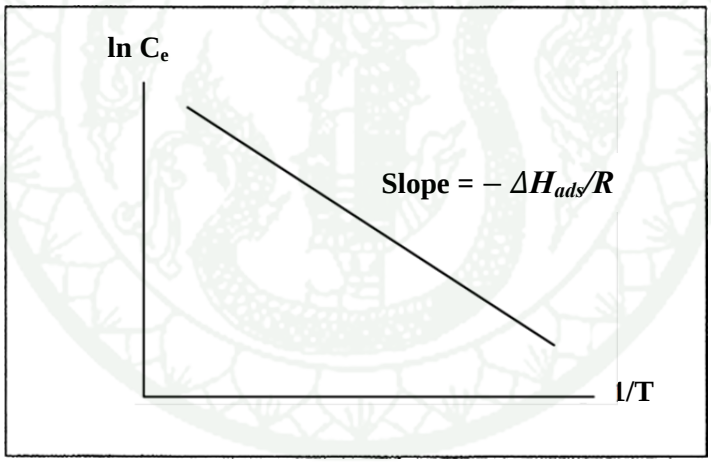

Figure 7 The Clausius-Clapeyron plots at various temperatures 1/T versus ln C_e for adsorption.

Source: Alberty and Silbey (1992)

3. Thermodynamic of adsorption

The thermodynamic relates the change in temperature (T) to the change in the equilibrium constant (K) given the standard enthalpy change (ΔH^o) for the adsorption process.

$$\frac{d \ln K}{d\mathrm{T}} = \frac{\Delta H^o}{RT^2} \quad \text{..... (20)}$$

The equation (20) can be rewritten as follows;

$$\frac{d \ln K}{d\frac{1}{\mathrm{T}}} = -\frac{\Delta H^o}{R} \quad \text{..... (21)}$$

The enthalpy change of reaction is assumed to be constant with temperature; the definite integral of this differential equation between temperatures T_1 and T_2 are combined with the natural logs, the integrated form of the van't Hoff equation as follows;

$$\ln\left(\frac{K_2}{K_1}\right) = -\frac{\Delta H^o}{R}\left(\frac{1}{T_2} - \frac{1}{T_1}\right) \quad \text{.....(22)}$$

where K_1 is the equilibrium constant at absolute temperature T_1

K_2 is the equilibrium constant at absolute temperature T_2

ΔH^o is the standard enthalpy change

and R is the gas constant

Since, thermodynamic parameters such as standard free energy change (ΔG^o), enthalpy change (ΔH^o), and entropy change (ΔS^o) for the adsorption of adsorbent were determined using the following equations:

$$\Delta G^o = \Delta H^o - T\Delta S^o \quad \text{..... (23)}$$

and $$\Delta G^o = -RT \ln K_D \quad \text{.....(24)}$$

$$\ln K_D = -\frac{\Delta H^o}{RT} + \frac{\Delta S^o}{R} \quad \text{.....(25)}$$

where K_D is the equilibrium constant
R is the gas constant (8.314 J/(mol.K))
T is absolute temperature (K)

For equation (22), a plot of the natural logarithm of the equilibrium constant ($\ln K_D$) versus the reciprocal temperature (1/T) gives a straight line. The slope of the line is equal to minus the standard enthalpy change divided by the gas constant, $-\Delta H^o/R$ and the intercept is equal to the standard entropy change divided by the gas constant, $\Delta S^o/R$. Differentiation of this expression yields the Van't Hoff equation.

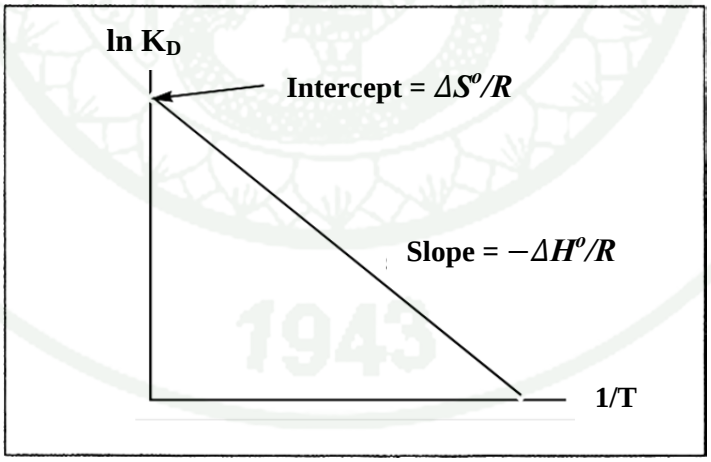

Figure 8 The Van't Hoff plots at various temperatures 1/T versus ln K_D for adsorption.

Source: Scienceblogs (2011)

4. Rainmaking

The process of rainmaking and moving cloud using 'Royal Rainmaking Technology' is described for weather modification by means of chemical seeding comprises steps of "Triggering", to activate cloud formation; "Fattening", to promote cloud growth; "Moving", to move cloud to a designated area, and "Attacking" to initiate rainfall from cloud. Attacking can be done by at least 3 different techniques; by 'Sandwich Seeding Technique' for 'warm cloud', by 'Glaciogenic Seeding Technique' for 'cool cloud', or by 'Super Sandwich Seeding Technique' for mixed phase cloud. 'Enhancing' is for enhancing amount of rainfall and prolonging raining duration including increasing area coverage. Weather modification extends to dispersion of cloud into clear flight path, prevention of hail formation, and inducing rainfall from stratiform clouds onto a valley or any catchment areas. Seeding may be performed inside or outside a cloud or to the top or underneath (His Majesty King Bhumibol Adulyadej, 2003). The process of rainmaking is comprised to 6 processes as follows.

4.1 Triggering process

The triggering is processes to activate cloud formation and enrich newborn cloud by dispersing cloud condensation nuclei of hygroscopic chemicals into volume of air. This process was used the powder of sodium a spreads upwind of a designated target area at a few of 7,000 – 8,000 feet.

4.2 Fattening process

The fatting is processes to promote raindrop formation by use the powder of sodium chloride. The powder of sodium chloride was spread into the cloud at level 8,000 feet. The raindrop is building up of cloud volume by dispersing exothermic-hygroscopic chemical into the updraft portion of cloud at a level above the cloud base.

4.3 Attacking the warm rain process

This process, the cloud was initiated to the rainfall, and floated to target area at 10,000 feet. The warm rain process are attacked the rain by used sandwich technique. The powder of sodium chloride is dispersed upwind into top of cloud at level 9,000 – 10,000 feet. The base of cloud was spreaded by the urea in angle of 45 degree.

4.4 Enhancing process

Enhance of rainfall are dispersed the dry ice below of cloud base about 1,000 feet. The dry ice was increased of the relative humidity in air and decreasing the temperature below of cloud base. Which are decreased the evaporation of the rainfall.

4.5 Attacking the cold rain process

Attacking the cold rain process by silver iodide was used the silver iodide flare. It is shoot top of cloud at level 21,500 feet. This process was increased the precipitation of rainfall. Silver iodide has a crystalline structure similar to that of ice and hence the moisture in the clouds condenses around the molecules.

4.6 Attacking by super sandwich model

The attacking by super sandwich model was used the silver iodide flare at top of cloud. The shoulder of cloud was dispersed powder of sodium, and dispersed the urea at base of cloud. These water droplets fall from the sky as rain. The silver iodide acts as an ice-forming agent by providing additional nuclei for water vapor condensation, dry ice lowers the temperature as it evaporates.

5. Bamboo

The bamboos are a group of woody pennanial evergreen, except for certain temperature species, plants in the true grass family Poaceae, subfamily Bambusoideae, and tribe Bambuseae. Some are giant bamboos, the largest members of the grass family. Bamboos are the fastest growing woody plants in the world. Their growth rate (up to 60 centimeters/day) is due to a unique rhizome-dependent system, but is highly dependent on location soil and climate condition. They are of economic and high cultural significance in East Asia and South East Asia where they are used extensively in gardens, as a building material, and as a food source.

Dendrocalamus brandisii

Familia: *Poaceae*
Genus: *Bambusa*
Synomyms: *Dendrocalamus brandisii*
Common name: Phai-Bongyai

Figure 9 The images of *Dendrocalamus brandisii.*

Source: Tropicalbamboo (2011)

Origin and geographic distribution: Indian and Southeast Asia.

Stem: up to 20-40 m, 10-12 cm in diameter, wall ca.3 cm thick, internodes usually 34–43 cm long and green to bright yellow.

The dimensions of fibres in the culm: length 20-40 mm, diameter 12.5–20 µm, and wall thickness ca. 10 µm.

The chemical composition of the culm: cellulose 53.19 %, Klason lignin 22.06%, xylan 20.47 %, arabinan 0.75%, galactan 0.28%, rhamnan 0.15%, glucuronic acid 0.17% and galacturonic acid 0.05%.

Propagation and planting: Phai-Bongyai is propagated by seed, rhizome cutting and tissue culture. Fresh seed germinates readily in 5-10 days after sowing, with a germination percentage of up to 80 %. Seed remain viable for 6 months when stored at 5 ^{o}C or when strored dry in sealed containers at room temperature. Seed stored without lowering temperature or moisture content will lose viability completely within 3 months. The best time for planting is in the rainy season. The images of *Dendrocalamus brandisii* are shown in Figure 9.

Application and properties: The bamboo charcoal has a high porosity, large surface area and large specific surface area (usually charcoal 300m^2 / g, charcoal up to 700m^2 / g). It is ability to regulate the humidity in the air, odor adsorption, fuel, water purification, health-care products and cosmetology. The properties is porous structure and adsorption characteristics, it is used to sweat, saliva, interior moisture adsorption, control allergens, bacteria and viruses in air. The cosmetology has developed bamboo charcoal soap and soap, skin whitening refreshing, and on the skin has a certain role in the prevention and treatment. It is currently developing a toothbrush, toothpaste and other daily necessities (Greenearthbamboo, 2010).

6. Oil Palm

The oil palm is a tropical palm tree which it is a member of the family Arecaceae, subfamily Arecoideae and tribe Cocoeae. The oil palm comprises two species such *as Elaeis guineensis Jacq* and *Elaeis oleifera*. The fruit of *Elaeis guineensis Jacq* give up of oil highly, grows in large bunches and size of a large plum. *Elaeis oleifera* is resisted the lethal bud rot, unsaturated fatty acid and iodine value approximately 77%. They are used in commercial agriculture in the production of palm oil. The oil palm used in food, soap, substitute for diesel fuels and used in the commercial food industry in other part of the world.

Elaeis guineensis Jacq.

Familia: *Palmae* or *Arecaceae*
Subfamily: *Arecoideae*
Genus: *Elaeis*
Synomyms: *Elaeis guineensis* Jacq.
Common name: Oil Palm

Figure 10 The images of *Elaeis guineensis* Jacq.

Source: Palmplantations (2011)

Origin and geographic distribution: West Africa, Central America and South America.

The description of the coconut: Stem; up to 35-60 cm tall, 20-28 cm in diameter. Leaves; pinnate to 100-120 cm long, 4-6 cm in wide.

The fruit and oil palm shell: A fruit of oil palm up to 2-5 cm long and each fruit weigh to 3-30 g, bunch of fruit weigh to 40-50 kg. The fruit of oil palm is composted for exocarp and mesocarp is fiber. The oil palm shell was separated 3 type such as Dura; shell up to 2-8 mm thickness and outermost shell to 35-60%. Tenera; shell up to 0.5-4 mm thickness and outmost shell to 60-90%. Pisifora; shell to very thinness and the outmost shell to 90%.

The composition of the palm shell is shown in Table 1

Table 1 Composition of palm shell

Composition	Percentage
Hydrogen (H)	6.46
Carbon (C)	46.59
Sulfur (S)	0.03
Nitrogen (N)	0.11
Oxygen (O)	24.61

Source: Chaiyaomporn and Chavalparit (2010)

Propagation and planting: Oil palm is propagated by sowing the seeds, off shoot and tissue culture. The seed are germinated the four-leaf stage in 10 to 14 weeks after planting. Seedlings are usually kept in poly-bag nurseries for about 12-14 months and planted in the field when they have 18-24 leaves. Planted from nurseries at 9-15 months of age, after transplanting into the field which after eight months in the nursery, normal healthy plants should be 0.8–1 m in height and display 5 to 8 functional leaves. In the first two years, lateral growth of the trunk dominates, giving a broad base up to 35-75 cm, high and 60 cm in diameter. The palms with good management are in production in 2 to 2.5 years after field planting. The images of *Elaeis guineensis* Jacq are shown in Figure 10.

Application and properties: The oil palm shell charcoal is a good source of carbon. It is has highly surface area and large specific surface area. It is ability to the water purification, air pollution control, conditioned-air filtration, gas/vapour purification, deodorization and decolourization. The adsorption properties of palm oil shell charcoal are due to the functional groups, such as carboxylic, hydroxyl, and lactone, which have a high affinity for metal ions (Tan *et al.,* 1993).

7. Coconut

The coconut is a palm family which it is a member of the family Arecaceae, subfamily Arecoideae and tribe Cocoeae. The coconut is the most extensively grown and used nut in the world. It is an important commercial crop in many tropical countries, contributing significantly to their economies. Copra of coconut is the source of coconut oil, which is used for making soap, shampoo, and cosmetics, cooking oils and it also be used as a substitute for diesel fuels. It also has cultural and religious significance in many societies that use it.

Cocos nucifera Linn.

Familia: *Arecaceae*
Subfamily: *Arecoideae*
Genus: *Cocos*
Synomyms: *Cocos nucifera* Linn.
Common name: Coconut

Figure 11 The images of *Cocos nucifera*.

Source: Ookaboo (2011)

Origin and geographic distribution: the origin of coconut has been found in the Malay Archipelago or the South Pacific.

The description of the coconut: Stem up to 30 meters (98 ft) tall, the pinnate leaves 4-6 meters (13-20 ft) long, and pinnae 60-90 cm long.

A fruit of coconut up to 15 inches (38 cm) long and 12 inches (30 cm) wide, composed of a thick, fibrous husk surrounding a somewhat spherical nut with a hard, brittle hairy shell. The nut is 6 - 8 inches (15 - 20 cm) in diameter and 10-12 inches (25 - 30 cm) long. Three sunken holes of softer tissue called "eyes" are at one end of the nut.

The chemical composition of the shell is shown in the table 2.

Table 2 Coconut shell compound (dry basis)

Compound	Percent
Cellulose	33.61
Lignin	36.51
Pentosans	29.27
Ash	0.61

Source: Woodroof (1979)

Propagation and planting: Coconut Palm propagation is entirely from seed-the coconuts. It takes many months for germination to take place. Recommended temperature for faster germination is around 90-100 ^{o}F. Upon germination, the shoot

and root emerge through the side or one end of the fruit. The young coconut about 6 months old can be transplanted directly into the field or can be grown in pots in the nursery. Coconut like sandy soil adds 40% sand to the mix. The images of *Cocos nucifera* Linn. are shown in Figure 11.

Application and properties: The coconut shell charcoal is a good source of carbon because it has strongly in the structure of shell. It is used for fuel and a source of charcoal. Activated carbon from coconut shell is material sources of domestic and industrial fuel greatly contributes to the environment. The coconut shell charcoal has a small macropores structure which renders it more effective for the adsorption of gas and vapor and for the removal of color, oxidants, impurities and odor of compounds (Wikipedia, 2011).

8. Montmorillonite clay

8.1 Character of montmorillonite clay

Montmorillonite is a very soft phyllosilicate group of minerals. It is a member of the smectite family as shown in Figure 12. Montmorillonite is the main constituent of the volcanic ash weathering product such as bentonite. Chemical formula of montmorillonite clay is $(Na, Ca)_{0.33}(Al, Mg)_2(Si_4O_{10})(OH)_2 \cdot nH_2O$. Montmorillonite can be adsorbed and ion exchange within cave which it is interlayer space. The properties of ion exchange and swelling or expand within interlayer space of montmorillonite is applicable to the industrials and adsorbed pollutants in envelopments.

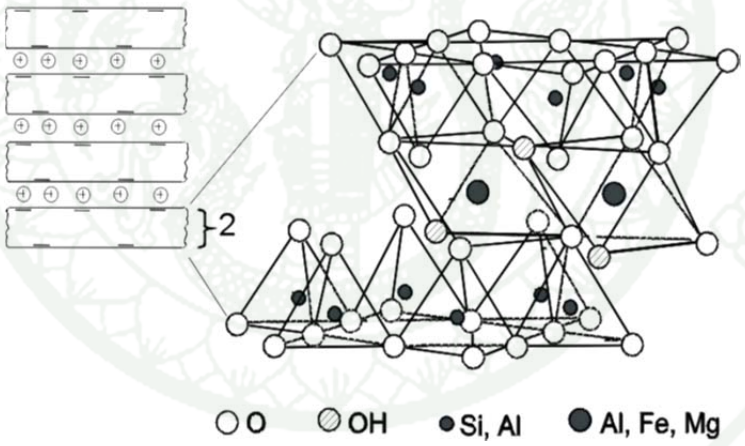

Figure 12 The structure composites of smectite minerals.

Source: Hofmann *et al.* (1956)

8.2 The properties and structure of montmorillonite clay

Montmorillonite is 2:1 clay, meaning that it as the silica tetrahedral sheet as shown in Figure 13 and aluminum octahedral sheet are shown in Figure 14. A single montmorillonite unit cell consists of two silica tetrahedral sheets sandwiching a central aluminum octahedral sheet as shown in Figure12.

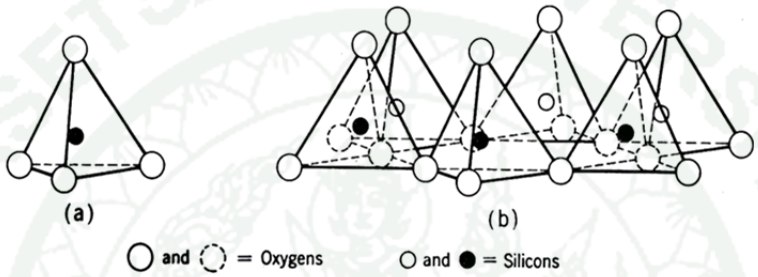

Figure 13 The structure of (a) a single tetrahedral unit and (b) the sheet structure of the tetrahedral unit.

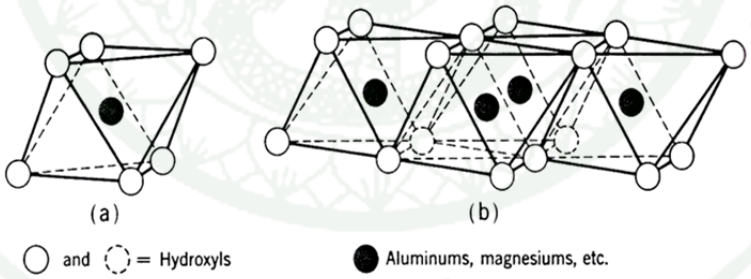

Figure 14 The structure of (a) a single octahedral unit and (b) the sheet structure of the octahedral unit.

Source: Smith and Bailey (1954)

The lengths and widths of montmorillonite flakes are from 10 to 100 times the thicknesses. The montmorillonite lattice is negative in charge, owing primarily to isomorphous replacements of ions within the structure. This negative character is

balanced by cations which are held on the surface of the flakes. Cations held in this fashion by the clay can be readily exchanged; the cations most commonly found in nature are sodium and calcium. The montmorillonite expand considerably more than other clays due to water penetrating the interlayer molecular spaces and concomitant adsorption. The amount of expansion is due largely to the type of exchangeable cation contained in the sample. The presence of sodium as the predominant exchangeable cation can result in the clay swelling to several times its original volume. The images montmorillonite clay is shown in Figure 15.

Figure 15 The images of Montmorillonite clay.

Source: Mindat (2011)

8.3 Application of montmorillonite clay

Montmorillonite is used in the oil drilling industry as a component of drilling mud, making the mud slurry viscous which helps in keeping the drill bit cool and removing drilled solids. It is also used as a soil additive to hold soil water in drought prone soils, to the construction of earthen dams and levees and to prevent the leakage of fluids. It is also used as a component of foundry sand and as a desiccant to remove moisture from air and gases.

9. Bentonite

9.1 Character of bentonite

The bentonite is a rock term; the origin of bentonite is attributed to the alteration of volcanic ash or glass. Bentonite largely composed of the clay mineral, montmorillonite. The bentonite is applicable in many industrials. Most industrial applications involve the swelling property of bentonite to form viscous water suspensions and large surface areas per unit weight of clay. The bentonite is 2 types such as sodium bentonite and calcium bentonite. The images bentonite is shown in Figure 16.

9.2 Structure of bentonite

The bentonite largely composed the clay mineral such as montmorillonite. Then structure of montmorillonite is applicable description to the structure of bentonite as well. The structure of montmorillonite is already shown in Figure 17.

Figure 16 The images of Bentonite.

Source: Mindat (2011)

9.3 Types and application of bentonite

9.3.1 Sodium bentonite

Sodium bentonite is swelling type or expands when wet, absorbing as much as several times its dry mass in water. Its excellent colloidal properties, and used in drilling mud for oil and gas wells and for geotechnical and environmental investigations.

9.3.2 Calcium bentonite

Calcium bentonite is non-swelling type. It is useful adsorbent of ions in solution because property of calcium bentonite is highly ion exchange. The high ion exchange of calcium bentonite are used the industrial cleaning agents, decolorize oils and adsorb the pollutant in wastewater.

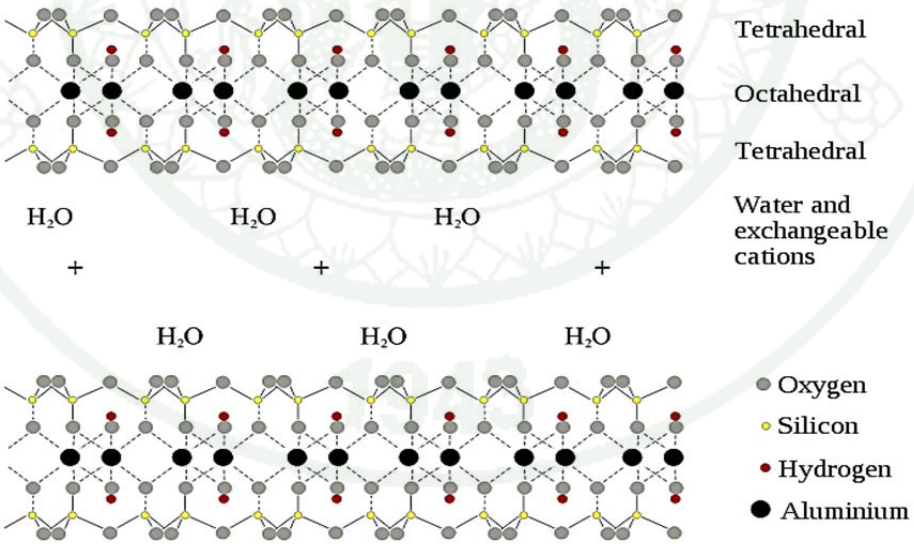

Figure 17 The crystalline structure of montmorillonite.

Source: Wikipedia (2011)

10. Pore structure and surface of carbon

Activated carbons are associated with pore starting from less than a nanometer to several thousand nanometers. This classification of pore by International Union of Pure and Applied Chemistry (IUPAC) is based on their width, while represent the distance between the wall of a slit-shaped pore and the radius of a cylindrical pore. The pores are divided into three groups as the micropores, the mesopores and the macropores. The classification of pores is shown in Figure 18.

Micropores have molecular dimension and the effective radius is less than 2 nm. The adsorption in these pore through volume filling, and there is no capillary condensation taking place. The adsorption energy in these pores is much larger compared to larger mesopores or to the nonporous surface because of the overlapping of adsorption forces the opposite walls of the macropores. Their specific surface area constitutes about 95% of the total surface area of the activated carbon.

Mesopores, also called transitional pores, have effective dimension in the 2 to 50 nm range, and their volume usually varies between 0.1 and 0.2 cm^3/g. The surface area of these pores does not exceed 5% of total surface area of the carbon.

Macropores are not of considerable importance to the process of adsorption in activated carbon because their contribution to the surface area of the adsorbate is very small and does not exceed 0.5 m^2/g, they have effective radii larger than 50 nm, and frequently in the 500 to 2,000 nm, with a pore volume between 0.2 and 0.4 cm^3/g. They act as transport for adsorbate into the micropore and mesopore.

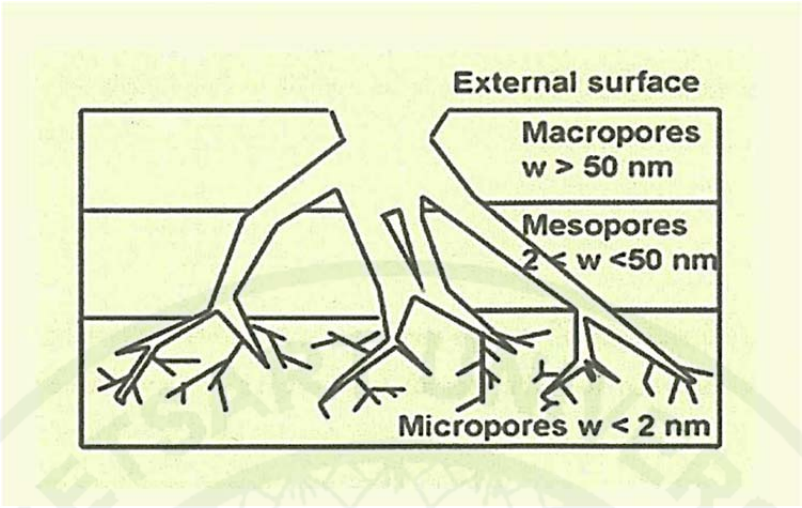

Figure 18 The classification of pore.

Source: Wikipedia (2008)

10. Phenol

10.1 Characteristics of phenol

Phenol, also known as carbolic acid, is a white crystalline solid with a sweet tarry odor, commonly referred to as a “hospital smell”. Its chemical formula is C_6H_5OH and is chemical name is hydroxybenzene. The structure of phenol is that of a hydroxyl group (-OH) bonded to phenyl ring. Thus, it is an aromatic compound which slightly acidic. The structure of phenol is shown in Figure 19. The phenol molecule has weak tendencies to lose the H^+ ion from the hydroxyl group, resulting in the highly water-soluble phenolate anion ($C_6H_5O^-$), and also called phenoxide anion. Compared to aliphatic alcohols, phenol shows much higher acidity. It even reacts with aqueous NaOH to lose H^+, whereas aliphatic alcohols do not. However, many carboxylic acids are more acidic than phenol. One explanation for the increased acidity over alcohols is resonance stabilization of the phenoxide anion by the aromatic ring. In this way, the negative charge on oxygen is shared by the ortho and para carbon atoms. In another explanation, increased acidity is the result of orbital overlap between the oxygen lone pairs and the aromatic system. In the third, the dominant effect is the induction from the sp^2 hybridized carbon the comparatively more powerful inductive withdrawal of electron density that is provided by sp^2 system compared to a sp^3 system, allow for great stabilization of the oxygen. The properties of phenol are shown in Table 3.

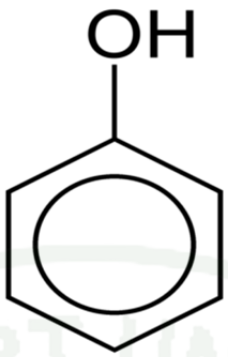

Figure 19 The chemical structure of phenol.

Source: Wolframalpha (2011)

10. 2 Application of phenol

Phenol is used in the production of drugs (it is the stating material in the industrial production of aspirin), herbicides, and synthetic resins (Bakelite, one of the first synthetic resin to be manufactured, is a polymer of phenol with formaldehyde). Phenol is the preferred chemical in use of embalming bodies for anatomical use and study because of its ability to preserve tissues for extended periods of time. Phenol is also used in the preparation of cosmetics including sunscreen, hair dyes, and skin lightening preparations. Compounds containing phenol moieties can be used to prevent ultraviolet light which induced damage to hair and skin due to the UV-absorbing properties of the aromatic ring of the phenol.

10.3 Toxicity of phenol

Inhalation and dermal exposure to phenol is highly irritating to the skin, eyes, and mucous membranes in humans. Phenol is considered to be varying toxic to humans through oral exposure, with ingestion of 1 g reported to be lethal, with symptoms including muscle weakness and tremors, loss of coordination, paralysis, convulsions, coma, and respiratory arrest. Blood changes, liver and kidney damage, and cardiac toxicity including weak pulse, cardiac depression, and reduced blood

pressure have been reported in human acutely exposed to phenol by the oral route. Acute (short-term) animal tests, such as the LD_{50} test in rats, mice and rabbits have shown phenol to have high acute toxicity from oral exposure. Long-term inhalation exposure to phenol in animal studies has shown effects on the liver, kidney, respiratory, cardiovascular, and central nervous systems.

Table 3 The properties of phenol.

Properties	
General	
Molecular formula	C_6H_5OH
Molar mass (g/mol)	94.11
Appearance	white crystalline solid
Physical and chemical properties	
Density (g/cm^3)	1.07
Melting point (^oC)	40.5
Boiling point (^oC)	181.7
Solubility in water (g/100 ml)	8.3 (20 ^oC)
Acidity (pK_a)	9.95

Source: Wikipedia (2008)

11. Chromium (VI)

11.1 Character of chromium

Chromium is a chemical element with the symbol Cr and atomic number 24. It is the first element in Group VIB. It is a steely-gray, lustrous, hard metal that takes a high polish and has a high melting point. It is also odorless, tasteless, and malleable. Chromium is a lustrous, brittle, hard metal. Its colour is silver-gray and it can be highly polished. It does not tarnish in air, when heated it borns and forms the green chromic oxide. Chromium is unstable in oxygen, it immediately produces a thin oxide layer that is impermeable to oxygen and protects the metal below. The properties of Cr are shown in Table 4.

11.2 Chromium in natural resources

Chromium is mined as chromite ($FeCr_2O_4$) ore. Chromium ores are mined today in South Africa, Zimbabwe, Finland, India, Kazakihstan and the Philippines. A total of 14 million tons of chromites ore are extracted. Reserves are hestimated to be of the order of 1 billion tones with unexploited deposits in Greenland, Canada and USA.

11.3 Application of chromium

Chromium main uses are in alloys such as stainless steel, in chrome plating and in metal ceramics. Chromium plating was once widely used to give steel a polished silvery mirror coating. Chromium is used in metallurgy to impart corrosion resistance and a shiny finish; as dyes and paints, its salts colour glass an emerald green and it is used to produce synthetic rubies; as a catalyst in dyeing and in the tanning of leather; to make molds for the firing of bricks. Chromium (IV) oxide (CrO_2) is used to manufacture magnetic tape.

Table 4 The properties of chromium.

Properties	
General	
Name	chromium (Cr)
Number	24
Atomic weight (g/mol)	51.9961
Electron configuration	[Ar] $3d^5$ $4s^1$
Electrons per shell	2, 8, 13, 1
Physical and chemical properties	
Phase	solid
Density (g/cm^3)	7.19
Melting point (^oC)	1907
Boiling point (^oC)	2671
Heat of fusion (kJ/mol)	21.0
Heat of vaporization (kJ/mol)	339.5
Atomic properties	
Crystal structure	body-centered cubic
Oxidation states	6, 5, 4, 3, 2, 1, -1 and -2
Electronegativity	1.66
Ionization energies	
1^{st} (kJ/mol)	651.1
2^{nd} (kJ/mol)	1590.1
3^{rd} (kJ/mol)	2987.0
Atomic radius (pm)	128
Covalent radius (pm)	139±5
Van der Waals radius (nm)	0.1270

Source: Wikipedia (2008)

11.4 Toxicity of chromium

Inhalation of hexavalent chromium compounds can result in ulceration and perforation of the mucous membranes of the nasal septum, irritation of the pharynx and larynx, asthmatic bronchitis, bronchospasms and edema. Respiratory symptoms may include coughing and wheezing, shortness of breath, and nasal itch. Chromium (VI) is mainly toxic to organisms. It can alter genetic materials and cause cancer. Chromium (VI) is a danger to human health, mainly for people who work in the steel and textile industry. Chromium (VI) is known to cause various health effects. When it is a compound in leather products, it can cause allergic reactions, such as skin rash. After breathing it in chromium (VI) can cause nose irritations and nosebleeds.

OBJECTIVES

There are four main objectives for this work.

1. To study the adsorption of water vapor onto chars and soil minerals.

2. To study the effect of temperature on adsorption capacity of phenol and water vapor onto chars and soil minerals.

3. To study the adsorption of phenol on the chars by used the Langmuir and Freundlich isotherms.

4. To study the adsorption of Chromium onto chars and soil minerals by used the Langmuir and Freundlich isotherms.

LITERATURE REVIEW

This section reviews the characterization techniques of adsorption water vapor and pollution by various adsorbent by previous researchers. The studies on adsorption of water vapor and pollution by various adsorbent are also reviewed.

1. Adsorption of water vapor and pollutants on chars

Foley *et al.* (1997) studied the adsorption of water vapor on highly microporous carbon derived from the carbonization of coconut shell. The carbonization was characterized by the adsorption of nitrogen at 77 K and carbon dioxide at 273 K. The micropore size distribution was determined using probe molecule vapors at relative pressure (P/P^0) was 0.5 and 301 K. The adsorption and desorption of water vapor on the activated carbon were investigated over the pressure range 0-2.41 kPa (P/P^0 = 0-0.9) in a static water vapor system. The results indicated that the mechanism of adsorption process on activated carbon is the fastest at low relative pressures. The slowest rate of adsorption and desorption were observed in the region of relative humidities in the range 40-70%. The relative humidities range 40-70% is the most commonly encountered range in real situation. The adsorption process involves the growth of clusters of water molecules on the primary adsorption centers. Which growths of clusters are leaded to water molecules bridging between pore walls and adjacent water molecules clusters, eventually lead to condensation of water vapor in pore.

Lee *et al.* (1999) studied the adsorption of water vapor on coal- and wood-based at room temperature (24^{o}C). The coal- and wood-based were prepared by chemical activation with varying heat treatment temperature using KOH and H_3PO_4 as chemical activates. The surface element distribution/concentration and chemical structure was characterized by X-ray photoelectron spectroscopy, BET and mesopore surface. The adsorption of water vapor was obtained using a gravimetric adsorption apparatus equipped with a Cahn 2000 electrobalance, about 50 mg of each activated

carbon sample, evacuation of volatile vapor at 523 K and equilibrium of relative pressure range of 10^{-3} to 0.9. The water vapor adsorption studies were fitted into the Dubinin-Serpinsky isotherm equation; sample has lower surface area adsorbed higher than a sample has higher surface area adsorbed in the low relative pressure range. Adsorption amount increases in relative pressure rang above 0.4; therefore surface area/imcroporosity has developed in the carbon samples.

Lee and Reucroft (1999) studied the adsorption of NH_3 and H_2S on coal and wood-based chemically activated carbon in the the low relative pressure ranges. Coal- and wood-based were prepared by chemical activated with varying heat treatment temperature using KOH and H_3PO_4 as chemical activates. The adsorption of carbon sample is measured by using gravimetric adsorption method. The adsorption characteristic of carbon sample was studied by compared with CCl_4, acetone and water vapor at the relative pressure (P/P^0) was 1. The results showed that the adsorption of NH_3 on the coal-based KOH activated carbon sample with high surface area was somewhat lower than on lower surface area carbon sample at very low relative pressure ($P/P^0 < 0.04$) because the limited of micropore volume in structure carbon. The NH_3 adsorption in the low relative pressure region was higher than H_2S due to the oxygen functional group on the carbon surface. The average micropore size and surface chemistry have effects on the adsorption process in vary low relative pressure ranges.

Cossarutto *et al.* (2001) studied the adsorption of water vapor on microporous carbon derived from carbonization of coconut shell. The adsorption isotherm and sorption kinetic of the activated carbon were characterized by using Intelligent Gravimetric Analyser (IGA) and system consists of a fully computerized microbalance, were investigated over the pressure range P/P^0 0-0.95 in water vapor system. The result showed that the rate of adsorption and desorption related with pressure region of the isotherm, the highest rate were observed at low relative pressure, the lowest rate were observed in an interval of relative pressure (P/P^0) from 0.55 to 0.7. The adsorption and desorption kinetics of water vapor on active carbon were followed a linear driving forces mass transfer rate low for more than 90% of the

adsorption pressure. The carbon derived from carbonization of coconut shell was higher surface polarity than unmodified carbon because the degree of burn-off has modified the microstructure of carbon surface.

Finqueneisel *et al.* (2005) studied the adsorption isotherm for co-adsorption of methanol and water vapor on activated carbon (AC). The AC was obtained by activation of coconut shell by steam at 1123 K. The adsorption was characterized by intelligent gravimetric analysis (IGA) and gravimetric microbalance. The co-adsorption was performed at relative humidity (RH) ranges from 25% to 74% and the methanol concentration from 0% to saturation. The result, a large part of the pore volume was already filled at low relative pressure. The adsorption of methanol/water vapor mixture on AC was higher when RH was 25% and then decreases with increasing RH.

Vartapetyan *et al.* (2005) studied the adsorption of water vapor by used carbonizates and active carbon (AC). They were prepared form the wood of tropical tree *Poltogyne* from surinan. The carbonizates structure was characterized by mass-spectrometric thermodesorption analysis, X-ray diffraction (XRD) and water vapor adsorption isotherm. Adsorption isotherm of heated and unheated can be measured by use a vacuum installation incorporating a spring quartz microbalance with sensitivity 10^{-5} g of 0.1 g. The results of samples had increased adsorption in region of medium and high pressure. The adsorption of the heating samples had decreased at low pressure. Decreasing samples mass with increasing water vapor pressure is due to the influence of impurity in structure. The XRD pattern of heat treatment could confirm the adsorption isotherm. The heating CA at 623 K were increased desorption because the active carbon were decreased of micropore size in structure.

Ozkaya (2006) studied the potential of activated carbon (AC) for phenol adsorption from aqueous solution. Four adsorption isotherms were carried out to evaluate the effect of contact time, initial concentration and desorption characteristics of AC. The physical properties of granular activated carbon are apparent density of 0.4 g/cm^3, particle size of 1.4 nm and average pore diameter of 18 Å^2. The adsorption

of phenol on activated carbon was studied using batch experiments and analyzed by the photometric method. The results found that the AC dosages as 0.5 g can be to remove 94% of phenol at adsorption equilibrium 1 hour. The adsorption of phenol on AC is fitted well with Langmuir isotherm.

Bedia *et al.* (2007) studied water adsorption capacity and kinetics of char and activated carbons with different burn-off and inorganic matter content prepared form kratf lignin. The activated carbon was characterized by temperature-programmed desorption (TPD), scanning electron microscopy (SEM), X-ray photoelectron spectroscopy (XPS), and atomic adsorption spectroscopy (AA). Water vapor adsorption isotherm had been obtained in a thermogravimetric system and had been fitted by a Dubinin-Serpinski equation. The kinetics of water vapor adsorption follows a linear driving force mass transfer (LDF) model. The results the adsorption isotherm of water on activated carbon produced at 41% burn-off show that the adsorption of water is higher at law relative pressure. The burn-off higher than 41% the carbon produced had a decreased in the water adsorbed at low relative pressure.

Dubey and Gopal (2007) studied the adsorption of chromium (VI) on low cost adsorption derived from agricultural waste material (Groundnut husk carbon and silver impregnated groundnut husk carbon). The adsorbent were prepared by activated carbon using sulfuric acid in 4:3 ratios and modified surface area of adsorbent by silver nitrated. The surface area was characterized by scanning electron microscope (SEM). The adsorption capacity was calculated by using Langmuir isotherm. The adsorption of chromium (VI) in aqueous solution was used batch technique and investigated the operation parameter such as pH, adsorbent doses, agitation speed, contact time and temperature. The results were found that percentage removal of chromium (VI) depended on the quantity of adsorbent, concentration of chromium ion and contact time. The adsorption capacity of the both groundnut husk carbon and silver impregnated groundnut husk carbon are 7.0104 mg/g and11.3990 mg/g, respectively. The adsorption capacity of silver impregnated groundnut husk carbon is higher than groundnut husk carbons due to silver ions and silver chromate were modified on the surface area.

Garg *et al.* (2007) studied the adsorption of chromium (VI) in aqueous solution onto different agricultural waste such as sugarcane bagasse, maize corn cob and Jatropha oil cake under various experimental conditions such as adsorbent dosage, chromium (VI) concentration, contact time and pH. The functional group and surface area of adsorbent were characterized by Fourier Transform Infrared spectra (FT-IR) and scanning electron microscope (SEMs). The concentration of chromium in the solution was determined by spectrophotometer. The results showed that the adsorption of chromium (VI) was highly dependent on pH, initial chromium concentration, adsorbents mass and contact time. The adsorptions of chromium (VI) on all the adsorbents are higher at pH 2. The adsorption capacities of all adsorbent were fitted with the Langmuir isotherm model. The percentage adsorption of chromium (VI) on the maize corn cob (62%) has lower than the Jatropha oil cake (97%) and sugarcane bagasse (92%).

Isa Hasnain *et al* (2008) studied the removal of chromium (VI) from aqueous solution using treated oil palm fibre under various experimental conditions. The adsorbent was prepared using concentration sulphuric acid and heat treatment for 24 hour at 150 ^{o}C. The surface area and functional group of adsorbent were characterized by scanning electron micrograph (SEM) and Fourier Transform Infrared spectra (FT-IR), respectively. The removals of chromium (VI) from aqueous solution were determined by using a Hach DR 2010 Spectrophotometer. The adsorption capacity data were described by Langmuir and Freundlich isotherm models. The adsorption kinetics was described by pseudo first order and pseudo secondary order models. The results were found that the adsorption capacity of treated oil palm fibre favored at low pH about 1.5. The amount of chromium (VI) adsorbed increased with increase in chromium (VI) concentration and contact time. Which the adsorption capacity of chromium could be adequately described by both Freundlich isotherm (R^2= 0.8775) and Langmuir isotherm (R^2= 0.8715). The Freundlich isotherm model was presented a slightly better fit.

Naoto *et al.* (2008) prepared microporous carbon foams for adsorption/desorption of water vapor in ambient air. The microporous carbon foams was charactered by SEM and BET method. The microporous carbon foam prepared from a fluorinated polyimide using melamine foam as a template at different temperatures, activated at 400^{o}C for 1 hour in air. Activation of carbon foams at 400^{o}C for 1 hour in air had increased the adsorptivity of water vapor, which found that adsorption of water vapor in wet air and the desorption into dry air were reversible, the adsorptivity of about 40% mass fraction for a microporous volume of 0.75 mL/g.

Do *et al.* (2009) studied a new isotherm model to describe the adsorption and desorption of water adsorption onto activated carbon. The new equation are tested with activated carbon and the described the isotherms of adsorption-desorption. The results new models are found that the adsorption capacities of water are depended on pore structure and concentration of functional group in the structure of activated carbon. The water capacity in the micropore is decreased with increases concentration of functional group due to the pore blockage by the functional group, and water cluster size is smaller due to the stabilization of small clusters by the functional group. The adsorption capacities of water are depended on pore structure and functional group in the structure of activated carbon.

Pastor-Villlegas *et al.* (2010) studied the adsorption-desorption of water vapor on chars prepared from commercial wood charcoals, in relation to their surface chemistry, pore structure and chemical composition. The charcoals were characterized by Fouier transform infrared (FT-IR) spectroscopy and scanning electron microscopy (SEM). The micropore structures of the charcoals were characterized by adsorption of carbon dioxide at 273 K. The adsorption and desorption isotherm of water vapor were determined at 25 or in quasi-equilibrium condition by mean of an automatic gravimetric apparatus. The adsorption data of water vapor were fitted to the Dubinin-Serpinsky (DS-2) and Dubinin-Astakhov (DA) equation. For the adsorption isotherm, the results show that the adsorptions of water vapor are occurred in micropore structure, and thereafter in the non-micropore structure at relative pressures higher

than 0.95. The adsorption isotherm is dependent on both the surface chemistry and the pore structure of the sample. The adsorption isotherm of water vapor on micropore structure was fitted to with the DA equation.

Horikawa *et al.* (2011) studied a new model adsorption and desorption of water in mesoporous carbon. The mesoporous carbon materials were prepared from resorcinol-formaldehyde carbon cryogels (RFCCs) by sol-gel polycondensation of resorcinol with formaldehyde in slightly basic aqueous solution. The mesoporous carbons were followed by drying with freeze-drying and then carbonizing the RF cryogels at high temperature under a nitrogen atmosphere. The surface functional group in RFCCs was measured by Boehm titration. The specific surface area, mesopore size distribution and the pore volume were determined by the BET equation adsorbed N_2 at 77 K. The result found that the new model can be described adsorption and desorption of water vapor in the mesopore and micropore. The experimental data indicated that water cluster size in mesopore was larger than that in micropore and the hysteresis loop of adsorption-desorption in mesopores was greater than that in microspores.

2. Adsorption of water vapor and pollutants on soil minerals

Khan *et al*. (1995) studied the adsorption of chromium (VI) on bentonite. The physical and chemical properties were determined by X-ray diffraction (XRD) analysis. The adsorption of adsorbate on bentonite clay had been studied by a batch technique. The adsorption results were analyzed in terms of Langmuir, Freundlich and Dubinin-Raduskevich (D-R) isotherm. The results showed that the uptake of chromate (VI) on bentonite was high at pH 2.0 and the concentration range 10^{-5} to 10^{-3} mol/dm^3. The adsorption capacity of chromium (VI) on bentonite at 20 ^{o}C is 0.63 mmol/100 g which increases to 1.1 mmol/100 g at 40 ^{o}C. The ΔG^{o} value of chromium (VI) was increased in the negative at high temperature which indicates that adsorption process was favoured at higher temperature.

Viraraghavan and Flor de Maria (1998) studied the effective of bentonite in removing the phenol from wastewater. The adsorption of phenol was studied in batch experiments by using orbital shaker. The sample was shaken at 175 rpm at room temperature (21± 1^{o}C). The concentration of phenol was determined by using a Spectronic 21 spectrophotometer at a wavelength 460 nm. The results showed that bentonite can adsorb phenol to the renege 40-45%. The equilibrium time of adsorption of phenol bentonite was 16 hours. The optimum pH for adsorption of phenol was between 4.0 to 5.0. The adsorption of phenol on bentonite was described by Freundlich isotherm. The adsorption capacity of phenol on bentonite was 42.5%.

Hocine *et al.* (2004) studied the adsorption of aromatic amines on treated bentonite by various experimental conditions such as pH, temperature and aqueous concentrations. The results showed that activated bentonite can be used to remove the aromatic amines from wastewater. The removals of p-aminobenzoic acid were depended on pH, contact time and temperature. The adsorption of p-aminobenzoic acid on treated bentonite was fitted with the Freundlich isotherm. For influence of temperature on adsorption of p-aminobenzoic acid onto bentonite was not great which the adsorption capacity were decreased at temperature higher than 40 ^{o}C. This indicated that the adsorption was exothermic process.

Bhattacharyya and Gupta (2006) studied the adsorption of chromium (VI) from water by used clay. The adsorbent was characterized by X-ray diffraction (XRD). The surface area and cation exchange capacity of clay were estimated by using Sears' method and the copper bis(ethylenediamine) complex method. The adsorption experiment was studied by the batch adsorption methods. The aqueous solution of chromium (VI) was determined by atomic adsorp spectroscopy (Varian SpectraAA 220 with air-acetylene oxidization flame, wavelength 429.1 nm, lamp current 5 mA, slit width 0.5 nm, working range 0.1-30 μm/mL). The result*s* found that the adsorption of chromium (VI) in aqueous solution was increased from pH 1.0 to 7.0, after that the adsorption was decreased suddenly. The adsorption of chromium (VI) was attained equilibrium within 240 min. The kinetic of adsorption was endothermic process.

Tahir and Naseem (2007) studied the adsorption of chromium (III) from tannery wastewater onto bentonite clay under various experimental conditions such as adsorbent dosage, pH, chromium (III) concentration, and temperature and contact time. The surface area was measured using a BET Quantasorb Sorption System, Model No. QS-11. The chemical compositions of bentonite were determined by high frequency bead sample (OYO Danki Co-Jappan) X-ray fluorescence spectrometer (XRF). The adsorption of chromium (III) was studied by batch experiment and column techniques. The adsorption data were fitted to the Langmuir and Freundlich isotherm models. Thermodynamic parameter such as ΔG^o, ΔH^o and ΔS^o were calculated from the slope and intercept of the linear plot of ln K_D against $1/T$. The concentration of chromium (III) after adsorption was determined by atomic adsorption spectrophotometer (AA). The results showed that max 93% of the adsorption had achieved on pre-treated (with sludge) wastewater samples with a shaking time for 15 min. While 76% is achieved in case of untreated samples with a shaking time of 45 min at a pH range of 2.4 to 2.5. The heat of adsorption of chromium (III) was endothermic process (positive values of ΔH^o and ΔS^o and negative values of ΔG^o).

Richards and Bouazza (2007) studied the adsorption of phenol by four organically modified clays which obtained from the base basaltic clay and bentonite.

The both clays organically were modified by the adsorption of Hexadecyltrimethyl-ammonium (HDTMA) and Phenyltrimethylammonium (TMPA). The both clays were characterized by X-ray diffraction. The adsorption of phenol was studied by batch adsorption test methods. The concentrations of phenol were analyzed using a HP6890 Gas Chromatograph with HP5973 Mass Spectrometer detector. The results indicated that the adsorption of phenol by HDTMA modified clays was fitted with the Freundlich equation. The adsorption of phenol on TMPA modified clays was described by the Langmuir equation. The adsorption capacities were increased with modified surface of clay by organic compound. The adsorptions are depended on surface area and polarity of the surface.

Ghorbel-Abid *et al.* (2009) studied the adsorption of chromium (III) from aqueous solution using bentonite clay from Jebel Chakir (northwest of Tunis, Tunisia, North Africa). The bentonite was purified by repeating the cation exchange with NaCl solution (1M). The mineralogical and chemical compositions of the bentonite clay were determined by X-ray diffraction (XRD), infrared spectroscopy (IR) and the inductively coupled plasma technique (ICP).The surface area was determined using the adsorption isotherm obtained with methylene blue. The specific surface area (SE) was calculated by applying the BET equation to the nitrogen adsorption isotherm at 77 K. The adsorption capacity was determined by using Langmuir and Freundlich isotherm. The results showed that the adsorption behaviour of bentonite clay was depended highly on pH. The adsorption was increased along with increasing of suspension pH in range of 3 to 5. The adsorption capacity of bentonite clay was fitted to the Langmuir isotherm.

Sokolowska *et al.* (2009) studied the adsorption isotherm by evaluate the specific surface area and the surface dimension of several sample containing organic matter. The kaolin and quartz sample were modified by using humic acid, sand and peat. The surface area was calculated using BET equation. The water vapor adsorption isotherm was measured by using the gravimetric method; temperature was kept constant at 294±1 K. The time of equilibrium was ranged from 48 hours up to 6 days. The results were found that some adsorbent, i.e. quartz modified with sand soil

and peat can be well modeled by a straight regression line and the correlation coefficients were high. The adsorption isotherms of water vapor were depended on the specific surface area and the surface fractal dimension on the percent content of organic matter. The monolayer capacities were determined from the adsorption data corresponding to rather low moistures. The fractal dimensions were calculated from the data obtained at high relative pressure.

Stathi *et al.* (2010) studied the role of permanent charge site onto the heavy metal uptake by a high cation exchange capacity montmorillonite. The high cation exchange capacity (HCM) montmorillonite clay was prepared by acetate treatment of Zenith clay. The HCM had evaluated for metal-uptake from aqueous solutions. The experiment data showed that the cation exchange site can play a significant role in the adsorption of metal in smectite clay. The result showed that the hydroxyl group on surface area of smectite clay has to play secondary role in adsorption of metal. The permanent charge has influence the ionic-strength sensitivity of the point of zero charge of the montmorillonite clay.

MATERIALS AND METHODS

Materials

1. Apparatus

1.1 UV-Vis spectrophotometer (UV-Vis: Jasco, Model 7800)

1.2 Fourier transforms infrared spectrometer (FT-IR: Perkin Elmer, System 2000)

1.3 Scanning electron microscope (SEM: LEO, 1450 VP)

1.4 Microweight balance (Mettler Toledo, AL 204)

1.5 Rotary shaker (Clifton, NE5-2BD CE)

1.6 Centrifuge (Adams, Compact II)

1.7 pH meter (Inolab level 1, 8F93)

1.8 Heater (Eyela, UA-10S)

1.9 Oven (Precision, 16EG)

1.10 Blower

1.11 Desiccators

1.13 Sieve mesh 150 μm

1.14 Pump flow (Resun, P-1500)

1.15 Instrument for generate Water Vapor

2. Reagents

2.1 Phenol (C_6H_5OH, AR. grade, Carlo Erba, Rodano, Milan, Italy)

2.2 Potassium dichromate ($K_2Cr_2O_7$, AR. grade, Ajax Finechem, Aukland, New Zealand)

2.3 Potassium bromide (KBr, AR. Grade, Merck, Dermstadt, Germany)

2.4 Nitric acid (HNO_3 69-70%, A.S.C.R. Grade, Thailand)

2.5 Sodium hydroxide (NaOH, AR. Grade, Ajax Finechem, Aukland, New Zealand)

2.6 Citric acid monohydrate ($C_6H_8O_7.H_2O$, AR. Grade, RFCL, New Delhi, India)

2.7 tri Sodium phosphate (tert) Dodecahydrate ($Na_3PO_4.12H_2O$, AR. Grade, Fluka, Berlin, Germany)

2.8 Boric acid (H_3BO_3, AR. Grade, Leicester shire, Lougborough, United Kingdom)

2.9 Bentonite (Sigma Aldrich, Missouri, United States)

2.10 Montmorillonite K10 (Sigma Aldrich, Missouri, United States)

2.11 Pongyai Bamboo Charcoal powder

2.12 Palm shell Charcoal powder

2.13 Coconut shell Charcoal powder

Methods

1. Materials

Raw materials are charcoals from agriculture such as coconut shell, oil palm shell and bamboo. Raw materials are crushed to desired size and then washed with water, dried at 120 ^oC for 2 hours. The materials were sieved to 150 μm size and kept in desiccators.

2. The instrument to generate water vapor

The instrument used in adsorption water vapor experiments was designed by using the principle of Intelligent Gravimetric Analyzer instrument (IGA). The instrument comprises of 5 parts, a chamber, the water container, the heater, a pumps flow and blower are shown in Figure 20. The generations of water vapors are as followed:

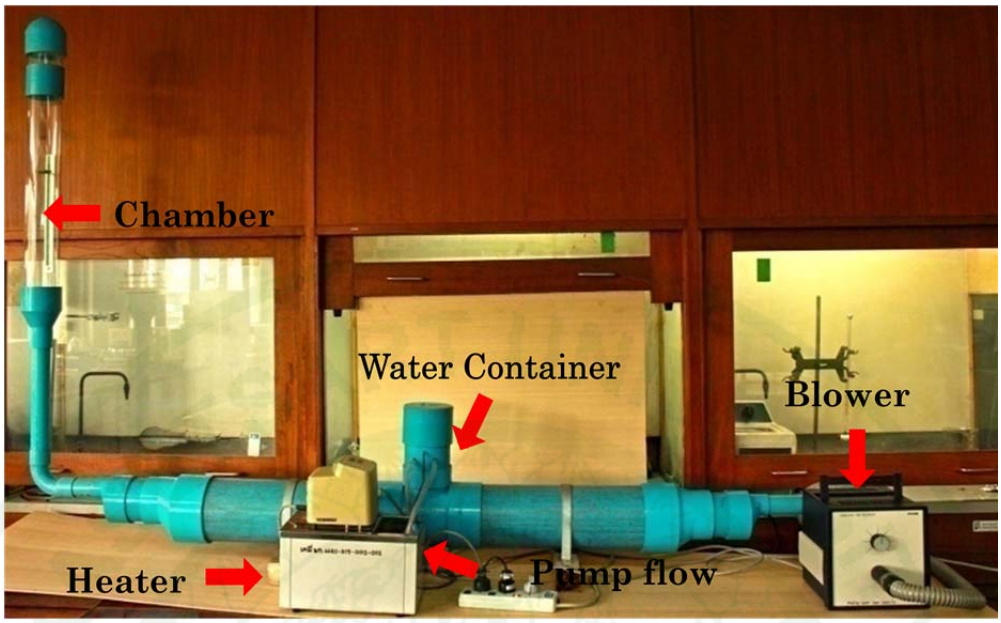

Figure 20 The comprises of instruments to generate water vapor.

Firstly, generate water vapors by heat water at 40±1 ^{o}C in a pipe. Then heated water was circulated in the system by a pump flow. The water vapors flow into the pipe and carrier the water vapor uptake to the sample chamber by pressure flow from a blower. The amount of water vapor will be determined from humidity which was measured every 30 min from thermo hygrometer for 3 hours.

3. The adsorption of water vapor on chars and soil minerals

3.1 Spring constant of a spring

The spring constant of a spring was studied by plot the force exerted by mass versus the displacement of spring when mass put on the spring. Which the force exerted by mass was calculated from Newton's Law.

The spring constant of a spring can be determined from the Hooke's Law.

$$F = kx$$

Where F is the restoring force exerted by the mass put on the spring (unit is N)
x is the displacement of spring at equilibrium (unit is m)
k is the spring constant (unit is N/m)

Displacement, or the distance the spring is stretched from the spring's equilibrium can be calculated by taking away the initial position from the final position.

The find of the spring constant, Hooke's Law equation can be switched into;

$$k = \frac{F}{x}$$

This equation states that the spring constant equals to the force exerted on the spring divided by the displacement of spring (final position – initial position). The calculation spring constant of a spring was presented in Appendix B.

3.2 The adsorption of water vapor

Adsorption of water vapor was studied by generated water vapor at temperature of 40, 45, 50 and 55 ^{o}C. Adsorption of water vapor on the adsorbate was measured from stretch out of spring. The spring is extended when the water vapor was adsorbed on surface of adsorbent. The distance the spring is stretched from the spring's equilibrium can be calculated by taking away the initial position from the final position. The amount of water vapor was determined from distance of spring which was collected every 30 min for 3 hours. Amount of water vapor which was

absorbed by adsorbent was calculated from distance of spring which was stretched according to the following equation:

$$F = kx$$

Where F is the restoring force exerted by the adsorbent (unit is N)
x is the displacement of spring at equilibrium (unit is m)
k is the spring constant (unit is N/m)

The amount of water vapor can be determined from the Newton's Law.

$$F = ma$$

Where F is the net force, m is mass in kilograms and a is acceleration in m/s^2.

Force is calculated from distance of spring and spring constant of a spring by used Hooke's Law. Mass is equal to amount of adsorbents (g) and a is equal to the gravity of earth (9.8 m/sec).

The calculation of amount of water vapor using Newton's Law equation can be switched into;

$$m = \frac{F}{a}$$

This equation state the m equals to the amount of water vapor adsorption onto adsorbent. The amount of water vapor adsorption was presented in Appendix B.

The relative pressure can be calculated by the Clausius-Clapeyron equation as followed;

$$\ln \frac{P_2}{P_1} = \left(-\frac{\Delta H_{vap}}{R}\right)\left(\frac{T_2 - T_1}{T_2 T_1}\right)$$

where T_1 is the absolute temperature

T_2 is the temperature at another point

P_1 is the corresponding vapor pressure

P_2 is the corresponding pressure at another point

ΔH_{vap} is the heat of vaporization of the liquid (J/mol)

and R is the universal gas constant (8.3143 J/mol.K)

Afterwards, the adsorption isotherm of water vapor plot of amount of adsorbed against the relative pressure (P/P^0) yields straight line for the adsorption water vapor onto chars and soil minerals. The Langmuir plots of x/m against P/P^0 yields straight line for the adsorption of water vapor onto chars and soil minerals. The Langmuir constant Q_o and b are obtained from slope and intercept of the respective plot. The Freundlich plots of log x/m versus log P/P^0 yields straight line for the adsorption of water vapor onto the chars and soil minerals. The Freundlich constant n and K_F are obtained from the slope and intercept of the respective plot. The applicability of isotherm models of the adsorption was compared by judging the correlation coefficient (R^2) values. The heat of adsorption plot of ln K_D versus 1/T yields straight line for the adsorption of water vapor onto chars and soil minerals at vary temperatures. The ΔH^o and ΔS^o of adsorption are obtained from the slope and intercept of respective plot. The thermodynamic of the adsorption was compared by judging the ΔH^o, ΔS^o and ΔG^o values. The calculation thermodynamic parameters of adsorption were presented in Appendix G.

4. Adsorption properties of char and soil minerals

4.1 Phenol adsorption on char and soil minerals

4.1.1 The adsorbent dosage

The optimum amount of adsorbent was studied by varies amount of adsorbent in range 0.0500 to 1.0000 g. The different amounts of adsorbents were added to the phenol solution (25 ml) with concentration of 100 mg/L. The adsorptions were taken in a set of 50 ml flasks and kept in a shaker of 200 rpm for 5 hours. The flasks were then removed from the shaker and the samples were filtrated through Whatman filter paper (No. 2 and 3) and centrifuge for 15 min. The final concentrations of phenol in the filtrates were determined by UV-Vis spectrophotometer at 270 nm wavelength.

4.1.2 The initial concentration of phenol

The initial concentration of phenol was studied in ranges of 50 to1000 mg/L. The different initial concentration of phenol (25 ml) with the optimum amount of adsorbent were added in a set of 50 ml flasks and kept in a shaker of 200 rpm for 5 hours. The flasks were then removed from the shaker and the samples were filtrated through Whatman filter paper (No. 2 and 3) and centrifuge for 15 min. The final concentrations of phenol in the filtrates were determined by UV-Vis spectrophotometer at 270 nm wavelength.

4.1.3 The contact time

The contact time of phenol on adsorbents were studied at different contact times (1-8 hours). The adsorption was taken in a set of 50 ml flasks and kept in a shaker of 200 rpm, the phenol solution will be collected every 1 hours. The samples were filtrated through Whatman filter paper (No. 2 and 3) and centrifuge for

15 min. The final concentrations of phenol in the filtrates were determined by UV-Vis spectrophotometer at 270 nm wavelength.

4.1.4 Adsorption isotherms

Adsorption isotherms were performed in a set of 50 ml flasks. The solutions of phenol (25 ml) with different initial concentrations and the optimum mass of each adsorbent were placed in these flasks. The adsorptions were kept in a shaker of 200 rpm at 30±2 ^{o}C. The contact time to reach equilibrium of the solid-solution mixture of 4, 6 and 6 were fixed for the adsorption of phenol on bamboo, oil palm shell and coconut shell, respectively. The flasks were then removed from the shaker and the samples were filtrated through Whatman filter paper (No. 2 and 3), the phenol solution was centrifuged for 15 min. The final concentrations of phenol in the filtrates were determined by UV-Vis spectrophotometer at 270 nm wavelength.

4.1.5 Effect of temperature

The effect of temperature on adsorption was performed in a set of 50 ml flasks where solution of phenol (25 ml) with a fixed temperature at 40, 50, and 60 ^{o}C. The instrument is shown in Figure 21. The optimum mass of adsorbent, the concentration of phenol and contact time will be selected from adsorption isotherm of phenol on bamboo, oil palm shell and coconut shell and kept in a water bath shaker of 200 rpm. The flasks were then removed from the shaker and the samples were filtrated through Whatman filter paper (No. 2 and 3) and centrifuge for 15 min. The final concentrations of phenol in the solution were determined by UV-Vis spectrophotometer at 270 nm wavelength.

Afterwards, the Langmuir plots of C_e/q_e against C_e yields straight line for the adsorption of phenol onto chars. The Langmuir constant Q_o and b are obtained from slope and intercept of the respective plot. The Freundlich plots of log q_e versus log C_e yields straight line for the adsorption of phenol onto the chars. The Freundlich constant n and K_F are obtained from the slope and intercept of the respective plot. The

applicability of isotherm models of the adsorption was compared by judging the correlation coefficient (R^2) values. The heat of adsorption plot of $\ln K_D$ versus 1/T yields straight line for the adsorption of phenol onto chars at various temperatures. The ΔH^o and ΔS^o of adsorption are obtained from the slope and intercept of respective plot. The thermodynamic of the adsorption was compared by judging the ΔH^o, ΔS^o and ΔG^o values.

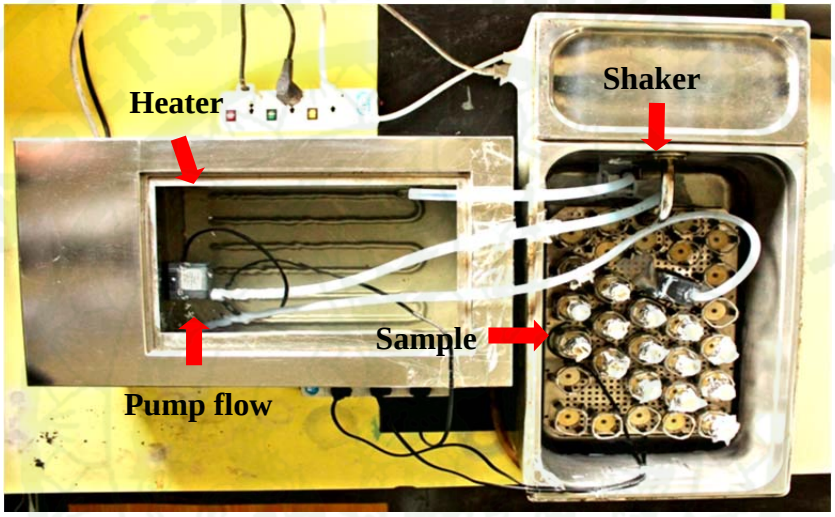

Figure 21 The comprises of instruments to adsorption experiments of phenol and chromium (VI) on char.

4.2 Chromium (VI) adsorption on the chars

4.2.1 The adsorbent dosage

The optimum amount of chars were studied by varies amount of chars in range of 0.0500 to 1.0000 g. The different amounts of chars were added to the chromium (VI) solution (25 ml) with concentration of 50 mg/L and fixed pH 2. The adsorptions were taken in a set of 50 ml flasks and kept in a shaker of 350 rpm for 2 hours. The flasks were then removed from the shaker and the samples were filtrated through Whatman filter paper (No. 2) and centrifuge for 15 min. The final

concentrations of chromium (VI) in the filtrates were determined by UV-Vis spectrophotometer at 420 nm wavelength.

4.2.2 The pH solution

The optimum pH of the solution was studied in the range of 1-4. The pH of solution was adjusted by the addition of 0.01 M H_3BO_3 and 0.01 M $Na_3PO_4.12H_2O$ and $C_6H_8O_7.H_2O$. The optimum amount of adsorbents adding to chromium (VI) solution (25 ml) with concentration of 50 mg/l were taken in a set of 50 ml flasks and kept in a shaker of 350 rpm for 2 hours. The flasks were then removed from the shaker and the samples were filtrated through Whatman filter paper (No. 2) and centrifuge for 15 min. The final concentrations of chromium (VI) in solutions in the filtrates were determined by UV-Vis spectrophotometer at 420 nm wavelength.

4.2.3 The initial concentration of chromium (VI)

The initial concentration of chromium (VI) was studied in ranges of 30 to 400 mg/L. The different initial concentration of chromium (VI) (25 ml), pH 2 with the optimum amount of chars were added in a set of 50 ml flasks, pH of solution about 2 and kept in a shaker of 350 rpm for 2 hours. The flasks were then removed from the shaker and the samples were filtrated through Whatman filter paper (No.2) and centrifuge for 15 min. The final concentrations of chromium (VI) in the filtrates were determined by UV-Vis spectrophotometer at 420 nm wavelength.

4.2.4 The contact time

The contact time of chromium (VI) on chars were studied at different contact time (30-240 min). The adsorption was taken in a set of 50 ml flasks and kept in a shaker of 350 rpm. The chromium (VI) solution will be collected every 30 minute. The flasks were then removed from the shaker and the samples were filtrated through Whatman filter paper (No. 2) and centrifuge for 15 min. The final

concentrations of chromium (VI) in the filtrates were determined by UV-Vis spectrophotometer at 420 nm wavelength.

4.2.5 Adsorption isotherms

Adsorption isotherms were performed in a set of 50 ml flasks. The solutions of chromium (VI) (25 ml) with different initial concentrations pH 2 and the optimum mass of each adsorbent were placed in these flasks. The adsorptions were kept in a shaker of 350 rpm at 30±2 ^{o}C. The contact time to reach equilibrium of the solid-solution mixture of 90, 120 and 180 min were fixed for the adsorption of chromium (VI) on bamboo, coconut shell and oil palm shell, respectively. The flasks were then removed from the shaker and the sample was filtrated through Whatman filter paper (No. 2), the chromium (VI) solution was centrifuged for 30 min. The concentrations of chromium (VI) in the filtrates were determined by UV-Vis spectrophotometer at 420 nm wavelength.

Afterwards, the Langmuir plots of C_e/q_e against C_e yields straight line for the adsorption of chromium (VI) onto chars. The Langmuir constant Q_o and b are obtained from slope and intercept of the respective plot. The Freundlich plots of log q_e versus log C_e yields straight line for the adsorption of chromium (VI) onto the chars. The Freundlich constant n and K_F are obtained from the slope and intercept of respective plot. The applicability of isotherm models of the adsorption was compared by judging the correlation coefficient (R^2) values.

4.3 Chromium (VI) adsorption on the soil minerals

4.3.1 The adsorbent dosage

The optimum amount of soil minerals were studied by varies amount of adsorbent in range 0.0500 to 1.0000 g. The different amounts of soil minerals were added to the chromium (VI) solution (50 ml) with concentration of 50 mg/L and fixed pH 2. The adsorptions were taken in a set of 125 ml flasks and kept in a shaker of 120

rpm for 2 hours. The flasks were then removed from the shaker and the samples were filtrated through Whatman filter paper (No. 2) and centrifuge for 30 min. The final concentrations of chromium (VI) in the filtrates were determined by UV-Vis spectrophotometer at 420 nm wavelength.

4.3.2 The pH solution

The optimum pH of the solution was studied in the range 1-4. The pH of solution was adjusted by the addition of 0.01 M HNO_3 and 0.01 M NaOH. The optimum amount of adsorbents adding to chromium (VI) solution (50 ml) with concentration of 50 mg/l were taken in a set of 125 ml flasks and kept in a shaker of 120 rpm for 2 hours. The flasks were then removed from the shaker and the samples were filtrated through Whatman filter paper (No.1) and centrifuge for 30 min. The final concentrations of chromium (VI) in the filtrates were determined by UV-Vis spectrophotometer at 420 nm wavelength.

4.3.3 The initial concentration of chromium (VI)

The initial concentrations of chromium (VI) were studied in ranges of 30 to 250 mg/L. The different initial concentration of chromium (VI) (50 ml) pH 2 with the optimum amount of soil minerals were added in a set of 125 ml flasks and kept in a shaker of 120 rpm for 2 hours. The flasks were then removed from the shaker and the samples were filtrated through Whatman filter paper (No.1) and centrifuge for 30 min. The final concentrations of chromium (VI) in the filtrates were determined by UV-Vis spectrophotometer at 420 nm wavelength.

4.3.4 The contact time

The contact time of chromium (VI) on soil minerals were studied at different contact time (5-120 min). The adsorption was taken in a set of 125 ml flasks and kept in a shaker of 120 rpm. The chromium (VI) solution will be collected 5, 10, 15, 30, 60, 90 and 120 min. The flasks were then removed from the shaker and the

samples were filtrated through Whatman filter paper (No.1) and centrifuge for 30 min. The final concentrations of chromium (VI) in the filtrates were determined by UV-Vis spectrophotometer at 420 nm wavelength.

4.3.5 Adsorption isotherms

Adsorption isotherms were performed in a set of 125 ml flasks. The solutions of chromium (VI) (50 ml) with different initial concentrations pH 2 and the optimum mass of each adsorbent were placed in these flasks. The adsorptions were kept in a shaker of 120 rpm at 30±2 ^{o}C. The contact time to reach equilibrium of the solid-solution mixture of 30 min. was fixed for the adsorption of chromium (VI) on soil minerals. The flasks were then removed from the shaker and the sample was filtrated through Whatman filter paper (No. 2), the chromium (VI) solution was centrifuged for 15 min. The concentrations of chromium (VI) in the filtrates were determined by UV-Vis spectrophotometer at 420 nm wavelength.

Afterwards, the Langmuir plots of C_e/q_e against C_e yields straight line for the adsorption of chromium (VI) onto soil minerals. The Langmuir constant Q_o and b are obtained from slope and intercept of the respective plot. The Freundlich plots of log q_e versus log C_e yields straight line for the adsorption of chromium (VI) onto the soil minerals. The Freundlich constant n and K_F are obtained from the slope and intercept of respective plot. The applicability of isotherm models of the adsorption was compared by judging the correlation coefficient (R^2) values.

5. Analysis of structure and functional groups of charcoal from agricultural and soil minerals

5.1 Scanning electron micrograph analyses

The surface morphology of char samples and soil minerals were determined by SEM. The samples were scattered on a stub and coated with gold before the analysis.

5.2 Fourier transforms infrared spectrometer (FT-IR)

The char samples and soil minerals were analyzed using FT-IR spectroscopy to study the functional group on the surfaces. The samples were mixed with potassium bromide and the mixture was pressed into pellets to be used in the analysis.

RESULTS AND DISCUSSIONS

1. Analyses of structure and functional group of chars and soil minerals

1.1 Scanning electron micrograph analyses

The surface area and pore structure of chars from bamboo, oil palm shell and coconut shell could be observed by SEM. The SEM micrographs of chars from bamboo, oil palm shell and coconut shell are presented in Figures 22 – 24. The pore sizes of chars from bamboo, oil palm shell and coconut shell were in the range of 0.05 – 5.88 μm. The char from bamboo had a greater number of macropores (0.7 – 4.2 μm) than chars from oil palm shell and coconut shell which it is primary xylem and phloem cells (lateral meristem). The char from oil palm shell had a greater distribution of mesopores and macropore (0.3 – 2.29 μm) which similar to char from coconut shell (0.15 – 0.60 μm). On the other hand, char from coconut shell had a greater number of mesopore than char from oil palm shell. Generally, the coconut shell based carbon will have a predominance of pore in the micropore range and these accounts for 95% of the available internal surface area (Cameron Carbon Incorporated, 2006).

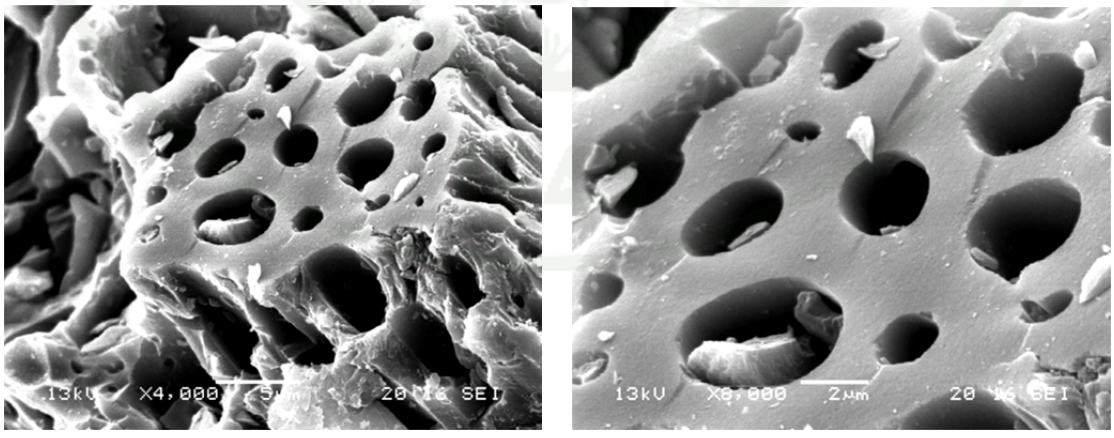

(a) (b)

Figure 22 The SEM image of (a) char from bamboo (4000x) and (b) bamboo (8000x).

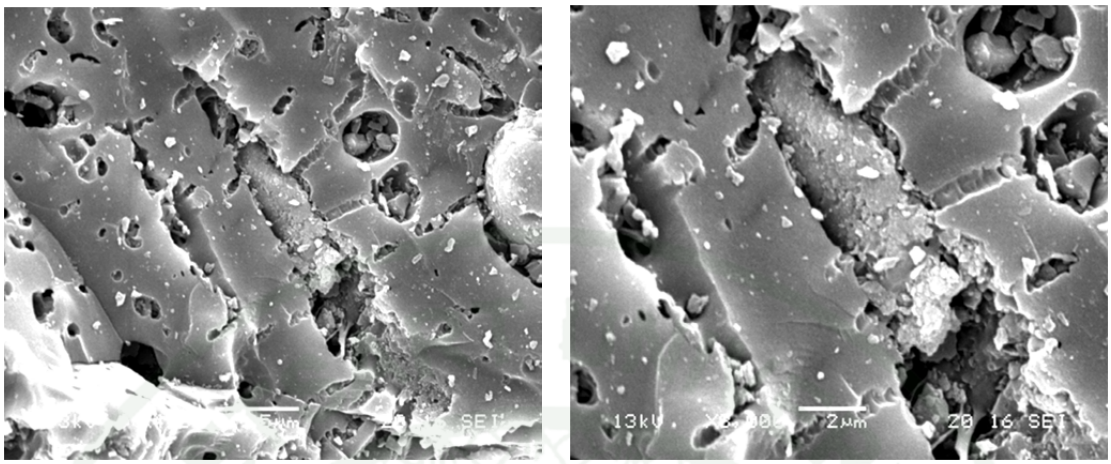

(a) (b)

Figure 23 The SEM micrograph of (a) char from oil palm shell (4000x) and (b) oil palm shell (8000x).

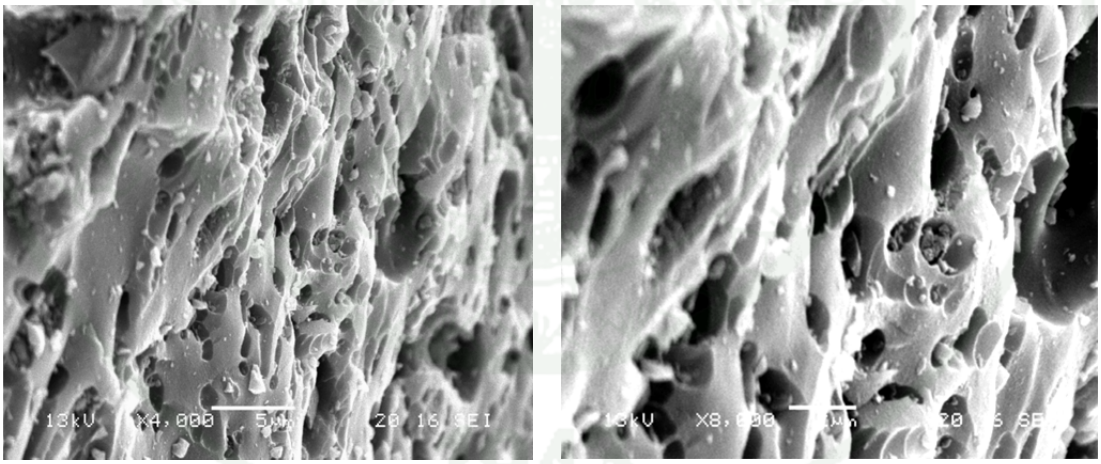

(a) (b)

Figure 24 The SEM image of (a) char from coconut shell (4000x) and (b) coconut shell (8000x).

1.2 Fourier Transform Infrared Spectroscopy (FT-IR) analyses

The different in the adsorption of chars and soil minerals might be attributed from functional group on surface area that could enhance the adsorption. Therefore, the functional groups on surface were studied by FT-IR. The band assignments of chars from bamboo, oil palm shell and coconut shell are shown in Table 5. And the band assignments of bentonite and montmorillonite K10 are shown in Table 6.

Table 5 Band assignments for FT-IR spectra.

Functional group	Wavenumber (cm^{-1})
Hydroxyl group (O-H Stretching, ROH)	3,450 - 3,350
Alkane (C-H Stretching)	2,950 – 2,800
Aromatic (C-C Stretching)	
Asymmetric and symmetric carboxylate ((C-O) Stretching)	1,580 – 1,540
Alkane (C-H Bending)	
Alcoholic (C-O Stretching)	1,200 – 1,050

Source: Pavia *et al.* (2001)

The FT-IR spectra and their assigned peaks of all chars were presented in Appendix A and Table 5, respectively. A board peak in the range of 3,450 – 3,350 cm^{-1} was attributed to O-H stretching vibration of hydroxyl group which it is the water on surface of chars. A very weak group and broad peak in range of 1,580 – 1,540 cm^{-1} were attributed to the aromatics could be observed through C–C stretching vibration. However, the spectrum of chars from bamboo, oil palm shell and coconut shell were difficult to assign because of all chars had a hard of structure. In term of hardness is somewhat difficult to measure on vibrational of carbonaceous by FT-IR spectroscopy because of the cross link structure of graphite or non-graphite is strictly

in the chars. In addition, the interlayer spacing in graphite is parallel with the interlayer spacing the non-graphite. The interlayer spacing in non-graphite carbon is 3.44 Å and graphite is 3.354 Å (March, 1992). The FT-IR spectroscopy was used to determine the fundamental vibration frequency. Which the results FT-IR spectra is not found the C– C or C=C of carbonaceous because the structure of chars was stricken of the carbonaceous.

Table 6 Band assignments for FT-IR spectra of soil minerals.

Functional group	Wavenumber (cm^{-1})
Aluminum hydroxide (Al-OH Stretching)	3,620
Hydroxyl group (O-H Stretching)	3,450 – 3,350
Silicon aluminum oxide (Si-O-Al Stretching)	2,911 – 2,838
Aluminum magnesium hydroxide (Al-Mg-OH Stretching)	1,673
Silicon oxide (Si-O Stretching)	1,191 – 1,036
Silicon hydroxide (Si-OH Bending)	915
Silicon oxide (Si-O-Si Bending)	
Silicon aluminum oxide (Si-O-Al Bending)	
Silicon magnesium oxide (Si-O-Mg Bending)	
Silicon oxide (Si-O Bending)	842 – 795
Aluminum magnesium hydroxide (Al-Mg-OH Bending)	623 – 465

Source: Vlasova *et al.* (2003)

The FT-IR spectra and their assigned peaks of all chars were presented in Appendix A and Table 6, respectively. The FT-IR spectra of bentonite and montmorillonite showed a weak band at 3,624 $cm^{-1}$was due to lattice hydroxyls OH stretching. The broad band at 3,392 cm^{-1} can be attributed to the H-O-H stretching vibration of H_2O. This band reflected the free H_2O adsorbed onto the structure of montmorillonite clay. Montmorillonite is typical for smectite with high amount of Al

in the octahedral. The band near 1,636 cm^{-1} and 1,664 cm^{-1} were due to the water of crystallization bending vibration. The Si-O-Si stretching vibration appeared near 1,004-1,036 cm^{-1} as a strong band. The 793 cm^{-1} band were due to Al-OH vibration.

Table 7 The FT-IR results of chars from bamboo, oil palm shell and coconut shell.

Sample	Wavenumber (cm^{-1})					
	3,450 – 3,350	2,950 – 2,800	1,750 – 1,650	1,580 – 1,540	1,400 – 1,000	800 – 400
Bamboo	(-)	(-)	broad, very weak 1,655	broad, very weak 1,560	(-)	(-)
Oil palm shell	broad, very weak 3,448	(-)	very weak 1,655	very weak 1,560	very weak 1,384	(-)
Coconut shell	broad 3,442	(-)	(-)	broad 1,540	(-)	(-)

Table 8 The FT-IR results of bentonite and montmorillonite K10.

Sample	Wavenumber (cm^{-1})						
	3,620 – 3,350	2,950 – 2,800	1,750 – 1,300	1,200 – 1,000	915– 840	800 – 400	623 – 450
Bentonite	broad, weak 3,624	(-)	weak 1,637	very weak ,very strong 1,121, 1,005	(-)	broad, weak 794	(-)
Montmorillonite K10	broad, very weak 3,392	(-)	weak 1,647	very strong 1,036	(-)	medium 794	(-)

2. Adsorption properties of chars and soil minerals

2.1 Water vapor adsorption

2.1.1 Amount of adsorbed water vapor onto chars and soil minerals.

The results founded that at high relative pressures ($P/P^0 > 3.01$) the adsorption of water vapor on chars from bamboo, oil palm shell and coconut shell have similar character which are not statistically significant difference at the 5% level. The char from coconut shell show a higher water vapor uptake at low relative pressure compared to other chars. Amount of adsorption water vapor onto chars and soil minerals at various relative pressures, P/P^0 are shown in Figure 25. The amounts of water vapor uptake on all chars are increase with increasing the relative pressures. The amounts of water vapor on chars are shown in Table 9.

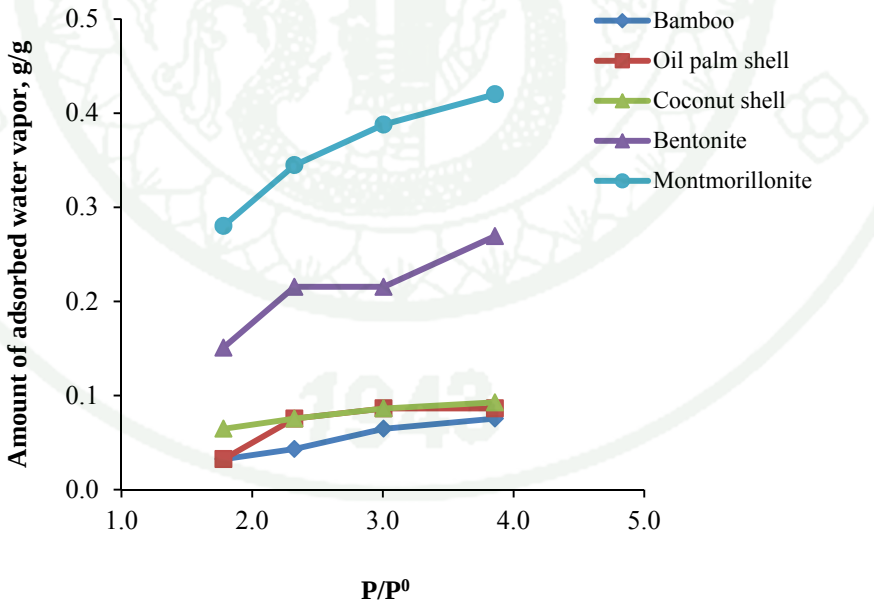

Figure 25 The adsorption of water vapor onto chars and soil minerals at various relative pressures.

The adsorption of water vapor on the chars from bamboo, oil palm shell and coconut shell was occurred on the surface and pore structure. At the water vapor pressured is an increase, the adsorption increased by the formation of hydrogen bond with the adsorbed molecules. The formation of cluster of water molecular located around the primary adsorption center (Foley *et al.,* 1997)

Table 9 The amount of adsorbed water vapor onto chars and soil minerals.

Relative pressure (10^3 torr)	The amount of uptake water vapor (g/g)				
	Bamboo	Oil palm shell	Coconut shell	Bentonite	Montmorillonite
1.780	0.0323±0.000	0.0323±0.000	0.0646±0.000	0.1508±0.057	0.2801±0.057
2.323	0.0431±0.028	0.0754±0.028	0.0754±0.028	0.2154±0.028	0.3447±0.028
3.005	0.0646±0.000	0.862±0.028	0.0862±0.028	0.2154±0.028	0.3878±0.086
3.858	0.0754±0.028	0.0862±0.028	0.0926±0.040	0.2693±0.028	0.4201±0.050

2.1.2 Adsorption isotherm of water vapor onto chars and soil minerals.

The adsorption isotherm indicated the adsorption molecules distribute between the vapor phases and the solid phase when the adsorption process reaches an equilibrium state. The analysis of the isotherm data by fitting them to different isotherm models was an important step to find the suitable model that could be used for the design purposes.

Adsorption isotherm study was carried out on two well-known isotherm models which were Langmuir and Freundlich isotherm. Langmuir isotherm assumes monolayer adsorption onto a surface containing a finite number of adsorption sites of uniform strategies of adsorption with no transmigration of adsorbate in the plane of surface. Meanwhile, Freundlich isotherm model assumed heterogeneous surface energies. The applicability of the isotherm models to the adsorption study was compared by judging the correlation coefficient (R^2) values.

Figures 26-35 showed the Langmuir plots of x/m versus P/P^0 and Freundlich plots of log x/m versus log P/P^0 for the adsorption of water vapor onto the chars and soil minerals.

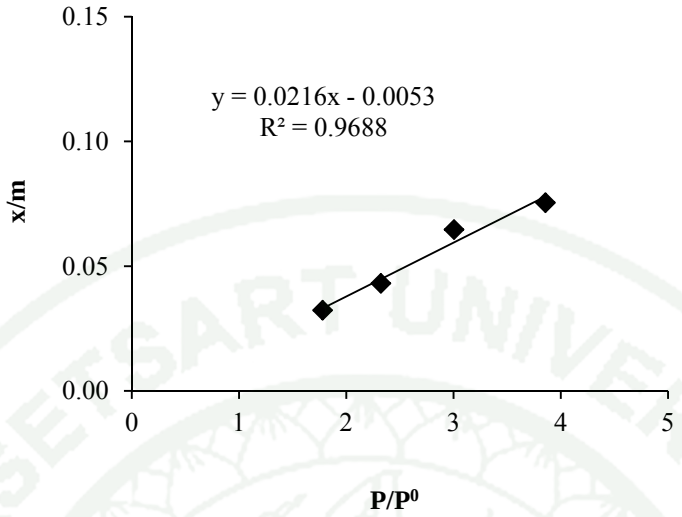

Figure 26 The Langmuir isotherm of water vapor onto char from bamboo.

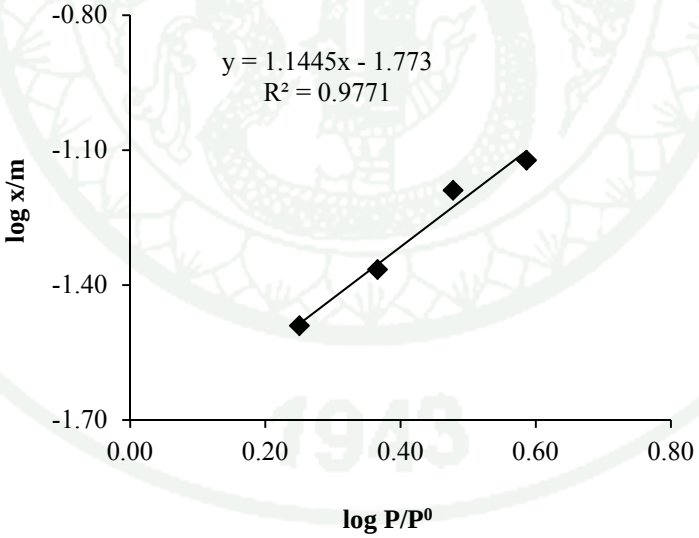

Figure 27 The Freundlich isotherm of water vapor onto char from bamboo.

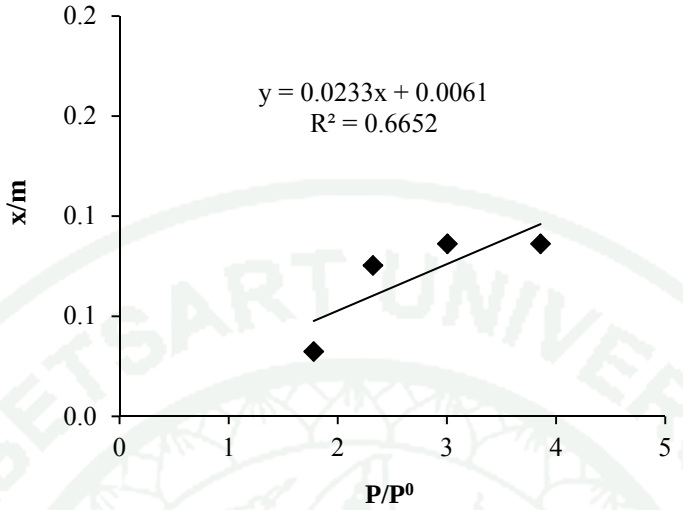

Figure 28 The Langmuir isotherm of water vapor onto char from oil palm shell.

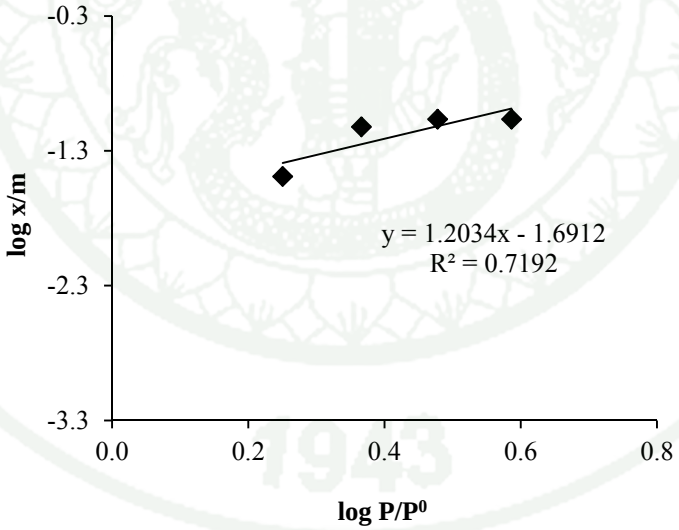

Figure 29 The Freundlich isotherm of water vapor onto char from oil palm shell.

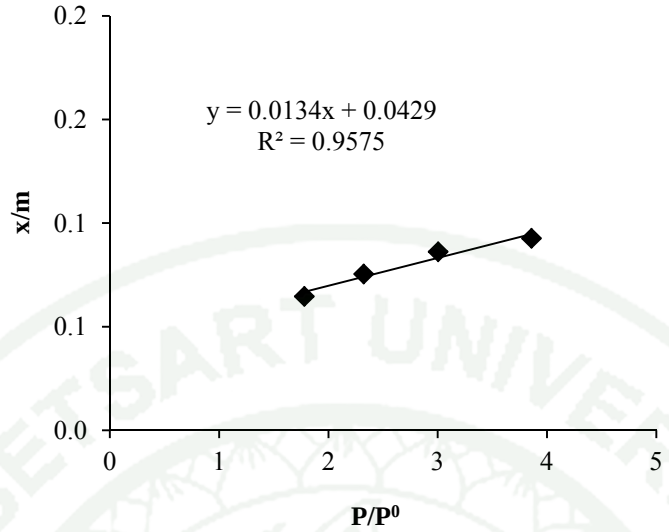

Figure 30 The Langmuir isotherm of water vapor onto char from coconut shell.

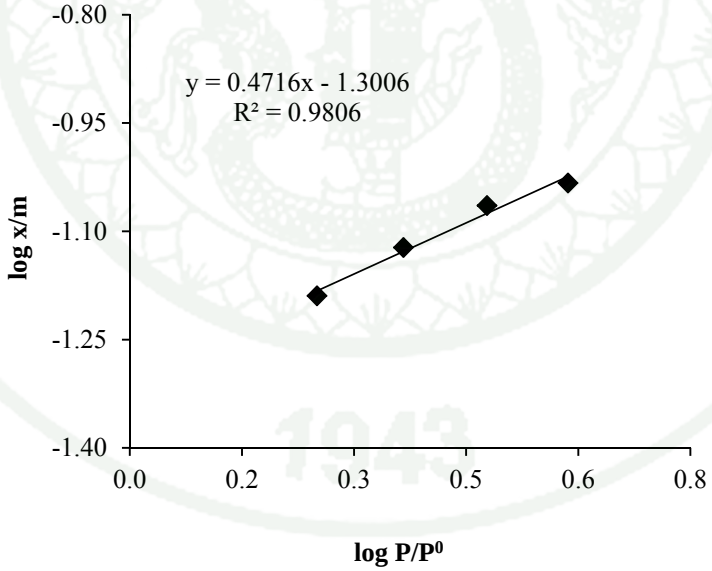

Figure 31 The Freundlich isotherm of water vapor onto char from coconut shell.

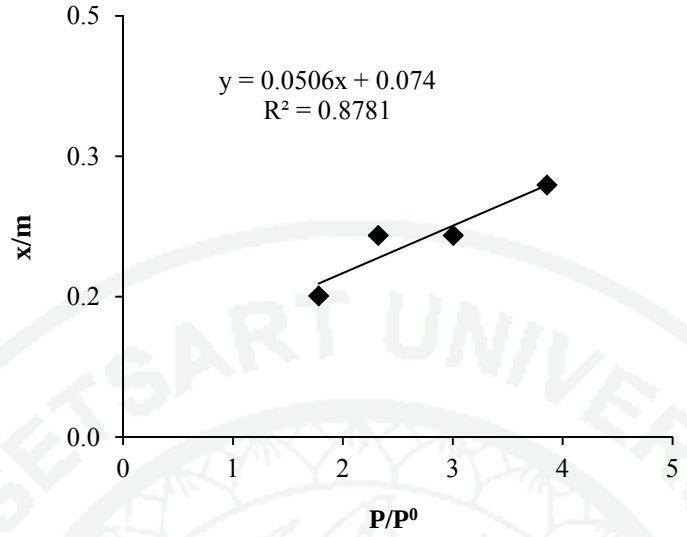

Figure 32 The Langmuir isotherm of water vapor onto bentonite.

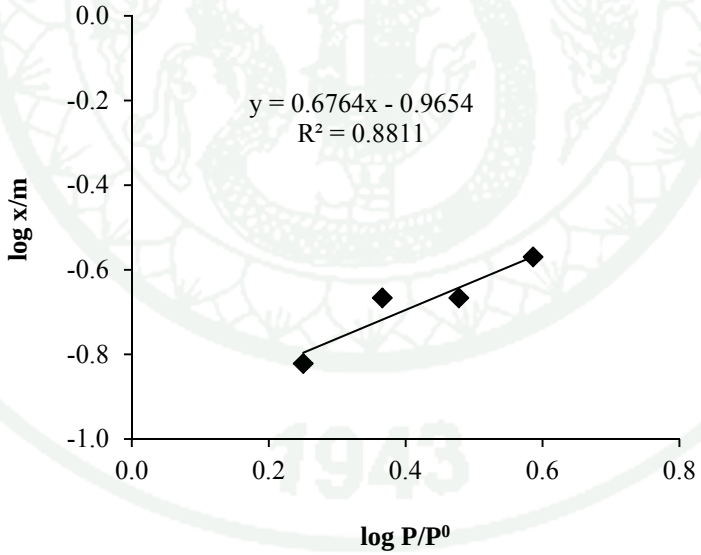

Figure 33 The Freundlich isotherm of water vapor onto bentonite.

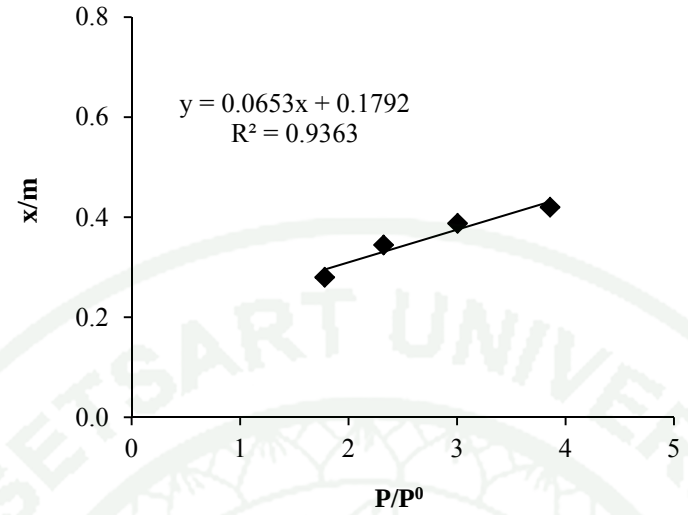

Figure 34 The Langmuir isotherm of water vapor onto montmorillonite K10.

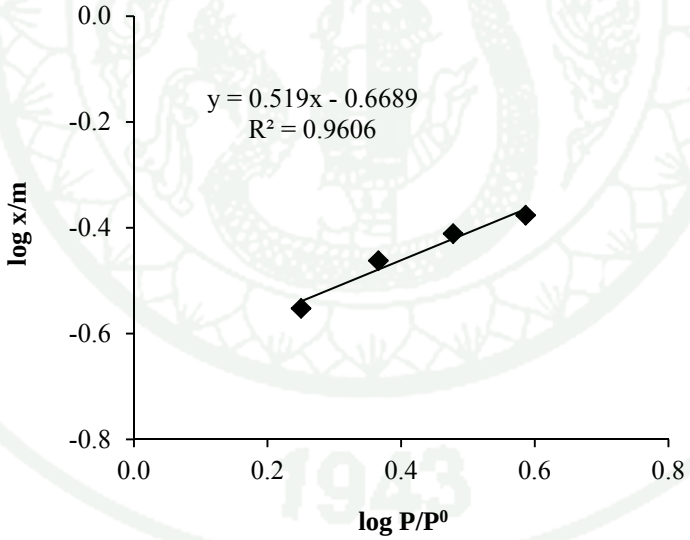

Figure 35 The Freundlich isotherm of water vapor onto montmorillonite K10.

The Langmuir and Freundlich adsorption isotherm constant for water vapor adsorption are given in Table 10. Apparently, the fitting to the Langmuir adsorption isotherm model was similar in comparison to the Freundlich model according to R^2 values. Therefore, the type of adsorption multilayer coverage of water molecules onto surface of chars from bamboo, oil palm shell, coconut shell, bentonite and montmorillonite K10. The Langmuir constants showed that the Q_0 of char from coconut shell was the highest when compared chars from bamboo and oil palm shell. The Q_0 value of montmorillonite is closely with bentonite. On the other hand, the b value of chars from bamboo and oil palm shell were a higher than that of char from coconut shell. And the b value of bentonite was closely with montmorillonite. For Langmuir constants indicate that the chars from bamboo and oil palm shell had the higher adsorption energy for adsorption monolayer. The Freundlich constants showed that the all n value was in the range of 0.8– 2.1. For the n value indicates that char from coconut shell is favorable multilayer adsorption of water vapor (char from coconut shell is 0.2120), compared to chars from bamboo and oil palm shell. However, the K_F value of char from oil palm shell was similar with bamboo which the K_F value of they were lower than char from coconut shell. The K_F value indicating that the char from coconut had the highest adsorption capacity. Furthermore, the Freundlich constants showed that the n value of bentonite was similar with montmorillonite. On the other hand, the K_F value of montmorillonite was higher than the bentonite which indicating that the montmorillonite had a higher adsorption capacity.

For the results, the Q_0 and K_F value indicating that the adsorption of water vapor on char from coconut shell had a higher than chars from bamboo and oil palm shell. The highest adsorption of water vapor on char from coconut shell was considered to the pores structure on the surface of itself compared to the chars from bamboo and oil palm shell. Because of the char from coconut shell had a high amount of mesoporosity. Mesopores in the adsorbent provide more room to allow multilayer adsorption of water vapor molecules (Lee and Reucroft, 1999). Thus the adsorption of water molecules was occurred to capillary condensation on pore structure of chars.

Furthermore, the K_F and n values for Freundlich isotherm indicate that the montmorillonite had a higher adsorption than the bentonite. The quantities of adsorbed water vapor on soil minerals are dependent on the interlayer cation which the adsorption of water vapor onto Na-montmorillonite was a higher than the Ca-montmorillnite (Salles *et al.*, 2009). The bentonite is Ca-bentoonite type which it is non-swelling type. Therefore, montmorillonite had a high water vapor adsorption amount because interlayer structure of montmorillonite can be swelling more than the bentonite. The Ca-montmorillonite had a limited swelling to a maximum interlayer spacing of 19 Angstrom (Theng, 1974). The Na-montmorillnite is not limited and the interlayer spacing can range from 10 Angstrom (oven-dry) to over 50 Angstrom (Theng, 1974). The highest swelling is characteristic of sodium-montmorillonite.

Table 10 Langmuir and Freundlich isotherm constants for water vapor.

Sample	Langmuir isotherm			Freundlich isotherm		
	Q_0 (mg/g)	b (L/mg)	R^2	n	K_F (mg/g)	R^2
Bamboo	46.296	4.075	0.968	0.874	0.0169	0.977
Oil palm shell	42.918	3.817	0.665	0.831	0.0204	0.719
Coconut shell	74.627	0.313	0.957	2.120	0.0500	0.980
Bentonite	19.763	0.685	0.878	1.479	0.1083	0.880
Montmorillonite	15.314	0.365	0.936	1.927	0.2143	0.961

2.2 Phenol adsorption

2.2.1 The optimization of adsorbent dosage

The adsorbent dosage on the adsorption of phenol was studied by varies doses of chars from bamboo, oil palm shell and coconut shell in range of 0.0500 – 1.000 g. The phenol concentration of 100 mg/L, contact time at 8 hours and the results were shown in Figure 36. The adsorptions of phenol onto chars found that the optimization dosages of chars from bamboo and coconut shell were 0.5000 g, and char from oil palm shell was 0.2500 g.

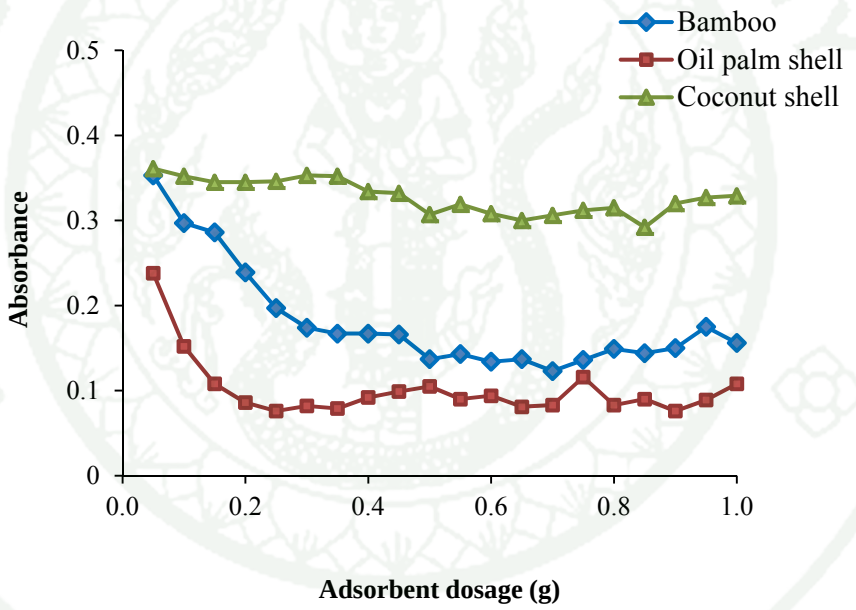

Figure 36 The adsorption of phenol onto chars by varies adsorbent in range of 0.0500 - 1.0000 g.

2.2.2 The optimization of initial concentration of phenol

The initial concentration of phenol adsorption on chars from bamboo, oil palm shell and coconut shell were studied in range of 50 – 1,000 mg/L, contact time 8 hours and fixed the optimization of adsorbent dosage are shown in Figure 37 and 38. The results found that the optimization of initial concentration of phenol adsorption on chars from bamboo and oil palm shell were used in range of 300 – 500 mg/L. The char form coconut shell was used in range of 800 -1,000 mg/L.

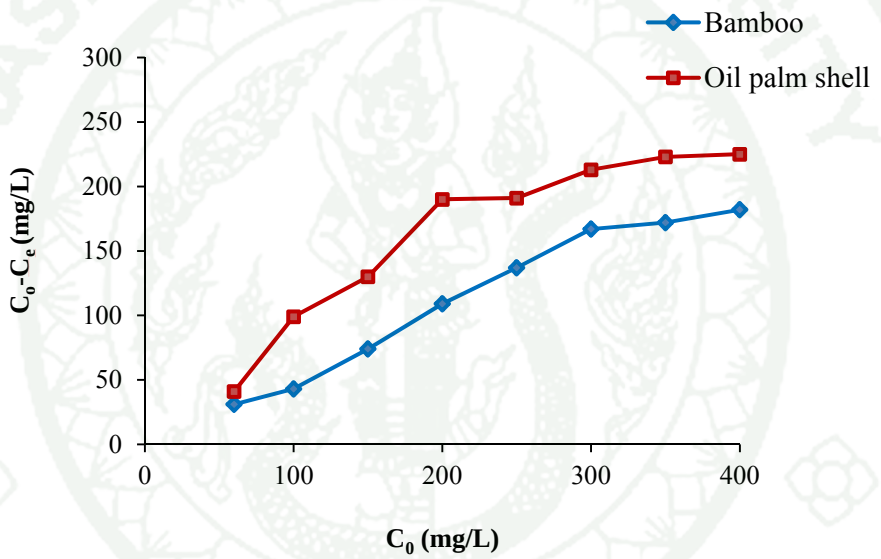

Figure 37 The adsorption of phenol onto chars from bamboo and oil palm shell by varies concentrations in rang of 50 – 400 mg/L.

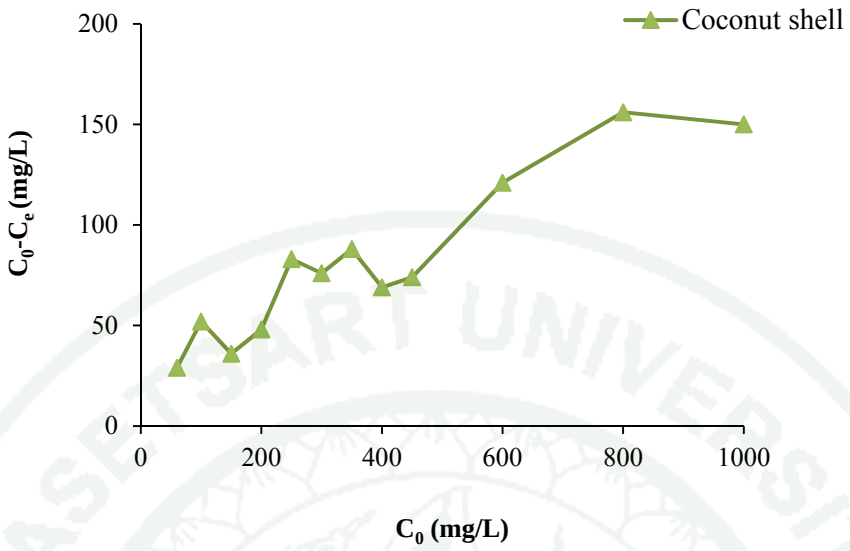

Figure 38 The adsorption of phenol onto char from coconut shell by varies concentrations in rang of 50 – 1,000 mg/L.

2.2.3 The optimization of contact time for adsorption of phenol

The optimization of contact time of phenol adsorption on chars from bamboo, oil palm shell and coconut shell were studied at different contact time from 1 – 8 hours by fixed the optimization of adsorbent dosage and fixed optimization of initial concentration of phenol are shown in Figure 39. The results shown that the optimization of contact time for adsorption of phenol on char from bamboo was found at 4 hour, the chars from oil palm shell and coconut shell were found at 6 hours.

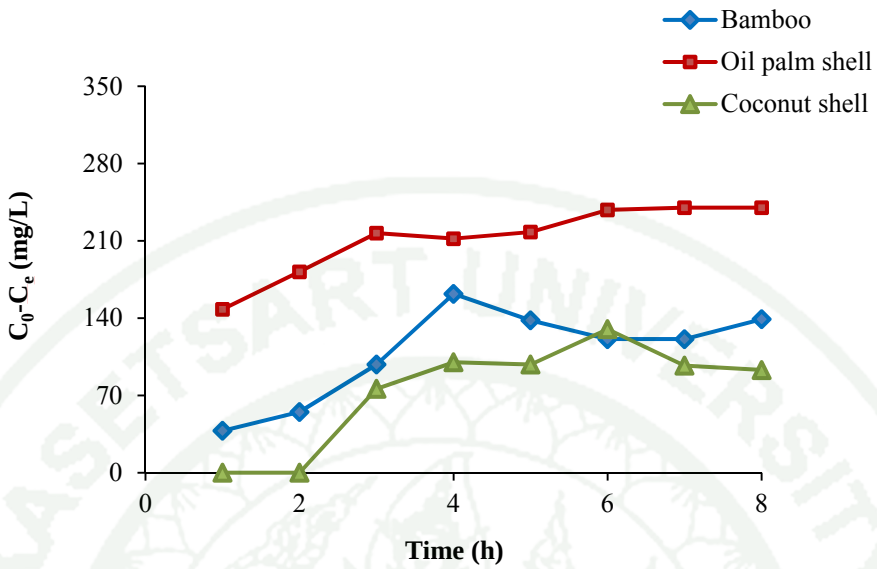

Figure 39 The adsorption of phenol onto chars by varies contact time in range from 1 – 8 hours.

2.2.4 Adsorption isotherm of phenol onto chars.

Figures 40 – 45 showed that Langmuir plots of C_e/q_e versus C_e and Freundlich plots of log q_e versus log C_e for the adsorption of phenol onto the chars from bamboo, oil palm shell and coconut shell.

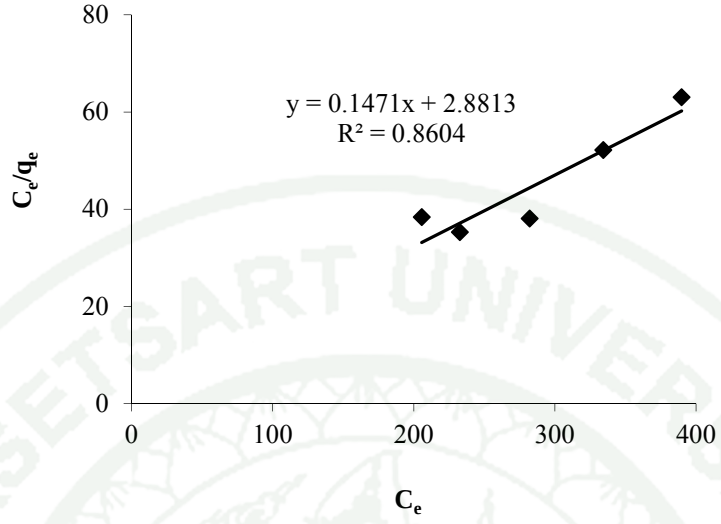

Figure 40 The Langmuir isotherm of phenol adsorption onto char from bamboo.

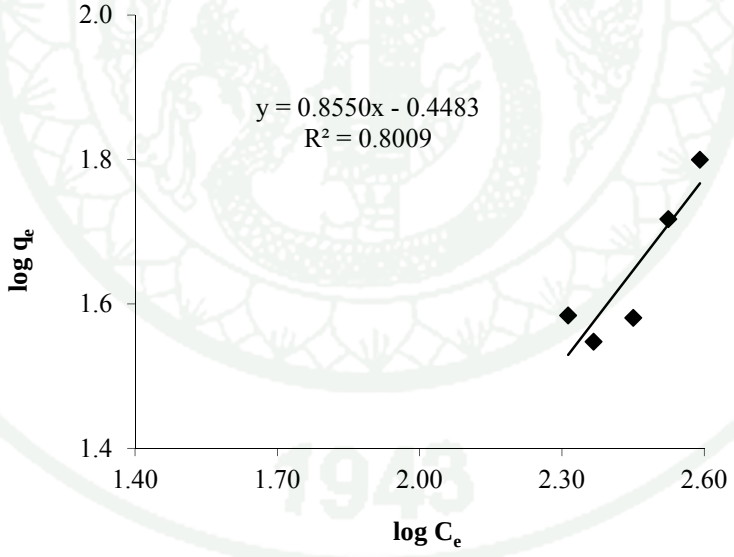

Figure 41 The Freundlich isotherm of phenol adsorption onto char from bamboo.

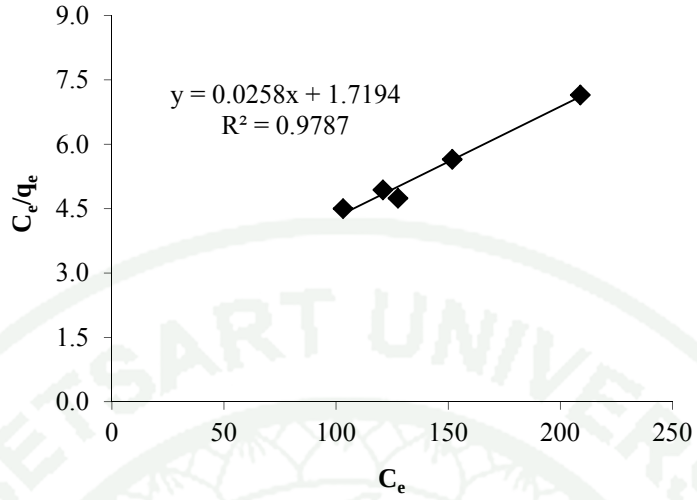

Figure 42 The Langmuir isotherm of phenol adsorption onto char from oil palm shell.

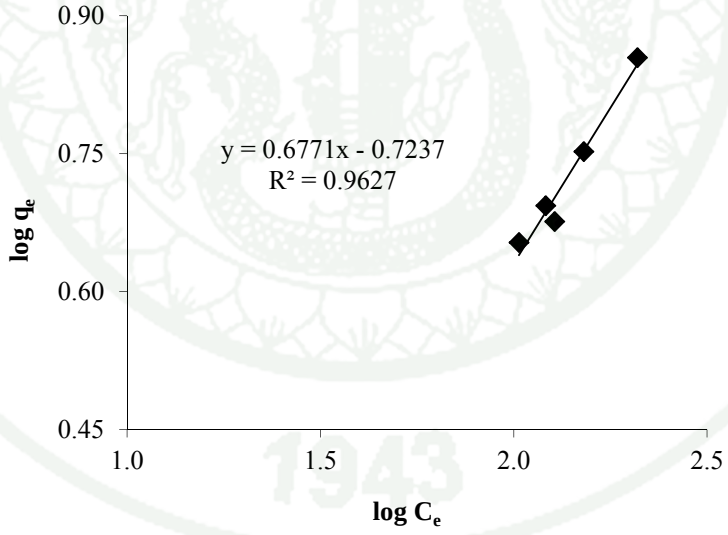

Figure 43 The Freundlich isotherm of phenol adsorption onto char from oil palm shell.

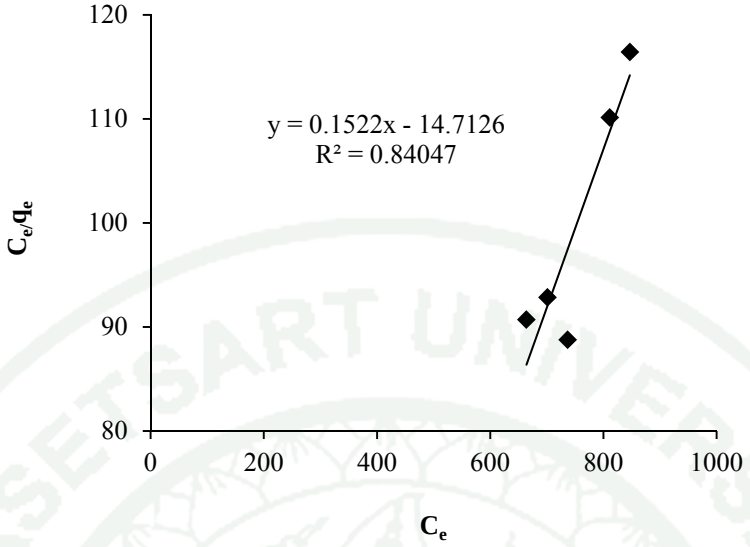

Figure 44 The Langmuir isotherm of phenol adsorption onto char from coconut shell.

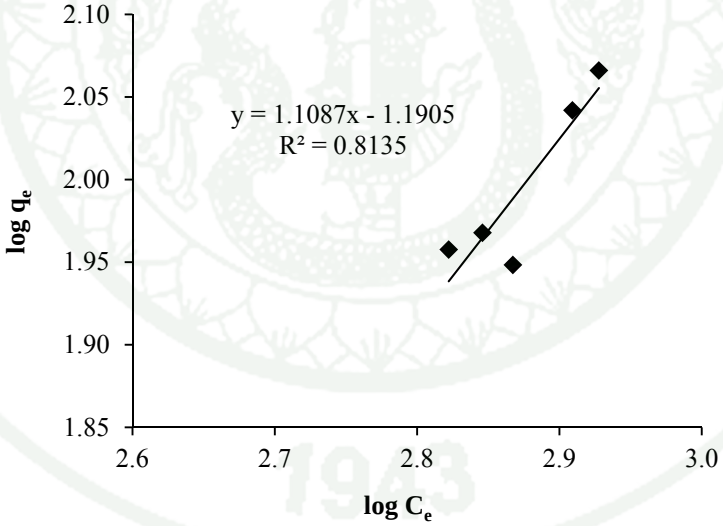

Figure 45 The Freundlich isotherm of phenol adsorption onto char from coconut shell.

The Langmuir and Freundlich adsorption isotherm parameters for phenol adsorption of chars were given in Table 11. It could be implied that sorption data were better fitted with Langmuir adsorption isotherm model than Freundlich model according to R^2 value. Therefore, the type of adsorption was monolayer coverage of phenol molecules onto surface of chars. The Langmuir constants, char from oil palm shell had the highest Q_0 value (38.7596 mg/g) which compared to other chars. However, the Q_0 value of chars from bamboo (6.9780 mg/g) and coconut shell (6.5677 mg/g) was lower than of oil palm shell. Furthermore, the b value of char from bamboo was similar with chars from oil palm shell and coconut shell which indicated that the all chars had the highest adsorption energy. However, the Freundlich constants showed that the K_F value of char from bamboo was a higher that of chars from oil palm shell and coconut shell. For the K_F value indicated that the char from bamboo had the highest adsorption capacity follow in the Freundlich isotherm. Furthermore, the n value of all chars were in the range of 0.9 – 1.4. Which the n value of char from bamboo was similar with chars from oil palm shell and coconut shell. The n value indicated that the all chars had the highest adsorption energy.

The adsorption of phenol onto soil minerals founded that the phenol not adsorbed on the surface of soil minerals. Because of the phenol molecules compete with water molecules for montmorillonite interlayer surfaces. Adsorption of phenol on soil minerals takes place only on the external surface.

The surface area of soil minerals are the major constituents of Alumina (Al_2O_3) and silica (SiO_2). Structurally, silica is described as composed of SiO_4 tetrahedral in which each oxygen atom is shared between two adjacent tetrahedral. The Si-O bond is around 50% ionic due to the large difference in the electronegativity of oxygen and silicon (Kumar *et al.*, 1978). Thus, it not adsorbed the phenol molecules, which are polar molecules.

Table 11 Langmuir and Freundlich isotherm constants for phenol.

Sample	Langmuir isotherm			Freundlich isotherm		
	Q_0 (mg/g)	b (L/mg)	R^2	n	K_F (mg/g)	R^2
Bamboo	6.7980	0.0510	0.860	1.1696	0.3562	0.800
Oil palm shell	38.7596	0.0150	0.978	1.4769	0.1889	0.962
Coconut shell	6.5677	0.0130	0.840	0.9019	0.0645	0.813

Table 12 The specific surface area of samples for adsorption of phenol.

Sample	Specific surface area (m^2/g)
Bamboo	22.70
Oil palm shell	129.42
Coconut shell	21.57

According to the Langmuir isotherm in case of phenol, this pointed out the fact that phenol adsorption was the mono-layered adsorption, in which the specific surface area could be calculated by replacing the Q_0 value as shown in Table 11 on the equation 12. The obtained specific surface area of char from bamboo, oil palm shell and coconut shell were in the range of 21.57 – 129.42 m^2/g. The specific surface area value reflected the phenol adsorption ability of the chars, in that, the higher this value, the more adsorption ability. In case of char from bamboo, it had the highest adsorption ability although its specific surface area was lower than the specific surface area of chars from oil palm shell which may due to the multi-layered adsorption on the surface area of char from bamboo.

2.2.5 Adsorption isotherm of phenol onto chars at various temperature.

Figures 46 – 63 showed that Langmuir plots of C_e/q_e versus C_e and Freundlich plots of log q_e versus log C_e for the adsorption of phenol onto the chars from bamboo, oil palm shell and coconut shell.

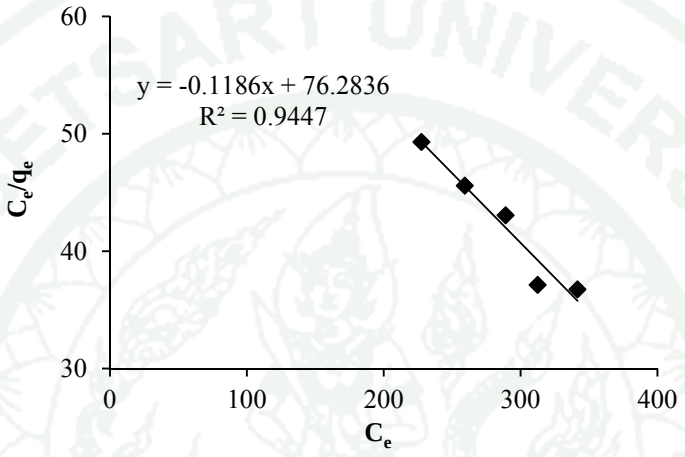

Figure 46 The Langmuir isotherm of phenol adsorption onto char from bamboo at temperature 40 °C.

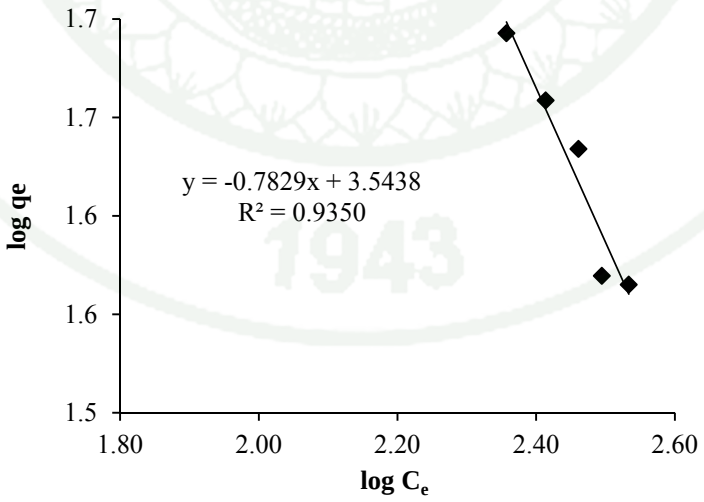

Figure 47 The Freundlich isotherm of phenol adsorption onto char from bamboo at temperature 40 °C.

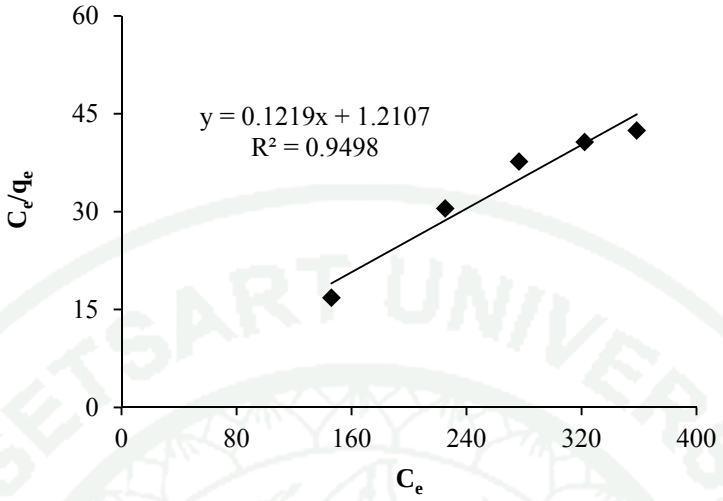

Figure 48 The Langmuir isotherm of phenol adsorption onto char from bamboo at temperature 50 ^{o}C.

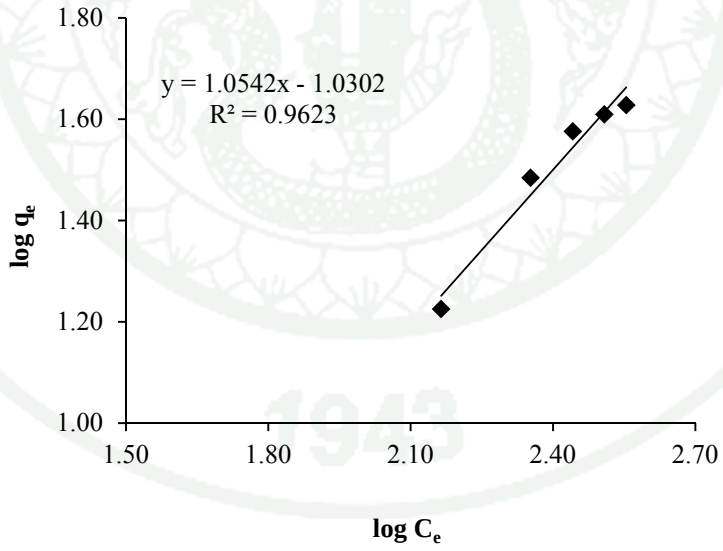

Figure 49 The Freundlich isotherm of phenol adsorption onto char from bamboo at temperature 50 ^{o}C.

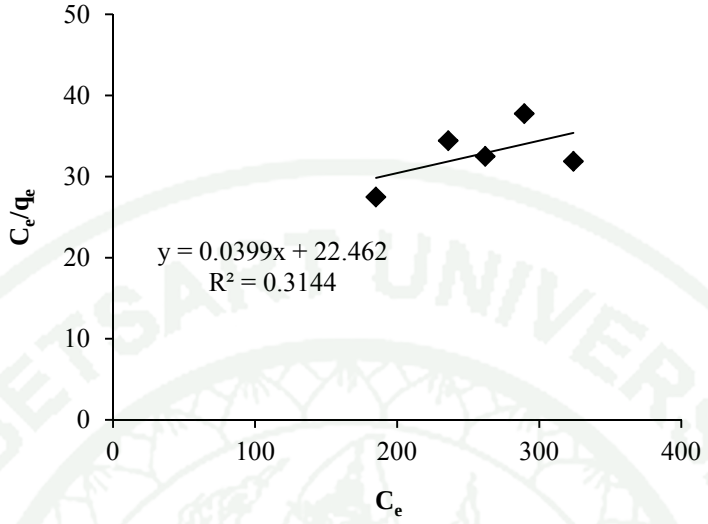

Figure 50 The Langmuir isotherm of phenol adsorption onto char from bamboo at temperature 60 ^{o}C.

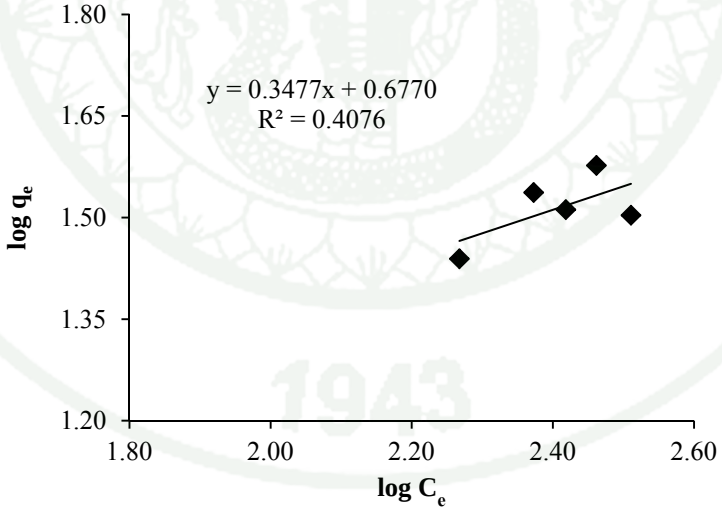

Figure 51 The Freundlich isotherm of phenol adsorption onto char from bamboo at temperature 60 ^{o}C.

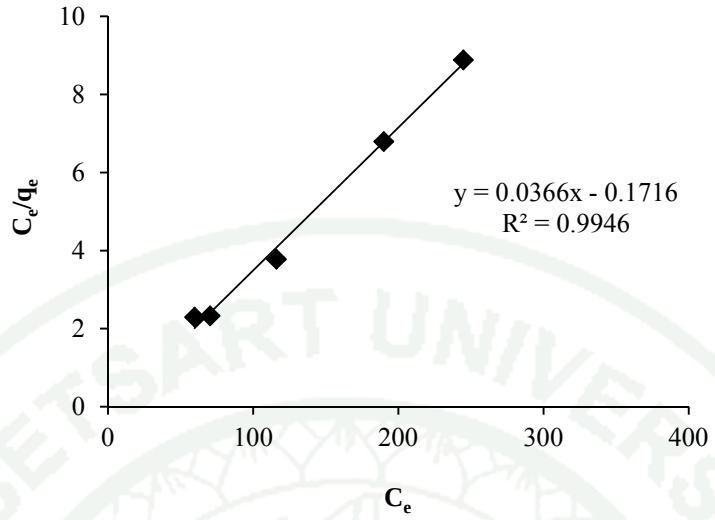

Figure 52 The Langmuir isotherm of phenol adsorption onto char from oil palm shell at temperature 40 ^{o}C.

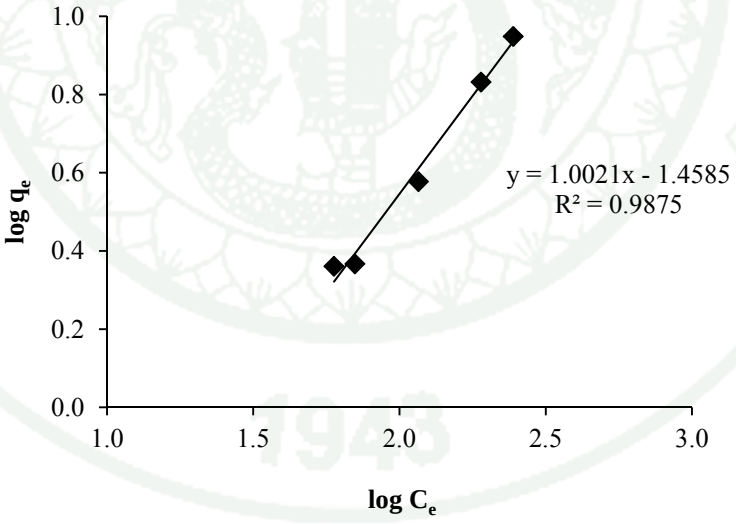

Figure 53 The Freundlich isotherm of phenol adsorption onto char from oil palm shell at temperature 40 ^{o}C.

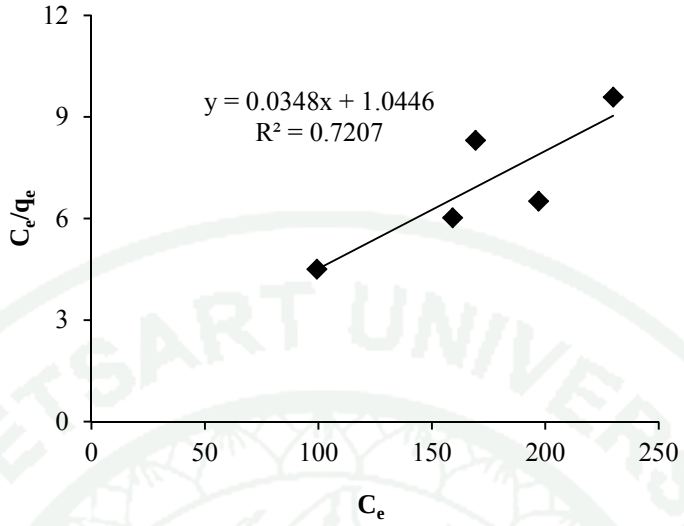

Figure 54 The Langmuir isotherm of phenol adsorption onto char from oil palm shell at temperature 50 ^{o}C.

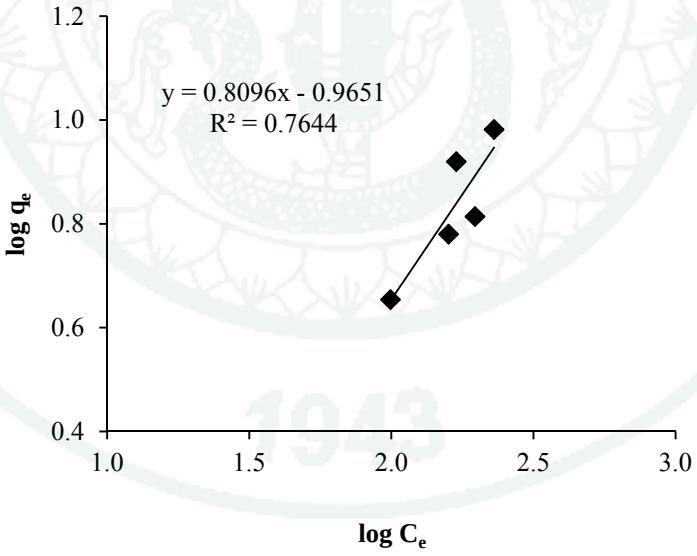

Figure 55 The Freundlich isotherm of phenol adsorption onto char from oil palm shell at temperature 50 ^{o}C.

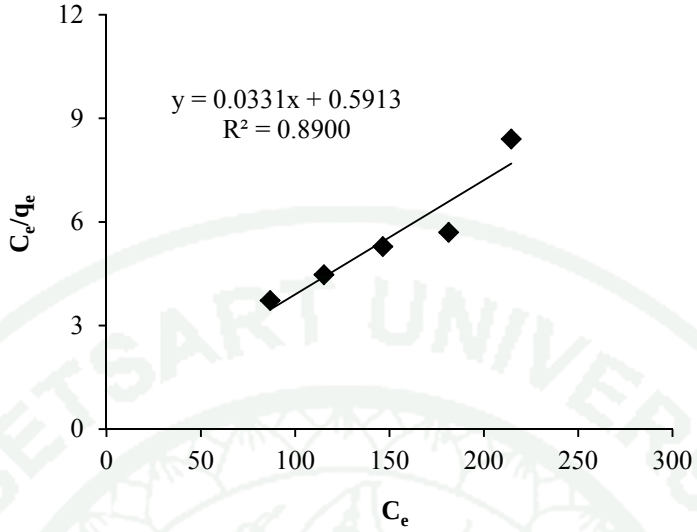

Figure 56 The Langmuir isotherm of phenol adsorption onto char from oil palm shell at temperature 60 °C.

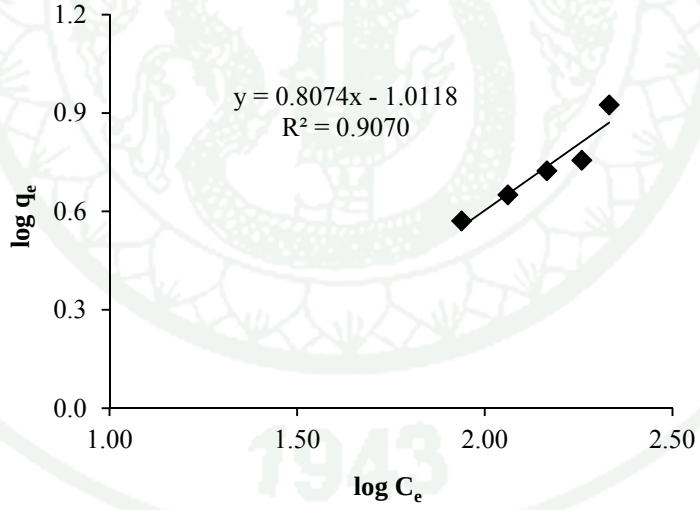

Figure 57 The Freundlich isotherm of phenol adsorption onto char from oil palm shell at temperature 60 °C.

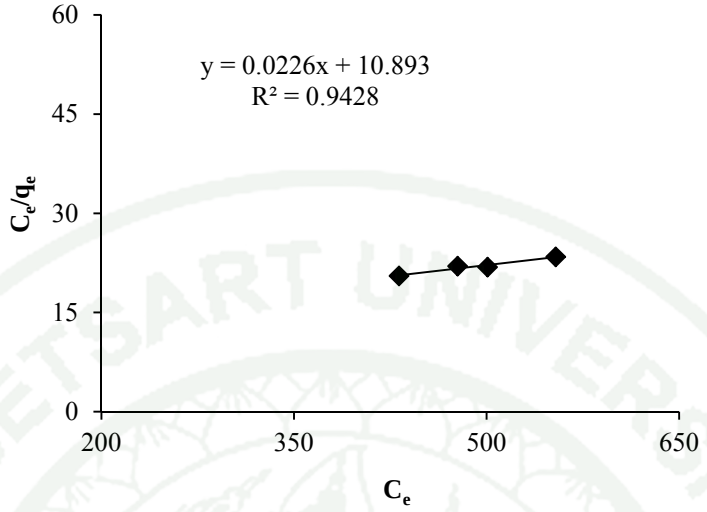

Figure 58 The Langmuir isotherm of phenol adsorption onto char from coconut shell at temperature 40 °C.

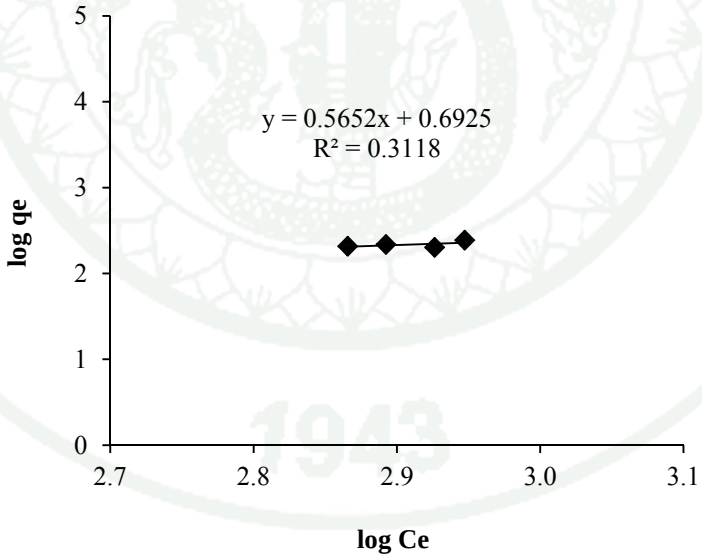

Figure 59 The Freundlich isotherm of phenol adsorption onto char from coconut shell at temperature 40 °C.

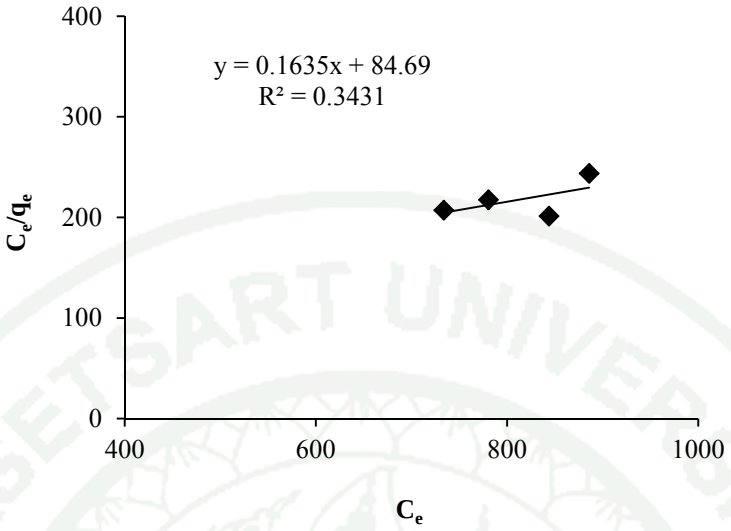

Figure 60 The Langmuir isotherm of phenol adsorption onto char from coconut shell at temperature 50 °C.

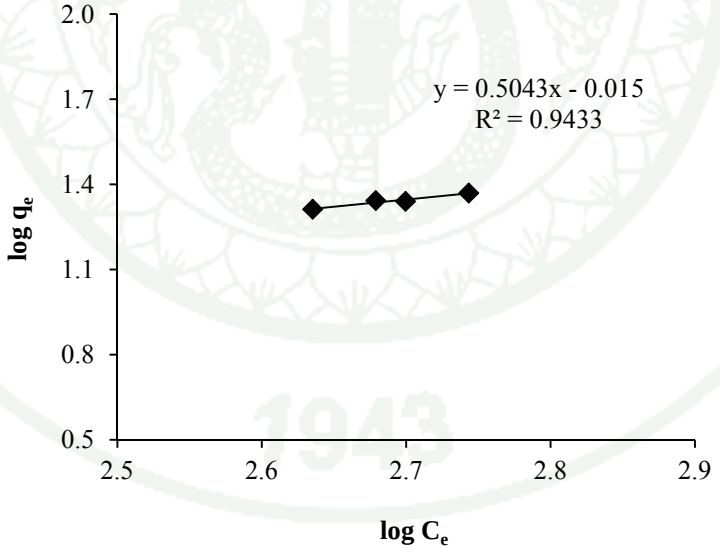

Figure 61 The Freundlich isotherm of phenol adsorption onto char from coconut shell at temperature 50 °C.

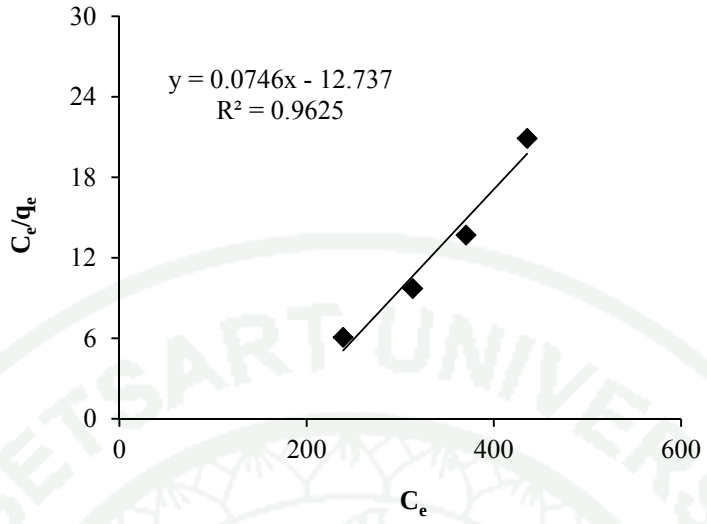

Figure 62 The Langmuir isotherm of phenol adsorption onto char from coconut shell at temperature 60 ^{o}C.

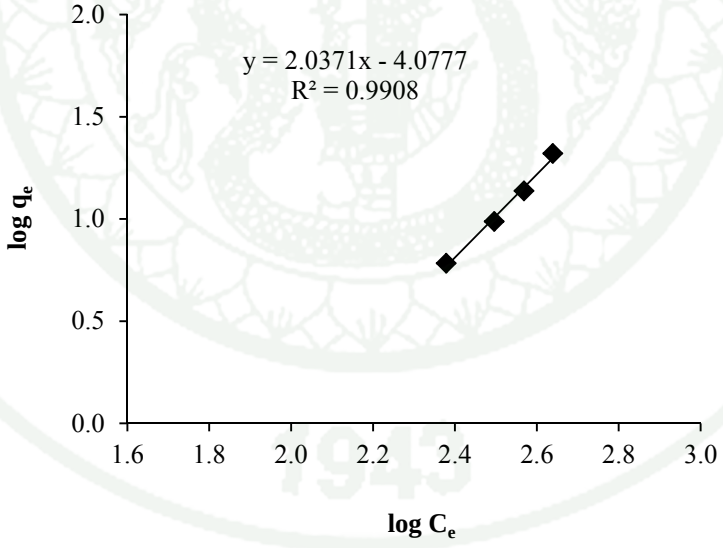

Figure 63 The Freundlich isotherm of phenol adsorption onto char from coconut shell at temperature 60 ^{o}C.

The Langmuir and Freundlich adsorption isotherm parameters for phenol adsorption of chars from bamboo, oil palm shell and coconut shell at various temperatures were given in Table 13 – 15. It could be implied that adsorption data were better fitted with Freundlich adsorption isotherm model than Langmuir model according to R^2 value when increases of the temperature. Therefore, the type of adsorption was multilayer coverage of phenol molecules onto surface of all chars. The K_F value indicates that the char from bamboo had a higher than chars from oil palm shell and coconut shell. For the K_F value indicates that the char from bamboo had a higher adsorption capacity. Furthermore, the n value of all chars were in the range of 0.4 – 2.8. The n value of char from bamboo was closely with chars from coconut shell and oil palm shell. Which the n value indicates that all chars had the highest adsorption energy. The Langmuir constant, chars from coconut shell had the highest Q_0 value (44.247 mg/g), compared to other chars from oil palm shell and bamboo. However, the Q_0 value of char from bamboo was a lower than char from oil palm shell. Furthermore, the b value of char form coconut shell had a higher than chars from oil palm shell and bamboo. For the b value indicating that the char from coconut shell had the highest adsorption energy.

The results, Langmuir and Freundlich constant show that char from coconut shell had a high adsorbed of phenol when compared with chars from oil palm shell and bamboo. On the other hand, at normal state the adsorption of phenol on char from oil palm shell was a higher than the chars from coconut shell and bamboo. For the results SEM image show that the pore structure of char from oil palm shell was a similar to the char from coconut shell which composited of mesopores and macropore. However, the adsorption capacity of chars may be assign to the lignin and cellulose which main composited of chars from oil palm shell and coconut shell. Viraraghavan and Alfaro have suggested that the aromatic surfaces of lignin and cellulose polymer serve to adsorb the phenol molecule. The intermolecular distances and area within the lignocellulosic polymer could also be suitable for the phenol molecules to be adsorbed between basal lignin unite. The aromatic nature of lignin base structure is similar to the structure of phenol molecule (Cohen *et al.,* 1991).

Table 13 Langmuir and Freundlich isotherm constants for phenol onto char from bamboo at various temperatures.

Temperature	Bamboo					
	Langmuir isotherm			Freundlich isotherm		
(^{o}C)	Q_0 (mg/g)	b (L/mg)	R^2	n	K_F (mg/g)	R^2
40	8.4317	0.0015	0.944	1.2773	3,497.8400	0.935
50	8.2034	0.1007	0.949	0.9486	0.0933	0.962
60	25.0626	0.0017	0.314	2.8769	4.7533	0.407

Table 14 Langmuir and Freundlich isotherm constants for phenol onto char from oil palm shell at various temperatures.

Temperature	Oil palm shell					
	Langmuir isotherm			Freundlich isotherm		
(^{o}C)	Q_0 (mg/g)	b (L/mg)	R^2	n	K_F (mg/g)	R^2
40	27.3220	0.2133	0.994	0.9979	0.0348	0.987
50	28.7356	0.0333	0.720	1.2352	0.1084	0.764
60	30.2115	0.0600	0.890	1.2385	0.0973	0.907

Table 15 Langmuir and Freundlich isotherm constants for phenol onto char from coconut shell at various temperatures.

Temperature	Coconut shell char					
	Langmuir isotherm			Freundlich isotherm		
(^{o}C)	Q_0 (mg/g)	b (L/mg)	R^2	n	K_F (mg/g)	R^2
40	6.1162	0.0722	0.656	1.7693	4.9260	0.642
50	44.2478	4.0617	0.942	1.9829	0.9960	0.943
60	13.4048	0.0058	0.962	0.4908	$8.36x10^{-5}$	0.990

Table 16 The specific surface area of samples for adsorption of phenol onto chars from bamboo, oil palm shell and coconut shell at various temperatures.

Samples	Temperature (^oC)	Specific surface area (m^2/g)
Bamboo	40	28.15
	50	27.39
	60	83.69
Oil palm shell	40	91.23
	50	95.95
	60	100.88
Coconut shell	40	20.43
	50	147.75
	60	44.76

According to the Langmuir isotherm in case of phenol at various temperatures, this pointed out the fact that phenol adsorption was the mono-layered adsorption, in which the specific surface area could be calculated by replacing the Q_0 value as shown in Table 16 on the equation 12. The obtained specific surface areas of all chars were in the range of 20.43 – 147.75 m^2/g. The specific surface area value reflected the phenol adsorption ability of the chars were a higher this value, the more adsorption ability. In case of char form coconut shell, it had the highest adsorption ability although its specific surface area was lower than the specific surface area of other chars which may due to the multi-layered adsorption on the surface area of char from coconut shell.

2.3 Chromium (VI) adsorption

2.3.1 The optimization of adsorbent dosage

The adsorbent dosage on the adsorption of chromium (VI) was studied by varies doses of chars from bamboo, oil palm shell, coconut shell and bentonite in range of 0.0500 – 1.6000 g. The chromium (VI) concentration of 50 mg/L, contact times at 3 hours and 120 minute for bentonite. The initial pH solution was adjusted at 4. The results are shown in Figure 64. The adsorptions of chromium (VI) onto chars and soil minerals found that the optimization dosage of chars from bamboo, oil palm shell and coconut shell for adsorption of chromium (VI) were 0.5000 g, 0.7500 g and 1.400 g, respectively. And the optimization dosage of bentonite for adsorption of chromium (VI) was 0.7500 g.

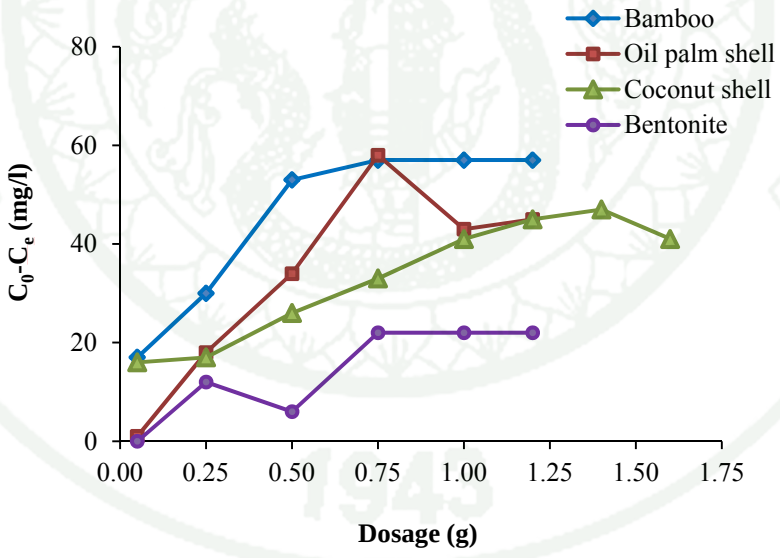

Figure 64 The adsorption of chromium (VI) onto chars and soil minerals by varies adsorbent in range of 0.0500 - 1.6000 g.

2.3.2 The optimization of contact time for adsorption of chromium (VI)

The optimization of contact time for adsorption of chromium (VI) on chars from bamboo, oil palm shell, coconut shell and bentonite were studied at different contact time from 15 -250 minute. The optimization dosage of each adsorbent was combined with 50 mg/L of initial concentration of chromium (VI) and the solution was adjusted pH 4.0. The contact time for adsorption of chromium (VI) on all chars and soil minerals are shown in Figure 65. The results shown that the chromium (VI) was adsorbed on chars from bamboo, oil palm shell and coconut shell within 1, 2 and 3 hours, respectively.

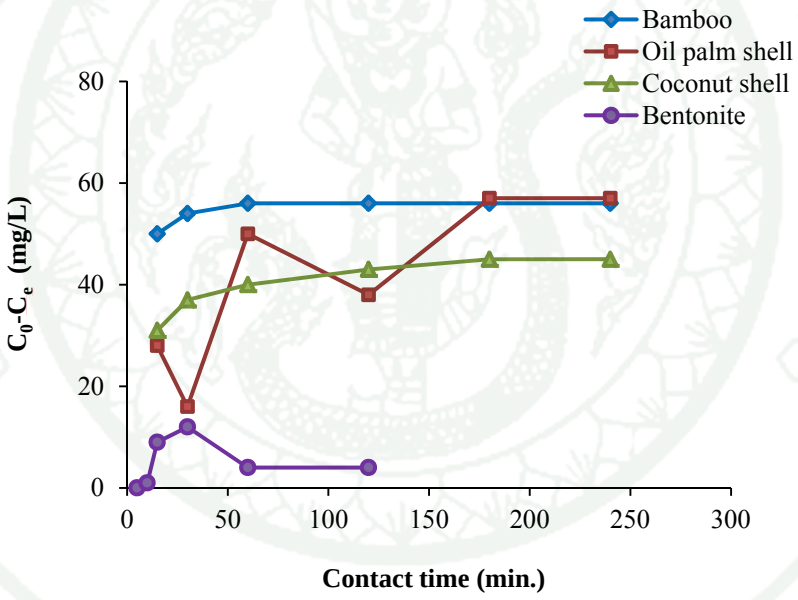

Figure 65 The adsorption of chromium (VI) onto chars and soil minerals by varies contact time in range from 15 – 250 min.

2.3.3 The optimization of initial pH solution

The initial pH of chromium (VI) solution was studied at different pH levels from 2 to 5. The pH solution on adsorption of chromium (VI) by all chars and soil minerals are shown in Figure 66. The results found that the adsorption of chromium (VI) by chars from bamboo, oil palm shell and coconut shell were seemed at pH of 2. The optimization of initial pH for adsorption of chromium (VI) on bentonite was founded to pH of 1.6.

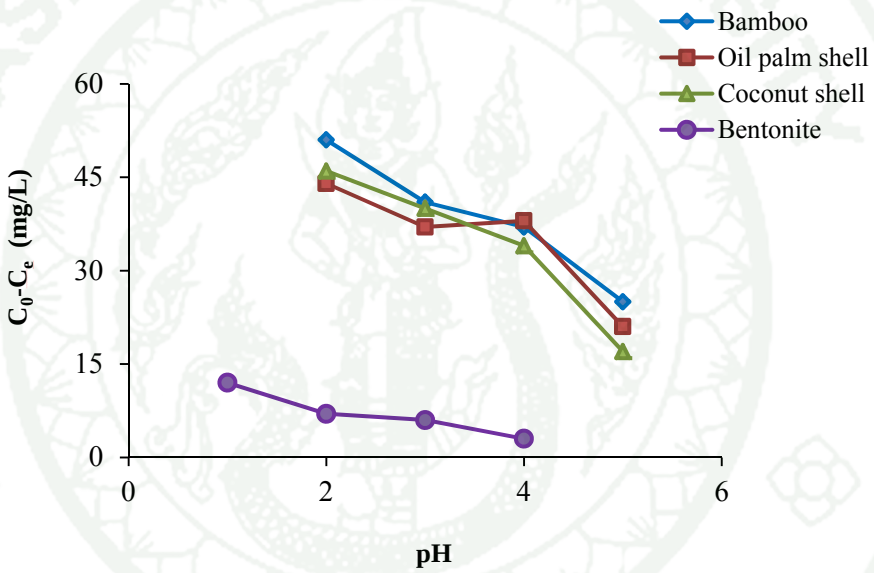

Figure 66 The adsorption of chromium (VI) onto chars and soil minerals by varies pH in range of 1.6 – 5.0.

2.3.4 The optimization of initial concentration of chromium (VI)

The initial concentration for adsorption of chromium (VI) on chars from bamboo, oil palm shell, coconut shell and bentonite were studied in range of 30 – 300 mg/L. The experiment was fixed the adsorbent dosage, contact time and pH of solution at optimization. The initial concentrations for adsorption of chromium (VI) on adsorbents are shown in Figure 67. The results found that the optimization of

initial concentration for adsorption of chromium (VI) on chars from bamboo were studied isotherm in range of 50 – 250 mg/L, oil palm shell in range of 200 – 400 mg/L and coconut shell in range of 100 – 300 mg/L. The optimization of initial concentration for adsorption of chromium (VI) on bentonite was studied in range of 10 – 50 mg/L.

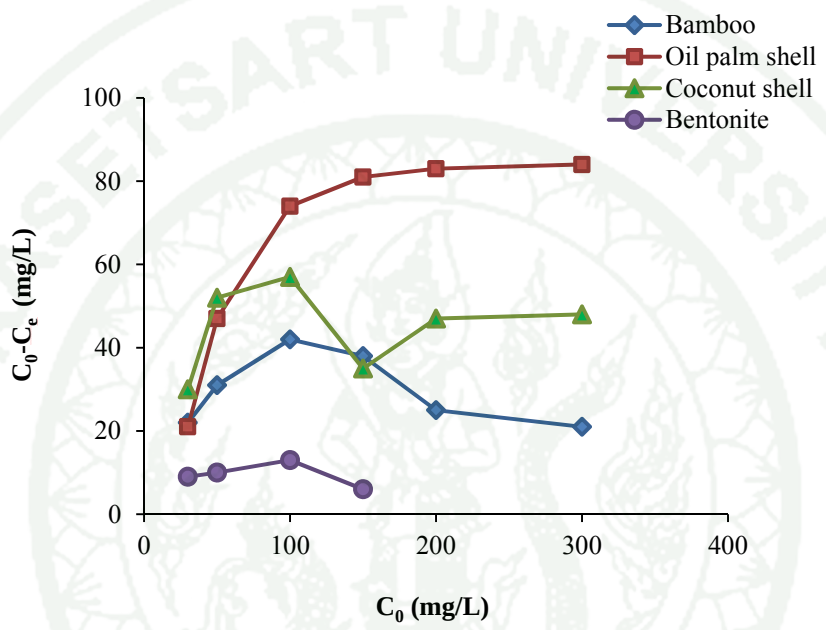

Figure 67 The adsorption of chromium (VI) onto chars and soil minerals by varies concentrations of chromium (VI) in range of 30-300 mg/L.

2.3.5 Adsorption isotherm of chromium (VI) onto chars and soil minerals.

Figures 68 – 75 showed that Langmuir plots of C_e/q_e versus C_e and Freundlich plots of log q_e versus log C_e for the adsorption of phenol onto the chars and soil minerals.

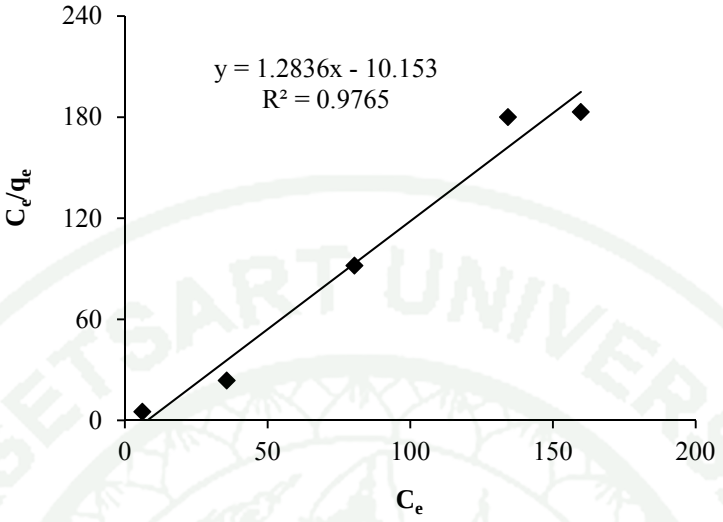

Figure 68 The Langmuir isotherm of chromium (VI) onto char form bamboo.

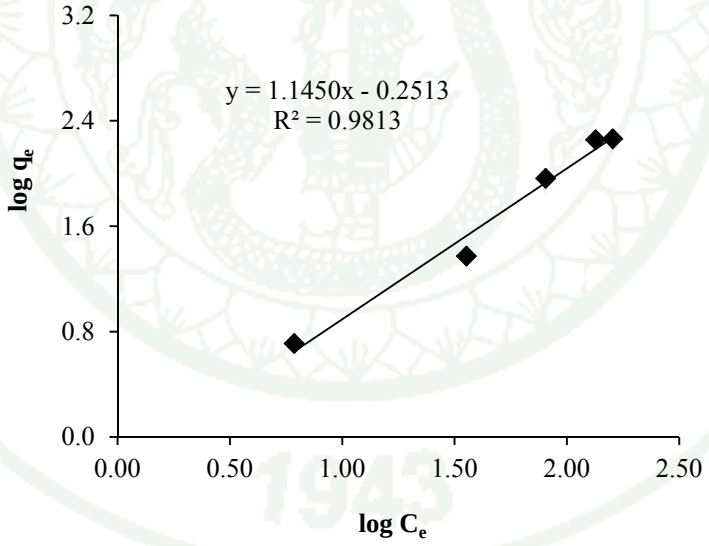

Figure 69 The Freundlich isotherm of chromium (VI) onto form bamboo.

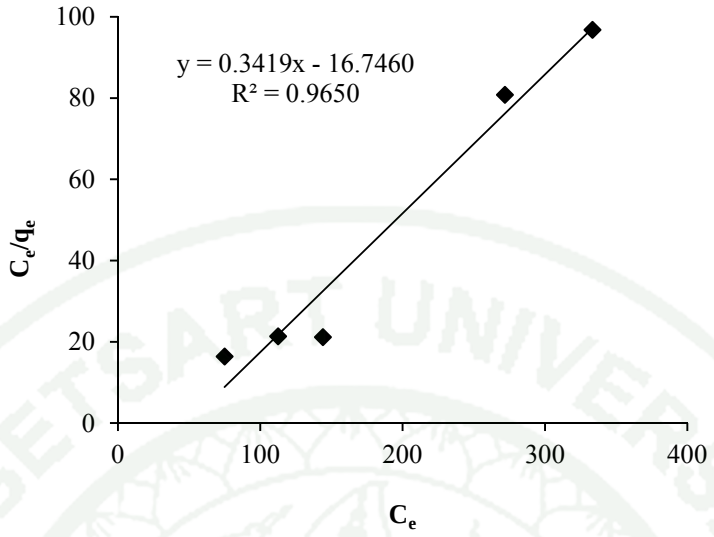

Figure 70 The Langmuir isotherm of chromium (VI) onto char from oil palm shell.

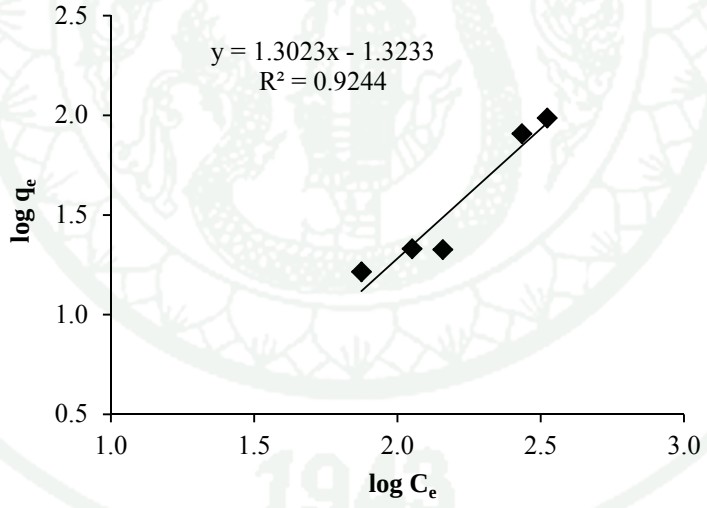

Figure 71 The Freundlich isotherm of chromium (VI) onto char from oil palm shell

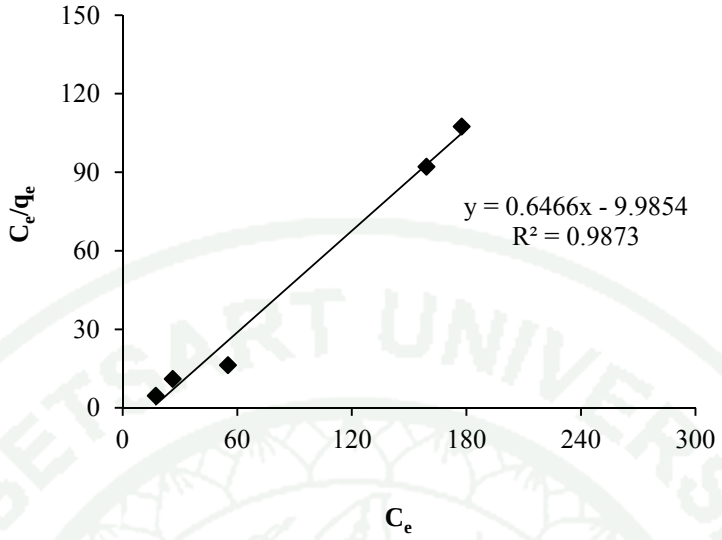

Figure 72 The Langmuir isotherm of chromium (VI) onto char from coconut shell.

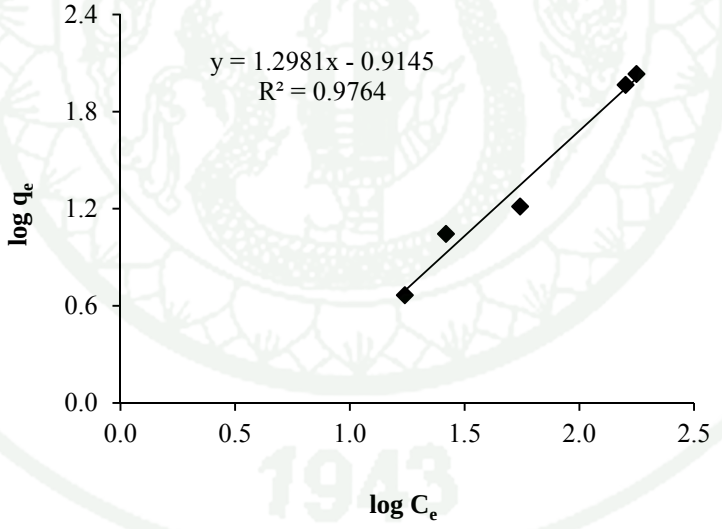

Figure 73 The Freundlich isotherm of chromium (VI) onto char from coconut shell.

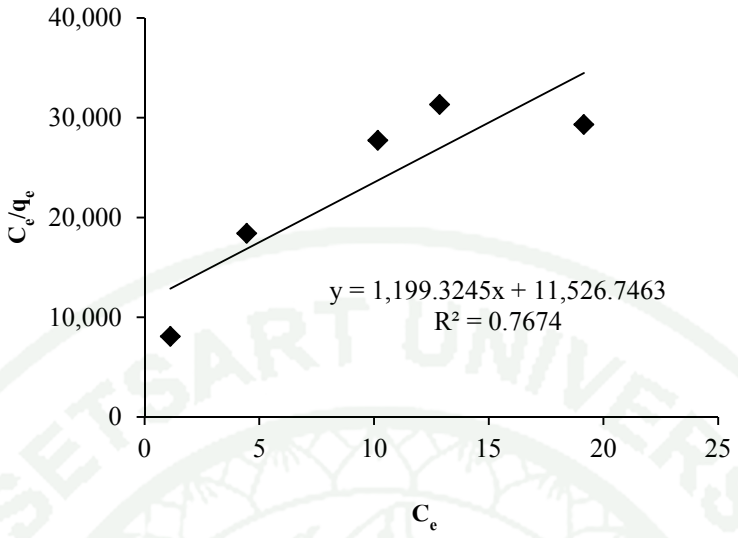

Figure 74 The Langmuir isotherm of chromium (VI) onto bentonite .

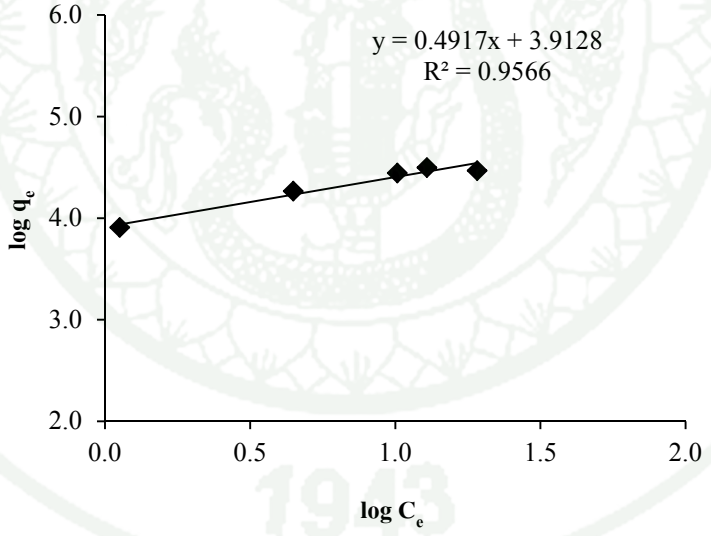

Figure 75 The Freundlich isotherm of chromium (VI) onto bentonite .

The Langmuir and Freundlich adsorption isotherm parameters for chromium (VI) adsorption of chars and soil minerals were given in Table 17. It could be implied that adsorption data of chars from oil palm shell and coconut shell were fitted with Langmuir adsorption isotherm model better than Freundlich model according to R^2 value. Therefore, the type of adsorption was monolayer coverage of chromium molecules onto surface of them. Which the adsorption of char from bamboo and soil mineral was fitted with the Freundlich isotherm model, the type of adsorption was multilayer coverage of chromium molecules onto surface of char from bamboo and soil mineral. The Langmuir constants shows indicated the char from oil palm shell had the highest Q_0 value, compared to other chars. Furthermore, the b value of char from bamboo was the highest, indicated the highest adsorption energy. The Freundlich constants showed the n value of char from bamboo had a closely chars from oil palm shell and coconut shell. On the other hand, the K_F value of char from bamboo had a higher than char from oil palm shell. Furthermore, the K_F value of bentonite was a higher than that of other adsorbent, indicated that the bentonite had the highest adsorption capacity.

For the adsorption results indicates that char from oil palm shell had a high the chromium (VI) adsorption when compared to all adsorbents. The adsorption of chromium (VI) on adsorbent was found to depend on pH of solution, contact time, quantity of adsorbent and initial concentration of adsorbate.

For adsorption of chromium on benotnite surface which the chromium (VI) ions bind to OH groups in the anionic from as $HCrO_4^-$ at very low pH as the surface gets positively charged, while cationic adsorption takes place at increasing pH (Khan *et al.,* 1995).

Table 17 Langmuir and Freundlich isotherm constants for chromium (VI).

Sample	Langmuir isotherm			Freundlich isotherm		
	Q_0 (mg/g)	b (L/mg)	R^2	n	K_F (mg/g)	R^2
Bamboo	0.7790	0.1264	0.976	1.1451	0.5607	0.981
Oil palm shell	2.9248	0.0204	0.965	1.3022	0.0475	0.924
Coconut shell	1.5466	0.0647	0.987	1.2982	0.1217	0.976
Bentonite	0.0008	9.6610	0.767	0.4916	8,180.88	0.956

Table 18 The specific surface area of samples for adsorption of chromium (VI).

Sample	Specific surface area (m^2/g)
Bamboo	0.2796
Oil palm shell	1.0498
Coconut shell	0.5548
Bentonite	0.0003

According to the Langmuir isotherm in case of chromium (VI), this pointed out the fact that chromium (VI) adsorption was the mono-layered adsorption, in which the specific surface area could be calculated by replacing the Q_0 value as shown in Table 18 on the equation 12. The obtained specific surface area of all chars and soil mineral were in the range of 0.0003 – 1.0498 m^2/g. The specific surface area value reflected the chromium (VI) adsorption ability of the chars and soil minerals, in that, the higher this value, the more adsorption ability. In case of bentonite, it had the highest adsorption ability although its specific surface area was lower than the specific surface area of other adsorbent which may due to the multi-layered adsorption on the surface area of bentonite, compared from the K_F values of other adsorbents.

3. Study of thermodynamic of water vapor and phenol onto chars and soil minerals

3.1 Water vapor adsorption

3.1.1 Thermodynamic of water vapor adsorption by chars and soil minerals.

The thermodynamical study of the adsorption process between the liquid phase and solid phase when increasing temperatures to reaches an equilibrium state. The analysis of the thermodynamics parameters by plotting them to Clausius-Clapeyron and Van't Hoff equation were compared all parameters to find the adsorption process that cloud be used for the indicating purposes of adsorption process.

The thermodynamic study was carried out on two equations model which were Clausius-Clapeyron and Van't Hoff. Clauisius-Clapeyron assumes the heat of adsorption. Meanwhile, Van't Hoff assumed the enthalpy, entropy and free energy of specific adsorption. The applicability of the Clausius-Clapeyron equation to the different temperatures study was compared by judging the enthalpy of adsorption.

Figures 76 - 79 show Clausius-Clapeyron plots of ln C_e versus 1/T and Van't Hoff plots of ln K_D versus 1/T for the adsorption of water vapor onto the chars and soil minerals at 40 ^oC, 45 ^oC, 50 ^oC and 55 ^oC.

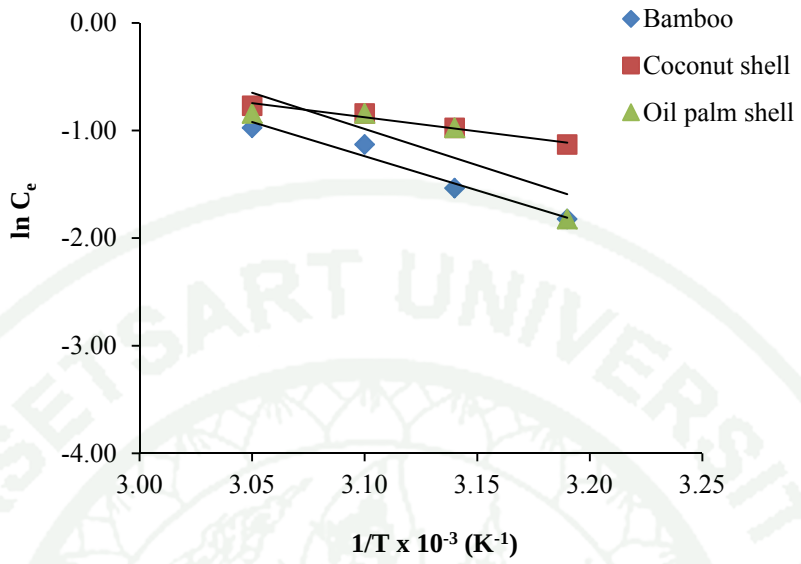

Figure 76 Clausius-Clapeyron plots for adsorption for water vapor onto chars from bamboo, oil palm shell and coconut shell at 40 °C, 45 °C, 50 °C and 55 °C.

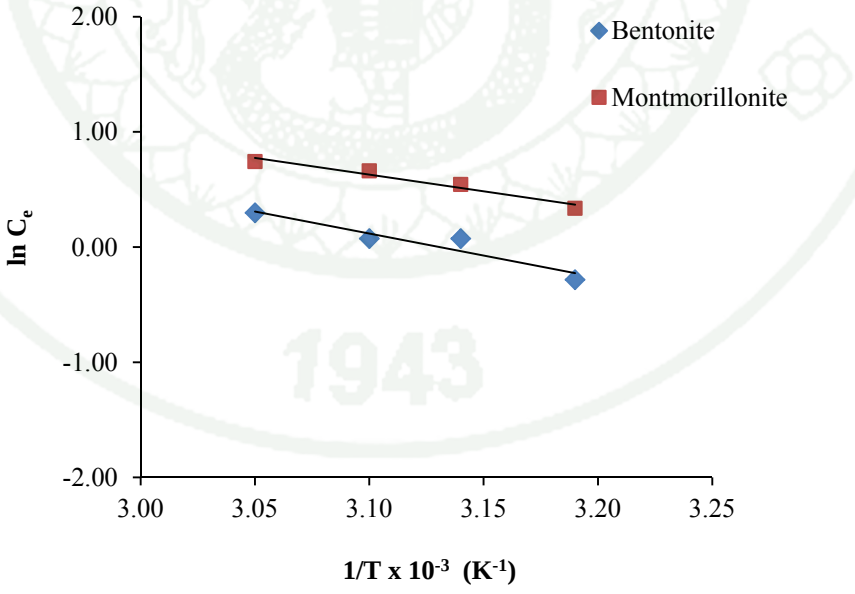

Figure 77 Clausius-Clapeyron plots for adsorption for water vapor onto bentonite and montmorillonite K10 at 40 °C, 45 °C, 50 °C and 55 °C.

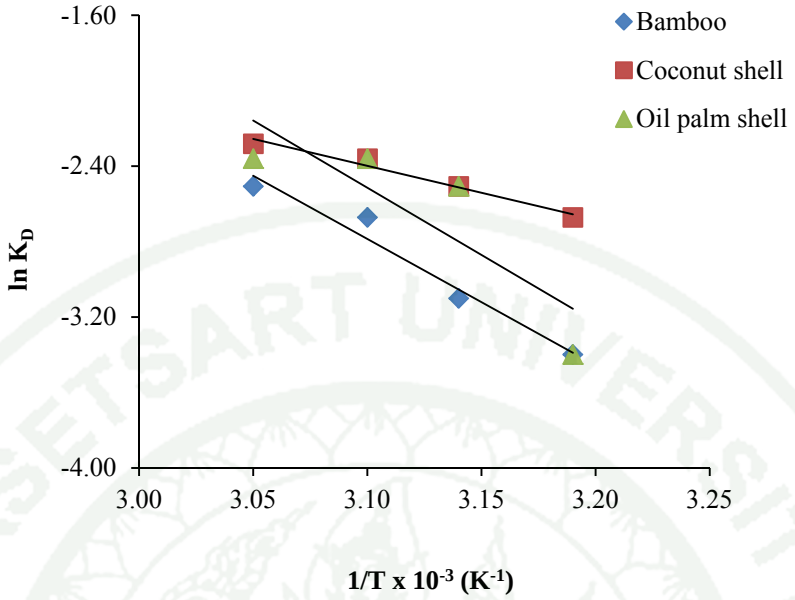

Figure 78 Van't Hoff plots for adsorption for water vapor onto chars form bamboo, oil palm shell and coconut shell at 40 °C, 45 °C, 50 °C and 55 °C.

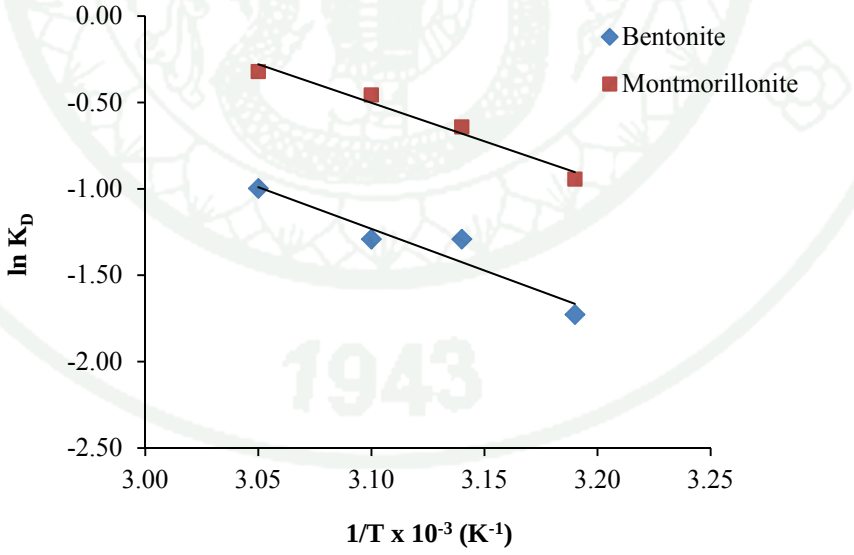

Figure 79 Van't Hoff plots for adsorption for water vapor onto bentonite and montmorillonite K10 at 40 °C, 45 °C, 50 °C and 55 °C.

The thermodynamic parameters of Clausius-Clapeyron and Van't Hoff equation for water vapor adsorption are given in Table 19-20. From the Clausius-Clapeyron equation, the ΔH_{ads} of all adsorbent were in range of 0.0218 – 0.0528 kJ/mol. The positive values of ΔH_{ads} suggested that the adsorption processes of water vapor onto all chars and soil minerals are endothermic reaction. The ΔH^o, ΔS^o and ΔG^o for the Van't Hoff equation showed that the values of entropy change, ΔS^o, of all adsorbents are in rage of 53.530 – 162.860 J/mol.K. The positive value of ΔS^o indicates the increasing randomness of the system. Furthermore, the negative values of free energy, ΔG^o, of all chars and soil minerals indicated that the adsorptions of water vapor on all chars and soil minerals are spontaneous by nature.

Table 19 The heat of adsorption (ΔH_{ads}**)** of water vapor onto chars and soil minerals at 40 ^{o}C, 45 ^{o}C, 50 ^{o}C and 55 ^{o}C.

Sample	ΔH_{ads} (kJ/mol)	R^2
Bamboo	0.0528	0.962
Palm shell	0.0558	0.717
Coconut shell	0.0218	0.973
Bentonite	0.0318	0.901
Montmorillonite	0.0241	0.956

Table 20 Thermodynamics parameter for the adsorption of water vapor onto chars and soil minerals at 40 ^{o}C, 45 ^{o}C, 50 ^{o}C and 55 ^{o}C.

Sample	ΔH^o (kJ/mol)	ΔS^o (J/mol.K)	ΔG^o (kJ/mol)			
			40	45	50	55
Bamboo	0.056	149.520	- 46.740	- 47.492	- 48.239	- 48.987
Oil palm shell	0.059	162.860	-50.917	-51.731	-52.545	-53.360
Coconut shell	0.024	53.530	-16.733	-17.001	-17.268	-17.536
Bentonite	0.037	110.684	-34.607	-35.161	-35.714	-36.267
Montmorillonite	0.040	114.010	-35.645	-36.215	-36.785	-37.355

3.2 Phenol adsorption

3.2.1 Thermodynamic of phenol adsorption by chars.

Figures 80 - 85 showed that Clausius-Clapeyron plots of ln C_e versus 1/T and Van't Hoff plots of ln K_D versus 1/T for the adsorption of phenol onto the chars at at 40 ^oC, 50 ^oC and 60 ^oC.

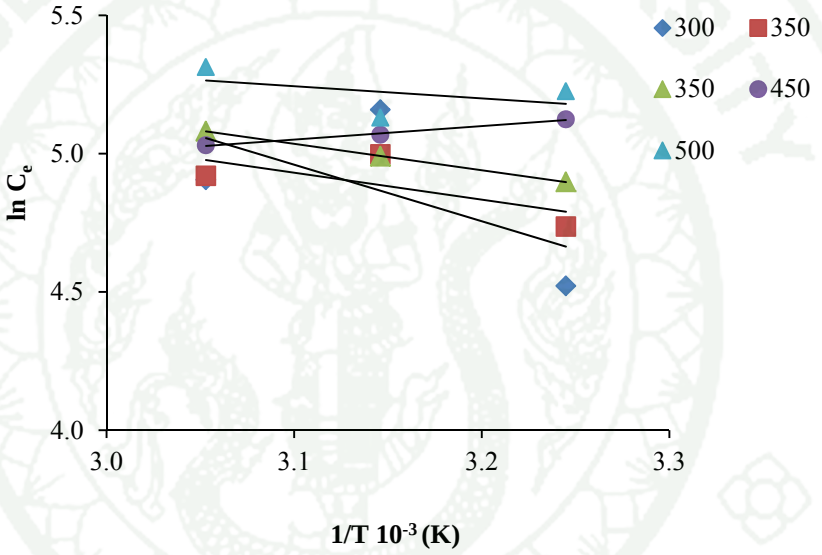

Figure 80 Clausius-Clapeyron plots for adsorption of phenol onto char from bamboo at 40 ^oC, 50 ^oC and 60 ^oC with the concentration of phenol in range of 300 – 500 mg/L.

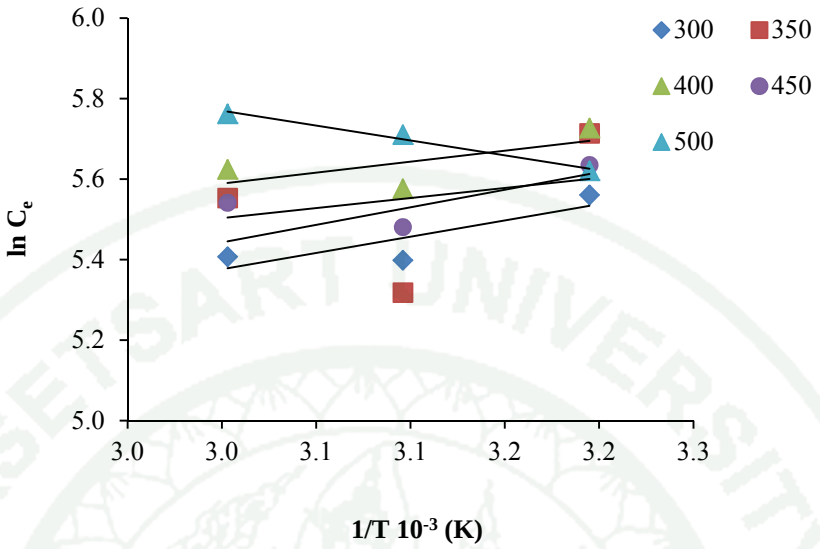

Figure 81 Clausius-Clapeyron plots for adsorption of phenol onto char from oil palm shell at 40 °C, 50 °C and 60 °C with the concentration of phenol in range of 300 – 500 mg/L.

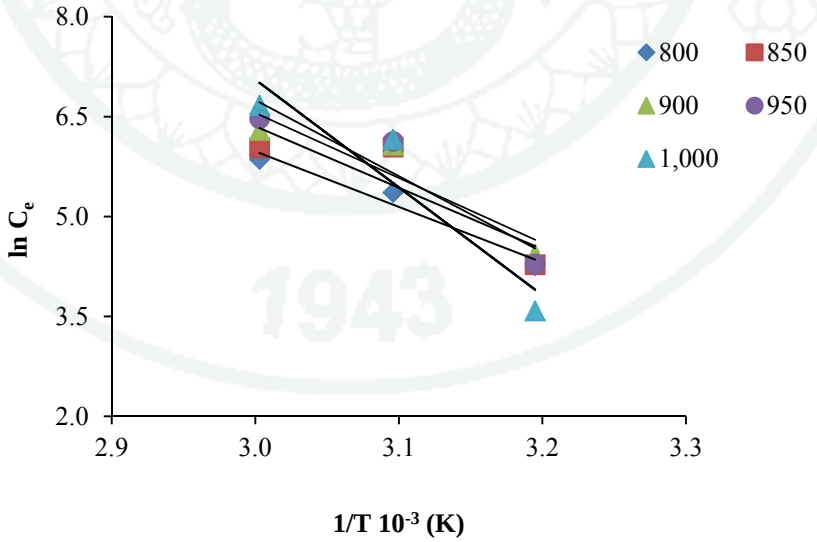

Figure 82 Clausius-Clapeyron plots for adsorption of phenol onto char from coconut shell at 40 °C, 50 °C and 60 °C with the concentration of phenol in range of 800 – 1,000 mg/L.

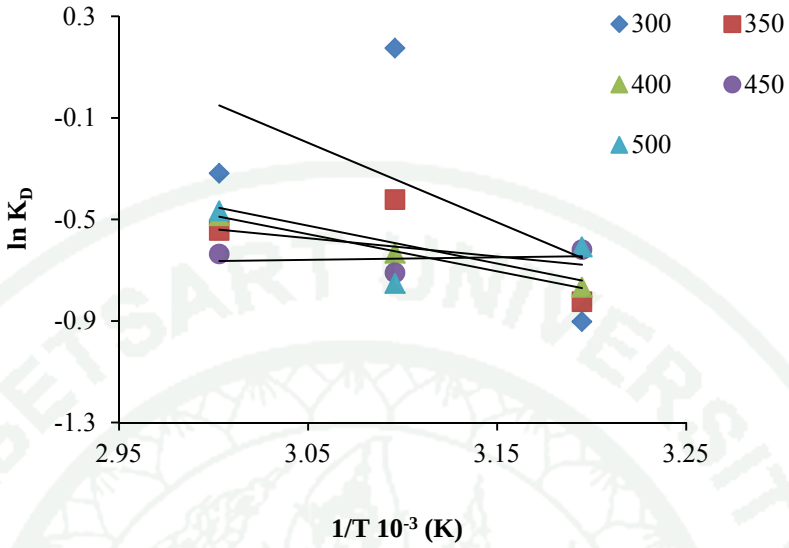

Figure 83 Van't Hoff plots for adsorption of phenol onto char from bamboo at 40 °C, 50 °C and 60 °C with the concentration of phenol in range of 300 – 500 mg/L.

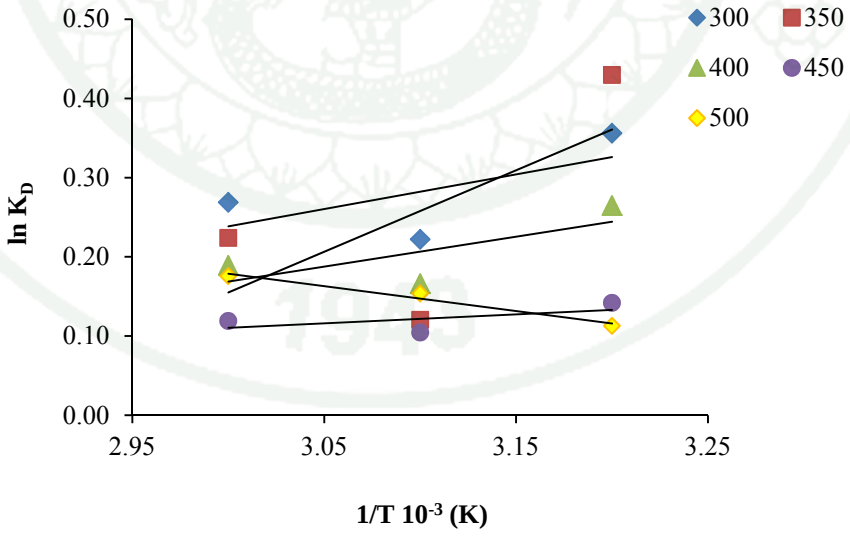

Figure 84 Van't Hoff plots for adsorption of phenol onto char from oil palm shell at 40 °C, 50 °C and 60 °C with the concentration of phenol in range of 300 – 500 mg/L.

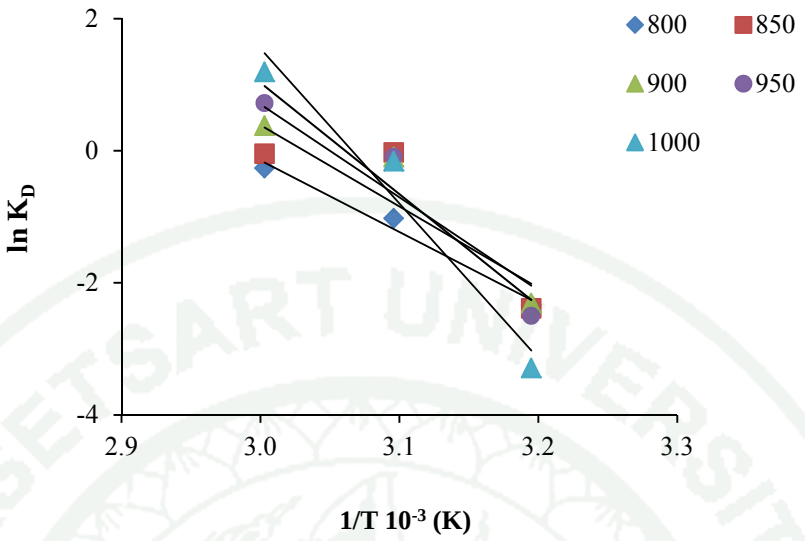

Figure 85 Van't Hoff plots for adsorption of phenol onto char from coconut shell at 40 °C, 50 °C and 60 °C with the concentration of phenol in range of 800 – 1,000 mg/L.

The thermodynamic parameters of Clausius-Clapeyron and Van't Hoff equation for phenol adsorption are given in Table 21– 26. The Clausius-Clapeyron equation showed that the value of the enthalpy change, ΔH_{ads}, of char from bamboo is 0.0037 – 0.0170 kJ/mol. The Van't Hoff equation showed that the value of the enthalpy change, ΔH^{o}, of char from bamboo is 0.001– 0.026 kJ/mol. The values of entropy change, ΔS^{o}, of char from bamboo is 7.930 – 77.773 J/mol.K and the values of free energy, ΔG^{o}, is -2.482 – -25.898 kJ/mol.

The Clausius-Clapeyron equation showed that the value of the enthalpy change, ΔH_{ads}, of char from oil palm shell is 0.0062 – - 0.0072 kJ/mol. The Van't Hoff equation showed that the value of the enthalpy change, ΔH^{o}, of char from oil palm shell is 0.099 – - 0.026 kJ/mol. The values of entropy change, ΔS^{o}, is 62.911 – -57.014 J/mol.K and the values of free energy, ΔG^{o}, is -8.613 – -27.745 kJ/mol.

The Clausius-Clapeyron equation showed that the value of the enthalpy change, ΔH_{ads}, of char coconut shell is 0.0694 – 0.1346 kJ/mol. The Van't Hoff equation showed that the value of the enthalpy change, ΔH^{o}, of char from coconut shell is 0.090 – 0.195 kJ/mol. The values of entropy change (ΔS^{o}) is 268.976 – 597.590 J/mol.K and the values of free energy, ΔG^{o}, is – 84.189 – -198.997 kJ/mol.

From Clausius-Clapeyron equation showed that the positive values of ΔH_{ads} suggest that the interactions of the phenol molecules with char from bamboo and coconut shell are exothermic processes by nature. On the other hand, the adsorption of phenol molecule on surface of char from oil palm shell is endothermic process by nature. Furthermore, the Van't Hoff equation showed that the free energy values, ΔG^{o}, of chars from bamboo and oil palm shell in range of -2.482 – -27.745 kJ/mol are indicated that the physisorption. Which the free energy values, ΔG^{o}, of char from coconut shell in range of -84.189 – 198.997 kJ/mol is suggested that the chemisorption.

The negative values of ΔG^{o} imply that the adsorption of phenol on char from bamboo, oil palm shell and coconut shell are spontaneous by nature. Generally, the absolute magnitude of the change in free energy for physisorption is between 0 and -20 kJ/mol, chemisorptions has a range of -80 and -400 kJ/mol (Gereli *et al.,* 2006).

Table 21 The heat of adsorption (ΔH_{ads}) of phenol onto char from bamboo at 40 ^{o}C, 50 ^{o}C and 60 ^{o}C with the concentration of phenol in range of 300 – 500 mg/L.

C_0 (mg/L)	Bamboo	
	ΔH_{ads} (kJ/mol)	R^2
300	0.0170	0.219
350	0.0081	0.422
400	0.0080	0.993
450	0.0041	0.463
500	0.0037	0.292

Table 22 The heat of adsorption (ΔH_{ads}) of phenol onto char from oil palm shell at 40 ^{o}C, 50 ^{o}C and 60 ^{o}C with the concentration of phenol in range of 300 - 500 mg/L.

C_0 (mg/L)	Oil palm shell	
	ΔH_{ads} (kJ/mol)	R^2
300	-0.0067	0.511
350	-0.0072	0.316
400	-0.0045	0.939
450	-0.0041	0.380
500	0.0062	0.497

Table 23 The heat of adsorption (ΔH_{ads}**)** of phenol onto char from coconut shell at 40 ^{o}C, 50 ^{o}C and 60 ^{o}C with the concentration of phenol in range of 800 – 1,000 mg/L.

C_0 (mg/L)	Coconut shell	
	ΔH_{ads} (kJ/mol)	R^2
800	0.0694	0.996
850	0.0769	0.788
900	0.0813	0.953
950	0.0950	0.996
1,000	0.1346	0.987

Table 24 Thermodynamics parameter for the adsorption of phenol onto char from bamboo at 40 °C, 50 °C and 60 °C.

Concentration (mg/L)	ΔH^o (kJ/mol)	ΔS^o (J/mol.K)	ΔG^o (kJ/mol)		
			40	50	60
300	0.026	77.773	-24.343	-25.121	-25.898
350	0.012	33.414	-10.459	-10.793	-11.127
400	0.012	32.556	-10.190	-10.516	-10.841
450	0.001	7.930	-2.482	-2.561	-2.641
500	0.006	13.453	-4.211	-4.345	-4.480

Table 25 Thermodynamics parameter for the adsorption of phenol onto char from oil palm shell char at 40 °C, 50 °C and 60 °C.

Concentration (mg/L)	ΔH^o (kJ/mol)	ΔS^o (J/mol.K)	ΔG^o (kJ/mol)		
			40	50	60
300	-0.021	-57.014	-17.846	-18.416	-18.986
350	-0.029	-83.317	-26.078	-26.912	-27.745
400	-0.015	-40.006	-12.522	-12.922	-13.322
450	-0.009	-27.516	-8.613	-8.888	-9.163
500	0.019	62.911	-19.691	-20.320	-20.950

Table 26 Thermodynamics parameter for the adsorption of phenol onto char from coconut shell char at 40 ^{o}C, 50 ^{o}C and 60 ^{o}C.

Concentration (mg/L)	ΔH^{o} (kJ/mol)	ΔS^{o} (J/mol.K)	ΔG^{o} (kJ/mol)		
			40	50	60
800	0.090	268.976	-84.189	-86.879	-89.569
850	0.103	310.764	-97.269	-100.377	-103.484
900	0.117	357.415	-111.871	-115.445	-119.019
950	0.140	429.400	-134.402	-138.696	-142.990
1000	0.195	597.590	-187.046	-193.021	-198.997

CONCLUSION AND RECOMMENTIDATIONS

Conclusion

From the results of water vapor adsorption on chars and soil minerals, it could be seen that the soil minerals had a higher amount of water vapor adsorption than chars from agricultural wastes (AW). This indicated that the soil minerals have higher surface area than chars. However, the uptake water vapor on montmorillonite K10 (0.4201 g/g) is a higher than the bentonite (0.2693 g/g). Furthermore, the chars from bamboo, oil palm shell and coconut shell seemed to have similar efficiency in adsorption of water vapor. The amount of water vapor adsorption of chars from bamboo, oil palm shell and coconut shell are 0.0754 g/g, 0.0862 g/g and 0.0926 g/g, respectively. The adsorption isotherm results, Langmuir constants show that the char from coconut shell (the value of Q_0 is74.50 mg/L) had the highest adsorption capacity than other adsorbents. On the other hand, the Freundlich constant indicated that the montrillonite (the value of K_F is 0.2143 mg/L) had higher adsorption capacity than other adsorbents. Which the adsorption of water vapor on all chars and soil minerals are fitted to the Freundlich isotherm, indicated the multilayer adsorption system. For the thermodynamics of adsorption results show the positive values of ΔH_{ads} suggest that the adsorption process of water vapor onto all chars and soil minerals are endothermic reactions. Additionally, the free energy, ΔG^o, of adsorption water vapor on chars form bamboo, oil palm shell, coconut shell, betonite and montmorillonite had a negative value which adsorption of water vapor onto all chars and soil minerals are spontaneous by nature.

In term of efficiency of phenol adsorption, the char from oil palm shell provided higher specific surface area than the chars from bamboo and coconut shell, indicated that the highest phenol adsorption capacity when compared to other chars. For the adsorption isotherm results, the phenol adsorptions on all chars were fitted to Langmuir isotherm, which suggest the monolayer adsorption. The adsorptions of phenol on all chars were fitted to Freundlich isotherm when increasing temperature. Therefore, the phenol adsorption capacities of all chars are increased with increasing

temperature, which indicates the multilayer adsorption system. Furthermore, thermodynamics of adsorption results showed that the ΔH_{ads} of chars from bamboo and coconut shell had a positive value. Therefore, the phenol adsorption on chars from bamboo and coconut shell is endothermic process. The negative values ΔH_{ads} of char from oil palm shell indicates that the phenol adsorption is exothermic process. In addition, the negative values ΔG^{o} of chars from bamboo and oil palm shell are indicated that the physisorption reaction which the char from coconut shell is chemisorptions reaction. This implied that the adsorptions of phenol on all chars are spontaneous by nature.

The adsorption of chromium (VI) on chars and soil minerals suggested that the oil palm shell provided the highest specific surface area when compared to other adsorbents. The adsorption isotherms results, the chromium (VI) onto chars from oil palm shell and coconut shell are fitted to Langmuir isotherm which the char from bamboo and bentonite are fitted to Freundlich isotherm. From the Langmuir constant indicates that the char from oil palm shell had a higher adsorption capacity. However, the adsorbents adsorption capability was strongly dependent on the pH of solution. Therefore, it can be conclusion that the Chromium (VI) adsorption capacities of all adsorbents were favored at low pH. The maximum adsorption of all adsorbents can be reached at pH 2.

Recommendations

1. In the adsorption process of water vapor, water drop or vapor should be attached to spring because it will expectedly increase the amount of water vapor on adsorbent which faulty in the adsorption of water onto adsorbents.

2. Regarding the adsorption of water, the efficiency of adsorption of each adsorbents might determine by N_2 adsorption/desorption isotherm which compared the adsorption capacity of each adsorbent.

3. In case of the rainmaking process, the soil minerals can be used to adsorb water vapor in the triggering process. The weight of soil minerals is heavy; therefore the char from coconut shell is well adsorbing water vapor in the triggering process. Because of weight of char from coconut shell are less than soil minerals. Usually, sodium chloride powder was used in the triggering process (Royal rainmaking, 1998) which the sodium chloride powder is heavy.

4. The used the chars from AW for adsorption should be cleaned because it has the impacts on the detection adsorbed values of solution.

5. Concerning the adsorption of pollution aspect, temperature or pH of solution should be considered because they might have the impacts on the adsorption abilities of each adsorbate.

LITERATURE CITED

Amphol, A., T. Paitip and N. Woranan. 2009. Preparation and characteristics of agricultural waste activated carbon by physical activation having micro- and mesopores. **Analy. and Apply. Pyro.** 82:279-285.

Alberty, R.A. and R. J. Silbey. 1992. Physical Chemistry.1st edition. John Wiley & Sons, Inc.,New York. pp. 187.

Bansal, R.C. and M. Goyal, 2005. Activated Carbon Adsorption.1st ed. CRC Press, New York.

Bedia, J., J. R. Mirasol and T. Cordero. 2007. Water vapor adsorption on lignin-based activated carbons. **Chem. Technol. Bio.** 82:548-557.

Bhattacharyya, K. S. and S. S. Gupta. 2006. Adsorption of chromium (VI) from water by clays. **Ind. Eng. Chem. Res.** 45:7232-7240.

Brack, A. 1998. **The Molecular Origins of Life: Assembling Piece of the Puzzle.** 1st ed. Cambridge University Press, New York, USA.

Cameron Carbon Incorporated. 2006. **Activated carbon.** Available Source: http://www.cameroncarbon.com/activated_carbons.html. March 12, 2012.

Chaiyaomporn, K. and O.Chavalparit. 2010. Fuel Pellets Production from Biodiesel Waste. **EnvironmentAsia**. 3(1): 103-110.

Cheremisinoff, P.N. and A.C. Morresi. 1987. Carbon adsorption application. In P.N. Cheremisinoff and F. Ellerbusch (eds.), **Carbon Adsorption Handbook.** Michigan: Ann Arbor Science.

Cohen, A.D., M.S. Rollins, W.M. Zunic and J.R. During. 1991. Effects of chemical and physical differences in peats on their ability to extract hydrocarbons from water. **Water Res.** 25(9): 1047-1060.

Cossarutto, L., T. Zimny., J. Kaczmarczyk., T. Siemieniewska., J. Bimer and J.V. Weber. 2001. Transport and sorption of water vapor in activated carbon. **Carbon.** 39:2339-2346.

Culp, G. L. and R.L. Culp. 1974. **New Concepts in Water Purification.** 1st ed. Van Nostrand Reinhold Company, New York, USA.

Do, D.D., S. Junpirom and H.D. Do. 2009. A new adsorption- desorption model for water adsorption in activated carbon. **Carbon.** 47:1466-1473.

Dubey, S.P. and K. Gopal. 2007. Adsorption of chromium (VI) on low cost adsorbents derived from agricultural waste material: A comparative study. **Hazard. Mater.** 114:465-470.

Fabrice, S., D. Jean-Marc, D. Renaud, B. Olivier, J. Michel, B. Isabella and V.D. Henri. 2009. Hydration sequence of swelling clay: Evolutions of specific surface area and hydration energy. **Colloid and Inter. Sci.** 333:510-522.

Finqueneisel, G., T. Zimny and J.V. Weber. 2005. On the prediction of adsorption isotherm of methanol/water vapor mixtures on microporous activated carbon. **Carbon.** 43:1084-1114.

Foley, N. J., K. M. Thomas, P. L. Forshaw, P. Stonton and P. R. Norman. 1997. Kinetic of water vapor adsorption activated carbon. **Langmuir.** 13:2083-2089.

Garg, U. K., M. P. Kaur, V. K. Garg and D. Sud. 2007. Removal of hexavalentchromium from aqueous solution by agricultural waste biomass. **Hazard. Mater.** 140:60-68.

Gereli, G., Y. Sek, I. Murat Kusoglu and K. Yurdakoc. 2006. Equilibrium and kinetics for the sorption of promethazine by hydrochloride onto K10 montmorillonite. **Colloid and Inter. Sci.** 299: 155-162.

Ghorbel-Abid, I., A. Jrad, K. Nahdi and M. Trabelsi-Ayadi. 2009. Sorption of chromium (III) from aqueous solution using bentonite clay. **Desal.** 246: 595-604.

Greeneartbamboo. 2010. **Bamboo charcoal.** Available Source: http://www.Greeneartbamboo.com/Bamboo_charcoal. December 15, 2011

Hofmann, U., A. Weiss, G. Koch, A. Mehler and A. Schoz. 1956. Intracrytalline Swelling, Cation Exchange, and Anion Exchange of Minerals of the Montmorillonite Group and of Kaolinite. **Acad. Sci., Publ.** 465: 273-287.

His Majesty King Bhumibol Adulyadej. 2003. Weather modifications for rainmaking. Thailand.

Hocine, O., M. Boufatit, A. Khouider. (2004) Use of montmorillonite clay as adsorbents of hazardous pollutants. **Desalination.** 167: 141-145.

Horikawa, T., T. Sekida, J. Hayashi, M. Katoh and D. D. Do. 2011. A new adsorption-desorption model for water adsorption in porous carbon. **Carbon.** 49: 416-424.

Isa Hasanain, M., I. Naimah, A. A. M. Hamidi, A. Nordin, Md. S. Nor Habsah, L. Z. Ali Akbar and M. K. Shamsul Rahman. 2008. Removal of chromium (VI) from aqueous solution using treated oil palm fibre. **Hazardous Materail.** 152: 662- 668.

Khan, S. A., R. U. Rehman. and M. A. Khan. 1995. Adsorption of chromium (III), chromium (VI) and silver (I) on bentonite. **Water Manage.** 15:271-282.

Kumar, S., S.N. Upadhya and Y.D. Upadhaya. 1978. Removal of phenols by adsorption of fly ash. **J. Chem. Technol. Biotechnol.** 37: 281-292.

Lee, W.H., and P.J. Reucroft 1999. Vapor adsorption on coal-and wood-based chemically activated carbons (I) Surface oxidation states and adsorption of H_2O. **Carbon**. 37:7-14.

_____. 1999. Vapor adsorption on coal- and wood-based chemically activated carbon (III) NH_3 and H_2S adsorption in the low relative pressure range. **Carbon.** 37:21-26.

Masel, R.I. 1996. **Principles of Adsorption and Reaction on Solid Surfaces.** 3rd ed. John Wiley & Sons, New York, USA.

March, J. 1992. In: **Advanced organic chemistry.** Reaction, mechanisms, and structure, Wiley, New York. pp 3-25.

Mindat .2011. **Bentonite.** Available Source: http://www.mindat.com/Bentonite**.** October 18, 2011

_____. 2011. **Montmorillonite clay.** Available Source: http://www.mindat.com/montmorillonite clay. October 18, 2011

Naoto, O., N. Yoko, M. Takahiro, I. Yumiko, I. Akifumi and I. Michio. 2008. Preparetion of microporous carbon foams for adsorption/desorption of water vapor in ambient air. **New Carbon Mater.** 23(3):216-220.

Ozkaya, B. 2006. Adsorption and desorption of phenol on activated carbon and a comparison of isotherm models. **Hazard. Mater.** B129: 158-163.

Ookaboo. 2011. ***Cocos nufifera.*** Available Source: http://www.Ookaboo.com/ Coconut_Cocosnufifera. October 18, 2011

Pastor-Villiegas, J., J. M. Meneses Rodriguez, J. F. Pastor-Valle, J. Rouquerol, R. Denoyel and M. G. Garcia. 2010. Adsorption-desorption of water vapor on chars prepared from commercial wood charcoals, in relation to their chemical composition, surface chemistry and pore structure. **Anal and App. Pyro.** 88:124-133.

Pavia, D., G. Lampman and G. Kriz. 2001. Introduction to spectroscopy. 3rd ed. Department of chemistry, Western Washington University, Bellingham, Washington.

Palmplantations. 2009. ***Elaeis guineensis* Jacq.** Available Source: http://www.Palmplantations.com/Oilpalm_Elaeisguineensis_Jacq. October 18, 2011.

Qingrong, Q., S. Sunohara, Y. Kato, M. A. Ahmad Zaini, M. Machida and H. Tatsumoto. 2008. Water vapor adsorption onto activated carbons prepared from cattle manure compost (CMC). **App. Surf. Sci.** 254:4868-4874.

Royal rainmaking. 1998. **Royal rainmaking.** Available Source: http://www.royalrainmaking.com/Royalrainmaking. October 18, 2011

Richards, S. and A. Bouazza. 2007. Phenol adsorption in organo-modified basaltic clay and bentonite. **Appl. Clay Sci.** 37:133-142.

Salles, F., J. M. Douillard, R. Denoyel, O. Bildstein, M. Jullien, I. Beurroies and H.V. Damme. 2009. Hydration sequence of swelling clays: Evolutions of specific surface area and hydration energy. **J. Colloid Inter. Sci.** 333: 510-522.

Scienceblogs. 2011. **Heat capacity**. Available Source: http://scienceblogs.com/worldsfair/2011/01/heat_capacity_101_detecting_an.php. October 29, 2011.

Smith, J. V. and S. W. Bailey. 1954. Review of Si-O and Al-O Distances. **Acta. Cryst.** 7: 479-481.

Sokolowaka, Z., P. Warchulska and S. Sokolowski. 2009. Trends in soil fractal parameters caused by accumulation of soil organic matter as resulting from the analysis of water vapor adsorption isotherms. **Eco. Com.** 6:254-262.

Stathi, P., I. T. Papadas, A. Tselepidou and Y. Deligiannakis. 2010. Heavy-metal uptake by high cation-exchange-capacity montmorillonite: the role of permanent charge sites. **Global. Nest.** 12:248-255.

Tahir, S. S. and R. Nasseam. 2007.Removal of Cr(III) from tannery wastewater by a dsorption onto bentonite clay. **Separation and Purification Technology**. 53: 312-321.

Tan, W.T., S.T. Ooi and C.K. Lee. 1993. Removal of chromium (VI) from solution by coconut husk and palm pressed fibers. **Environmental Technology.** 14(3): 277-282.

Tanada, S., N. Kawasaki, T. Nakamura, M. Araki and Y. Tachibana. 2000. Characteristics of nonafluorobutyl methyl ether (NFE) adsorption onto activated carbon fibers and differet-size-acti-vated carbon particles**. J. Colloid Inter. Sci.** 288: 220- 225.

Theng, B. K. G. 1974. The Chemistry of Clay-Organic Reactions: Adam Hilger, London, 343.

Tropicalbamboo.com. 2008. ***Dendrocalamus brandisii.*** Available Source: http://www.Tropicalbamboo.com/Dendrocalamus_brandisii. October 18, 2011.

Uchida, M., O. Shinohara, S. Ito, N. Kawasaki, T. Nakamura and S. Tanada. 2000. Reduction of iron (III) ion by activated carbon fiber. **J. Colloid Inter. Sci.** 224:347-350.

Vartapetyan, R.Sh., A.M Voloshchuk, A.K. Buryak, C.D. Artamonova., R.L. Belford., P.J. Ceroke., D.V. Kholine., R.B. Clarkson and B.M. Odintsov. 2005. Water vapor adsorption on char and active carbon-oxygen sensor prepared from a tropical tree wood. **Carbon.** 43:2152-2159.

Vlasova, M., G. Dominquez-Patina, N. Kakazcy, M. Dominquez-Patino, D. Juarez-Romero and Y. E. Mendez. 2003. Structural-phase transformations in bentonite after acid treatment. **Sci. of Sintering.** 35:155-166.

Viraraghavan, T. and Flor de Maria A. 1998. Adsorption of phenol from wastewater by peat fly ash and bentonite. **J. Hazard Mate.** 57: 59-70.

Webb, P.A. 2003. Introduction to chemical adsorption analytical techniques and their applications to catalysis. Micromeritics Instrument Corp., Norcross, Georgia 30093. US.

Woodroof, J. G.1979. **Coconuts: Production Processing Products.** 2nd ed. AVI Publishing Co. Inc.,

Wikipedia. 2008. **Crystalline structure of montmorillonite.** Available Source: http://en.wikipedia.org/wiki/Montmorillonite. October 19, 2011.

_____. 2008. **Propeties of chromium.** Available Source: http://www.wikipedia.com/chromium. October 18, 2011.

_____ . 2008. **Pore size.** Available Source: http://www.en.wikipedia.org/wiki/henol. October 18, 2011.

Wikipedia. 2009. **Propeties of phenol.** Available Source:
http://www.wikipedia.com/phenol. October 18, 2008.

Wolframalpha. 2011. **Phenol size.** Available Source:
http://www.wolframalpha.com/phenol. October 18, 2011.

APPENDICES

Appendix A

The FT-IR spectra of chars and soil minerals

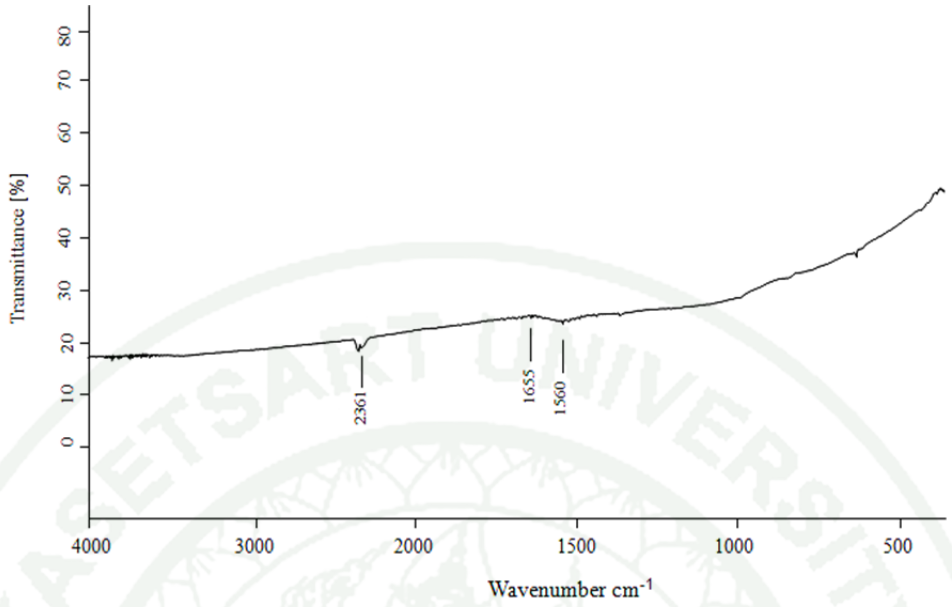

Appendix Figure A1 The FT-IR spectrum of char from bamboo.

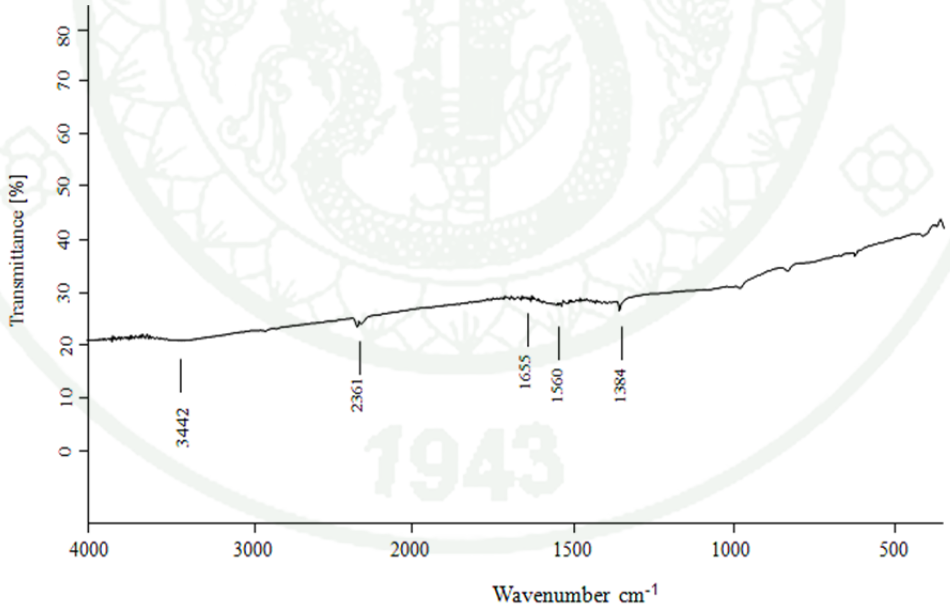

Appendix Figure A2 The FT-IR spectrum of char from oil palm shell.

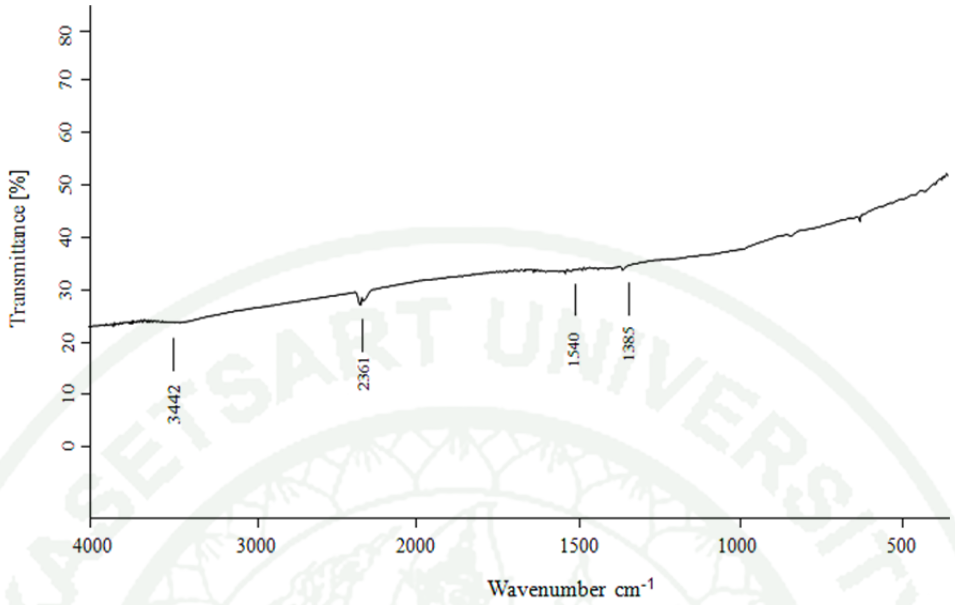

Appendix Figure A3 The FT-IR spectrum of char from coconut shell.

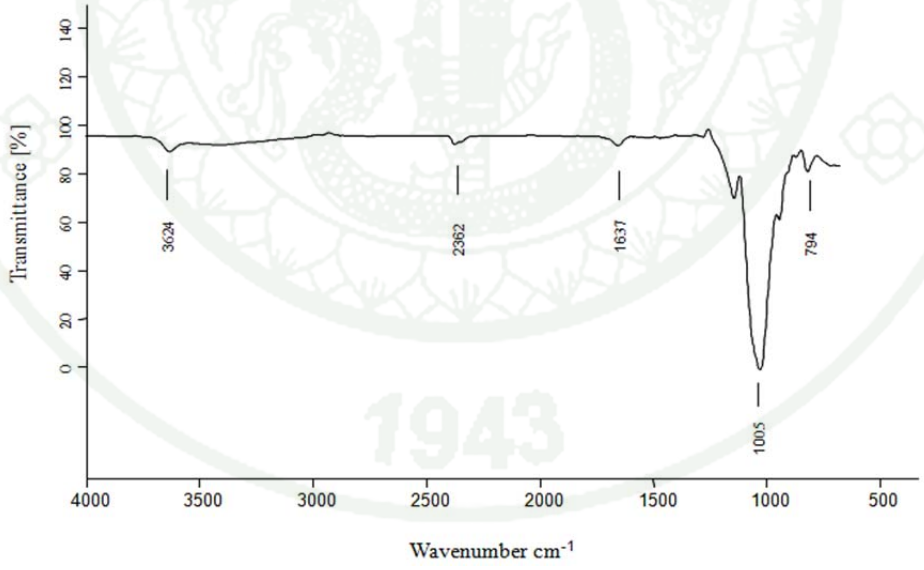

Appendix Figure A4 The FT-IR spectrum of bentonite.

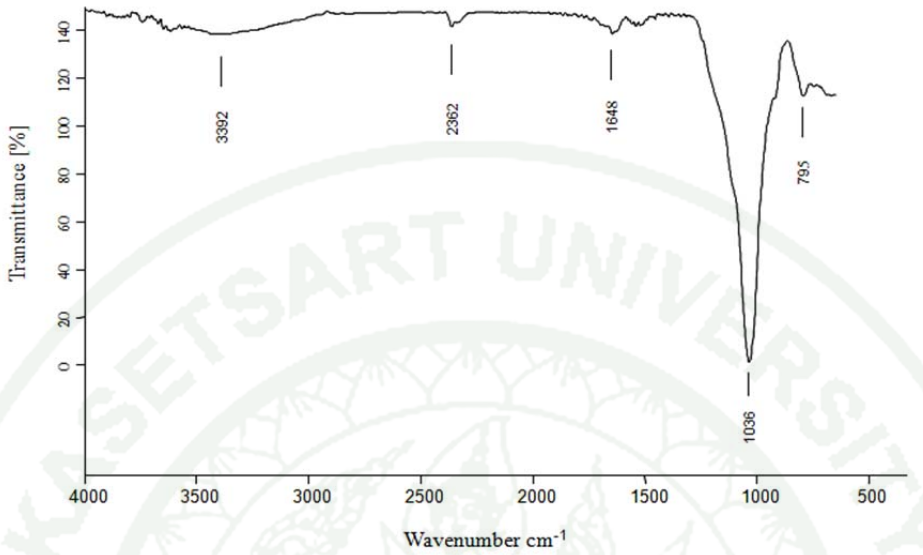

Appendix Figure A5 The FT-IR spectrum of montmorillonite K10.

Appendix B

Calculation the relative pressure, constant of spring and amount of water vapor

1. Calculation of relative pressure

The Clausius-Clapeyron equation

$$\ln \frac{P_2}{P_1} = \left(-\frac{\Delta H_{vap}}{R}\right)\left(\frac{T_2 - T_1}{T_2 T_1}\right)$$

where T_1 and P_1 = the corresponding absolute temperature and vapor pressure.

T_2 and P_2 = the corresponding temperature and pressure at another point.

ΔH_{vap} = the heat of vaporization of the liquid in (J/mol).

R = the universal gas constant whose value is 8.3143(J/mol.K).

For example, the temperature of heat of water vapor was calculated the relative pressure by the Clausius-Clapeyron equation as follows;

T_1 = 298 K

T_2 = 318 K

P_{298} = 1 atm or 760 torr

ΔH_{vap} = 43.990 kJ/mol; at temperature 25 ^{o}C

R = 8.3143 (J/mol.K)

$$\ln \frac{P_{318}}{760 \text{ torr}} = \left(\frac{\text{-43.990 kJ/mol}}{8.3143 \text{ J/mol.K}}\right)\left(\frac{313 \text{ K - } 298 \text{ K}}{313 \text{ K x } 298 \text{ K}}\right)$$

$$\ln \frac{P_{318}}{760 \text{ torr}} = \left(\frac{-43.990 \times 10^3}{8.3143}\right)\left(\frac{15}{93274}\right)$$

$$\ln P_{318} = \ln 760 \times (-5.2910 \times 10^3) \times (0.1610 \times 10^{-3})$$

$$\ln P_{318} = \ln 760 \times 0.8520$$

$$\ln P_{318} = \left(\frac{0.8520}{2.3026}\right) = 0.3700$$

$$\log X = 10^{0.3700}$$

$= \quad 2.3442$

$P_{318} \quad = \quad 760 \text{ x } 2.3442 \text{ torr}$

$P_{318} \quad = \quad 1781.61 \quad \text{torr or } 1.7816 \text{ x } 10^3 \text{ torr}$

Therefore, the relative pressure (P/P_0) of water vapor at 45 ^{o}C or 313 K was 1.7816 x 10^3 torr.

2. Calculation of constant of spring

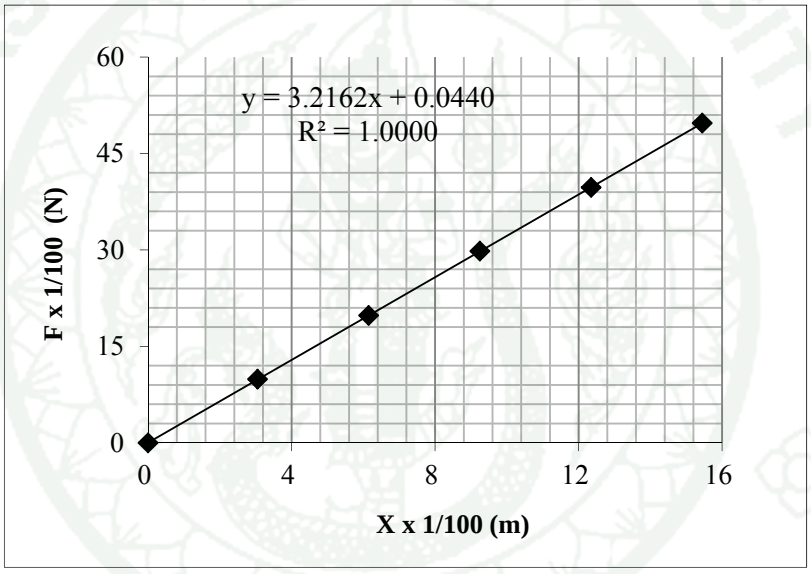

Appendix Figure B1 The standard curve of constant of spring.

Calculate the constant of spring as following;

$$k = \frac{\Delta F}{\Delta x} = \text{Slope}$$

$$= \frac{\Delta F}{\Delta x}$$

$$= \frac{38.50 - 10.0 \times 10^{-3}\ \text{N}}{12.00 - 3.05 \times 10^{-2}\ \text{m}}$$

$$= 0.3296\ \text{N/m}$$

Therefore, the constant of spring was 0.3296 N/m.

3. Calculation of water vapor value

$$F = kx$$

where F = the restoring force exerted by the material (unit is N)
x = the displacement of spring at equilibrium (unit is m)
k = the spring constant (unit is N/m)

$k = 0.3167$ N/m
$x = 0.1000 \times 10^{-2}$ m

$$F = (0.3167\ \text{N/m}) \times (0.1000 \times 10^{-2}\ \text{m})$$
$$= 3.1670 \times 10^{-4}\ \text{N}$$

Therefore, the force exerted by the water vapor was 3.1670×10^{-4} N.

From Newton's law

$$F = ma$$

where F is the net force, m is mass in kilograms and a is acceleration in m/s^2.

$F = 3.1670 \times 10^{-4}$ N
$M = 0.5000$ g

$$m = \frac{F}{a}$$

$$= \frac{3.1670 \times 10^{-4}\ N}{9.8} \times 1000\ g$$

$$= \frac{0.03232\ g}{0.5000\ g}$$

$$= 0.06463\ g/g$$

Therefore, the amount of water vapor onto coconut shell powder was 0.06463 g/g.

Appendix C

Calculation the specific surface area

1. Calculation of specific surface area

$$S = \frac{Q_o}{MW} \; x \; N \; x \; a$$

where S = the specific surface area (m^2/g)

Q_o = the maximum surface coverage (formation of monolayer) of sorbent (mg/g)

MW = the molecular weight (g/mol)

N = the Avogadro number (6.02×10^{23} molecule/mol)

a = the cross sectional area of adsorbate ($Å^2$)

For example, the specific surface area of bentonite for adsorption of chromium (VI) was calculated as follows;

Q_o = 0.8338 mg/g

MW = 51.9900 g/mol

N = 6.02×10^{23} molecule/mol

a = 3.1 $Å^2$

$$S = \frac{0.8338}{51.9900} \text{ x } 6.02 \text{ x } 10^{23} \text{ x } 3.1 = 0.0299 \text{ x } 10^{21} \; Å^2/g$$

$$= 0.2990 \; m^2/g$$

Therefore, the specific surface area of bentonite for adsorption of chromium (VI) was m^2/g.

Note: Cr (VI); MW = 51.99 g/mol, a = 3.1 $Å^2$

Phenol; MW = 94.11 g/mol, a = 52.2 Å

Appendix D

Calculation the values of phenol adsorption and chromium (VI) on chars

1. Calculation value adsorption of phenol

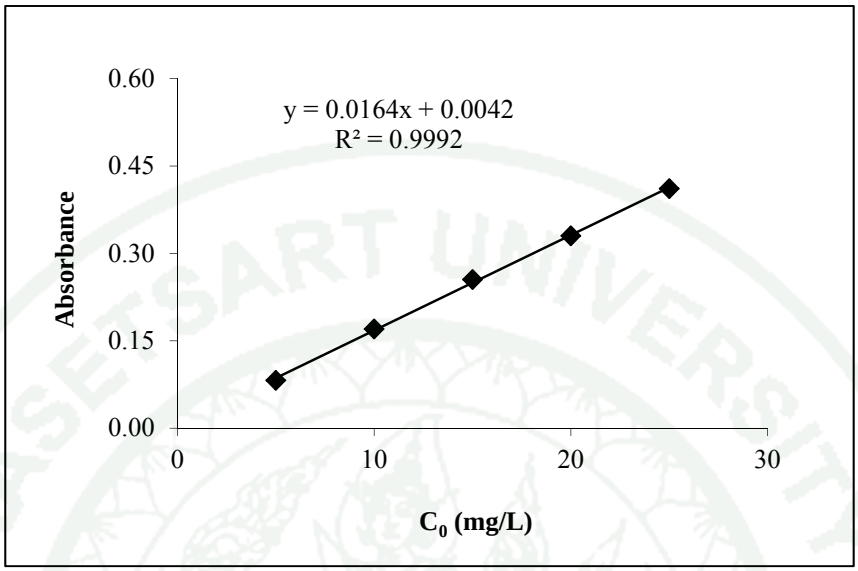

Appendix Figure D1 The standard curve of phenol

The values adsorption of phenol on char from bamboo was calculated as follows;

The phenol solution was diluted as 4 fractions

y = absorbance = 0.103

$$y = 0.0164x + 0.0042$$

$$x = \frac{y - 0.0042}{0.0164} = \frac{0.103 - 0.0042}{0.0164}$$

$$= 6.0244 \times 4$$

$$= 24.0976 \text{ mg/L}$$

Therefore, the phenol value of char from bamboo was 24.097 mg/L.

2. Calculation of chromium (VI) value

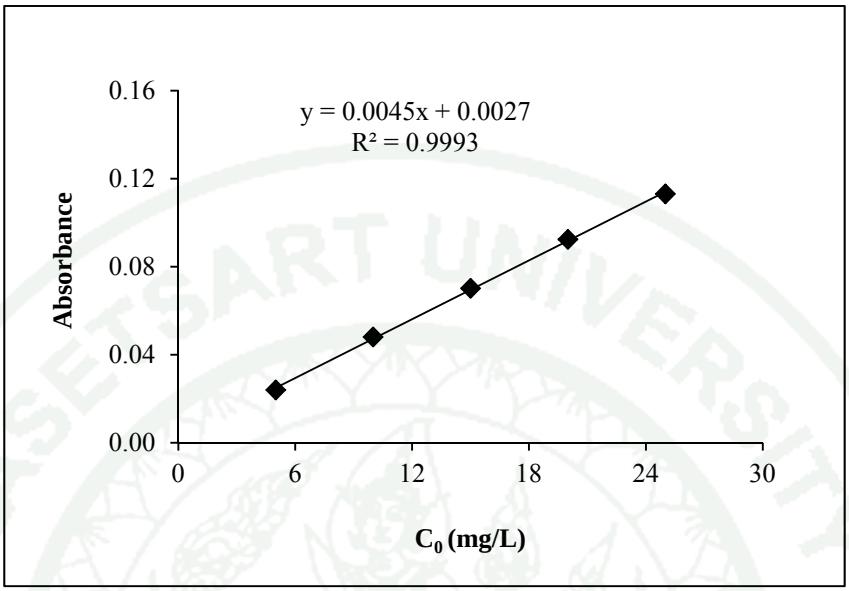

Appendix Figure D2 The standard curve of chromium (VI).

The values adsorption of chromium (VI) on char from bamboo was calculated as follows;

The chromium (VI) solution was diluted as 4 fractions

y = absorbance = 0.055

$$y = 0.0045x + 0.0027$$

$$x = \frac{y - 0.0027}{0.0045} = \frac{0.055 - 0.0027}{0.0045}$$

$$= 11.6222 \times 4$$

$$= 46.49 \text{ mg/L}$$

Therefore, the chromium (VI) value of char from bamboo was 46.49 mg/L.

Appendix E

Calculation the Langmuir and Freundlich constants for adsorption of phenol on chars

1. Calculation of Langmuir constants.

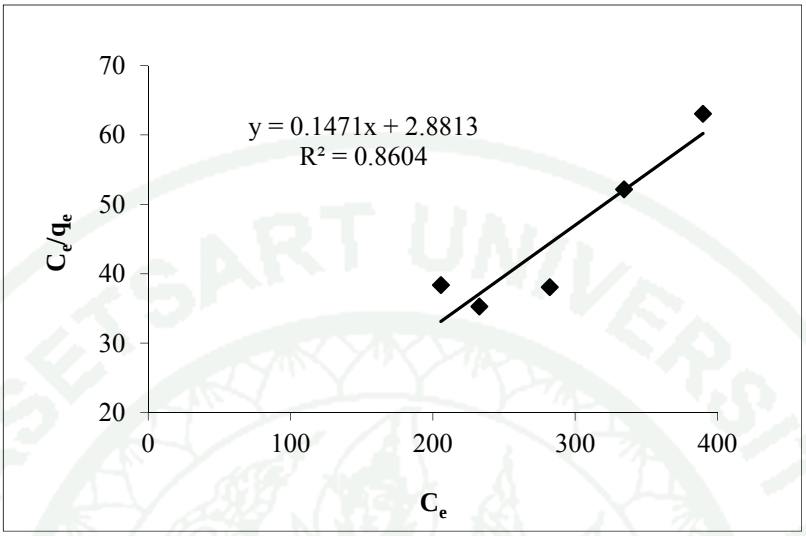

Appendix Figure E1 The Langmuir isotherm plots of C_e/q_e versus C_e for adsorption of phenol on char from bamboo.

Calculate the Langmuir constants as following;

$$\frac{C_e}{q_e} = \frac{1}{Q_0 b} + \frac{C_e}{Q_0}$$

where Ce is the equilibrium concentration of the adsorbate (mg/L)

qe is the amount of adsorbate per unit mass of adsorbent (mg/g)

Q_0 is the maximum surface coverage (formation of monolayer) of sorbent (mg/g)

b is the adsorption energy constant of Langmuir adsorption isotherm (L/mg)

For example, the adsorption isotherm of phenol adsorbed onto char from bamboo. The constants can be evaluated from the intercept and the slope of the linear plot of experimental data of C_e/q_e versus C_e.

$$\text{Slope} = \frac{1}{Q_o}$$

$$Q_o = \frac{1}{\text{Slope}}$$

$$Q_o = \frac{1}{0.1471}$$

$$= 6.7981 \text{ mg/g}$$

$$\text{Intercept} = \frac{1}{Q_o b}$$

$$b = \frac{1}{\text{Intercept x } Q_o}$$

$$b = \frac{1}{6.7981 \text{ x } 2.8813}$$

$$= \frac{1}{19.5874}$$

$$= 0.0510 \text{ L/mg}$$

Therefore, the Q_0 and b of Langmuir constants were 6.7981 mg/g and 0.0510 L/mg, respectively.

2. Calculation of Freundlich constants.

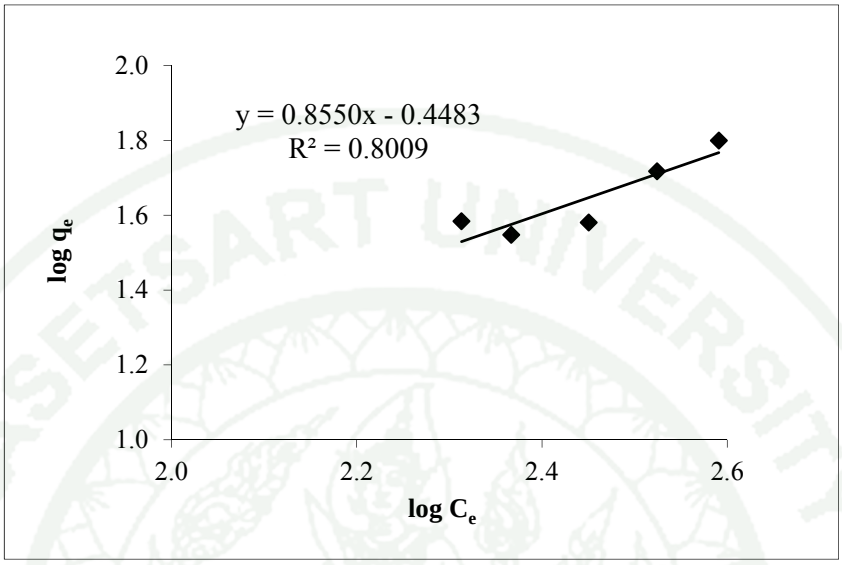

Appendix Figure E2 The Freundlich isotherm plots of log qe versus log Ce for adsorption of phenol on char forom bamboo.

Calculate the Langmuir constants as following;

$$\log q_e = \log K_F + \frac{1}{n} \log C_e$$

where q_e is the amount adsorbed at equilibrium (mg/g).

C_e is the equilibrium concentration of the adsorbate (mg/L).

K_F is the Freundlich isotherm constant related to adsorption capacity $((mg^{-1})(mg^{-1})^{1/n})$.

n is the Freundlich isotherm constant related to adsorption intensity.

For example, the adsorption isotherm of phenol adsorbed onto char from bamboo. The constants can be evaluated from the intercept and the slope of the linear plot of experimental data of log q_e versus log C_e.

$$\text{Slope} = \frac{1}{n} = 0.8550$$

$$\text{Intercept} = \log K_F$$

$$K_F = 10^{\text{Intercept}} = 10^{0.4483}$$

$$= 2.8074$$

Therefore, the 1/n and K_F of Freundlich constants were 0.8550 and 2.8074, respectively.

Appendix F

Calculate the distribution coefficient value of water vapor and phenol adsorption

1. Calculation K_D value of water vapor adsorption.

Calculate the distribution coefficient as following;

$$K_D = \frac{S}{1 - S}$$

where K_D = the distribution coefficient is defined as the concentration of a species adsorbed per gram of the adsorbent.

S = the adsorption coefficient at given temperature (g/g).

For example, the K_D value for the adsorption of water vapor on char from bamboo at temperature 40 ^oC was calculated as follows;

$$S = \frac{X}{m} = 0.06464 \text{ g/g}$$

m = 0.5000 g

x = 0.03232 g

$$K_D = \frac{0.06464}{1 - 0.06464}$$

$$= 0.0691$$

Therefore, the K_D value for the adsorption of water vapor on char from bamboo at temperature 40 ^oC was 0.0691.

.

2. Calculation K_D value of phenol adsorption.

$$K_D = \frac{C_e}{C_0}$$

Where C_e = the concentration of adsorbate on adsorbent at equilibrium (mg/L).

C_0 = the concentration of adsorbate in solution phase at equilibrium (mg/L).

For example, the K_D value for the adsorption of phenol concentration 320 mg/L on char from bamboo at temperature 60 ^oC was calculated as follows;

C_e = 135.00 mg/L.

C_0 = 185.00 mg/L.

$$K_D = \frac{135.00}{185.00}$$

$$= 0.7297$$

Therefore, the K_D value for the adsorption of phenol concentration 320 mg/L on char from bamboo at temperature 60 ^oC was 0.7297.

Appendix G

Calculate the ΔH_{ads} , ΔH^o, ΔS^o and ΔG^o value of water vapor and phenol adsorption

1. Calculation heat of adsorption, ΔH_{ads} value of adsorption.

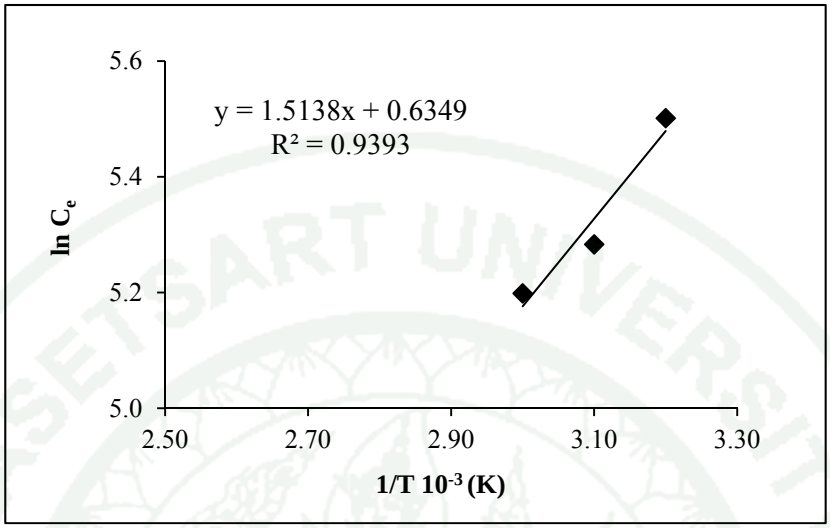

Appendix Figure G1 The Clausius-Clapeyron plots at various temperatures 1/T versus ln C_e for adsorption of phenol on char from bamboo.

Calculate the heat of adsorptin as following;

$$\ln C_e = -\frac{\Delta H_{ads}}{R}\frac{1}{T} + C$$

where ΔH_{ads} = the isosteric heat of adsorption (kJ/mol).

C_e = the equilibrium concentration (mmol/L).

T = absolute temperature (K).

R = the universal gas constant (8.314 J/K.mol).

C = the integration constant.

For example, the entropy, ΔH_{ads} value of phenol adsorption on char from bamboo was calculated as follows;

$$-\frac{\Delta H_{ads}}{R} = \text{Slope} = 1.5138$$

ΔH_{ads} = − Slope x R = −1.5138 x 8.314

= − 12.5857/1,000 J/mol

= − 0.01258 kJ/mol

Therefore, the ΔH_{ads} value for adsorption of phenol on char from bamboo was −0.01258 kJ/mol.

2. Calculation enthalpy and entropy value of adsorption.

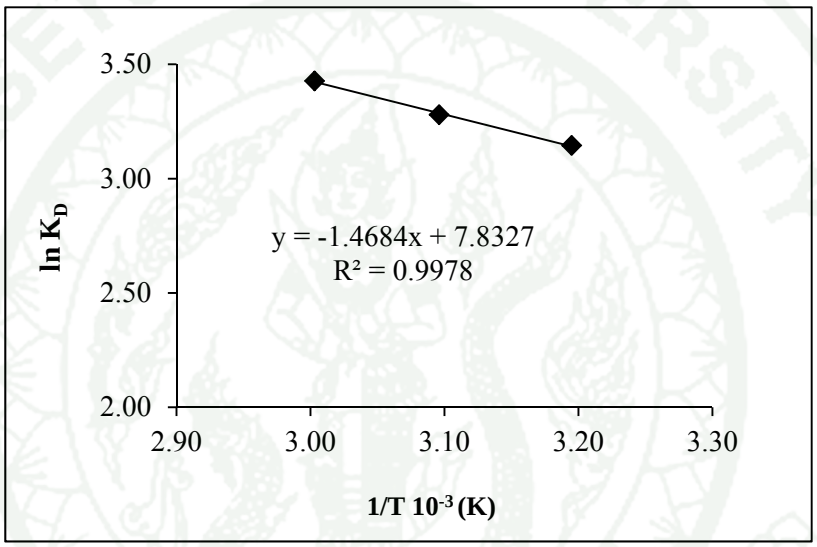

Appendix Figure G2 The Van't Hoff plots at various temperatures 1/T versus ln K_D for adsorption of phenol on char from bamboo.

Calculate the enthalpy, entropy as following;

$$\ln K_D = -\frac{\Delta H^o}{RT} + \frac{\Delta S^o}{R}$$

where K_D = the equilibrium constant.

ΔH^o = the enthalpy of adsorption (kJ/mol).

ΔS^o = the entropy of adsorption (J/mol.K).

R = the gas constant (8.314 J/mol.K).

T = absolute temperature (K).

For example, the enthalpy, ΔH^o value for adsorption of phenol on char from bamboo was calculated as follows;

$$-\frac{\Delta H^o}{R} = \text{Slope} = -1.4684$$

$$-\Delta H^o = -\text{Slope x R} = -(-1.4684 \text{ x } 8.314)$$

$$= 12.2083/1{,}000 \text{ J/mol.}$$

$$= 0.01220 \text{ kJ/mol.}$$

Therefore, the ΔH^o value value for adsorption of phenol on char from bamboo was 0.01220 kJ/mol.

For example, the entropy, ΔS^o value of phenol adsorption on char from bamboo was calculated as follows;

$$\frac{\Delta S^o}{R} = \text{Intercept} = 7.8327$$

$$\Delta S^o = \text{Intercept x R} = 7.8327 \text{ x } 8.314$$

$$= 65.1568 \text{ J/mol.K}$$

Therefore, the ΔS^o value value for adsorption of phenol on char from bamboo was 65.1568 J/mol.K.

3. Calculation free energy value of adsorption.

Calculate the free energy as following;

$$\Delta G^o = \Delta H^o - T\Delta S^o$$

For example, the free energy, ΔG^o value of phenol adsorption on char from bamboo at temperature 40 ^oC was calculated as follows;

$$\Delta G^{o} = 0.0122 - \frac{313 \times 65.16}{1{,}000}$$

$$= 0.0122 - 20.3951$$

$$= -20.383 \text{ kJ/mol.}$$

Therefore, the ΔG^{o} value value for adsorption of phenol on char from bamboo was -20.383 kJ/mol.

Appendix H

Raw data of phenol adsorption on chars and adsorption isotherm of phenol by various temperatures

Appendix Table H1 Adsorption of phenol onto char from bamboo by varies adsorbent dosage in range of 0.0500 –1.000 g.

Adsorbent dosage (g)	Absorbance				Concentration of phenol (mg/L)			S.D.
	Repeat 1	Repeat 2	Repeat 3	Average	C_0	C_e	(C_0-C_e)	
0.0500	0.355	0.361	0.342	0.353	100	82.32	18	±0.0097
0.1000	0.303	0.291	0.298	0.297	100	69.30	31	±0.0060
0.1500	0.344	0.249	0.265	0.286	100	66.64	33	±0.0509
0.2000	0.268	0.226	0.223	0.239	100	55.58	44	±0.0252
0.2500	0.193	0.201	0.198	0.197	100	45.77	54	±0.0040
0.3000	0.178	0.175	0.169	0.174	100	40.28	60	±0.0046
0.3500	0.178	0.165	0.159	0.167	100	38.71	61	±0.0097
0.4000	0.173	0.165	0.162	0.167	100	38.56	61	±0.0057

Appendix Table H1 (Continued)

Adsorbent dosage (g)	Absorbance				Concentration of phenol (mg/L)			S.D.
	Repeat 1	Repeat 2	Repeat 3	Average	C_0	C_e	(C_0-C_e)	
0.4500	0.172	0.195	0.13	0.166	100	38.32	62	±0.0330
0.5000	0.136	0.157	0.119	0.137	100	31.65	68	±0.0190
0.5500	0.132	0.161	0.135	0.143	100	32.91	67	±0.0159
0.6000	0.110	0.158	0.133	0.134	100	30.79	69	±0.0240
0.6500	0.125	0.166	0.119	0.137	100	31.50	69	±0.0256
0.7000	0.104	0.154	0.112	0.123	100	28.36	72	±0.0269
0.7500	0.119	0.164	0.125	0.136	100	31.34	69	±0.0244
0.8000	0.130	0.192	0.126	0.149	100	34.48	66	±0.0370

Appendix Table H1 (Continued)

Adsorbent dosage (g)	Absorbance				Concentration of phenol (mg/L)			S.D.
	Repeat 1	Repeat 2	Repeat 3	Average	C_0	C_e	(C_0-C_e)	
0.8500	0.103	0.179	0.149	0.144	100	33.15	67	±0.0383
0.9000	0.116	0.191	0.142	0.150	100	34.56	65	±0.0381
0.9500	0.123	0.195	0.207	0.175	100	40.52	59	±0.0454
1.0000	0.132	0.165	0.171	0.156	100	36.05	64	±0.0210

Appendix Table H2 Adsorption of phenol onto char from oil palm shell by varies adsorbent dosage in range of 0.0500 – 1.000 g.

Adsorbent dosage (g)	Absorbance				Concentration of phenol (mg/L)			S.D.
	Repeat 1	Repeat 2	Repeat 3	Average	C_0	C_e	(C_0-C_e)	
0.0500	0.284	0.253	0.238	0.258	100	60	40	±0.023
0.1000	0.115	0.178	0.164	0.152	100	35	65	±0.033
0.1500	0.104	0.106	0.114	0.108	100	25	75	±0.005
0.2000	0.082	0.074	0.102	0.086	100	20	80	±0.014
0.2500	0.081	0.062	0.084	0.076	100	17	83	±0.012
0.3000	0.082	0.079	0.086	0.082	100	19	81	±0.004
0.3500	0.080	0.067	0.089	0.079	100	18	82	±0.011
0.4000	0.129	0.061	0.084	0.091	100	21	79	±0.035

Appendix Table H2 (Continued)

Adsorbent dosage (g)	Absorbance				Concentration of phenol (mg/L)			S.D.
	Repeat 1	Repeat 2	Repeat 3	Average	C_0	C_e	(C_0-C_e)	
0.4500	0.135	0.070	0.091	0.099	100	23	77	±0.033
0.5000	0.140	0.076	0.100	0.105	100	24	76	±0.032
0.5500	0.068	0.109	0.094	0.090	100	24	76	±0.021
0.6000	0.082	0.091	0.108	0.094	100	25	75	±0.013
0.6500	0.079	0.094	0.070	0.081	100	22	78	±0.012
0.7000	0.101	0.072	0.077	0.083	100	22	78	±0.016
0.7500	0.093	0.127	0.127	0.116	100	31	69	±0.020
0.8000	0.082	0.083	0.084	0.083	100	22	78	±0.001

Appendix Table H2 (Continued)

Adsorbent dosage (g)	Absorbance				Concentration of phenol (mg/L)			S.D.
	Repeat 1	Repeat 2	Repeat 3	Average	C_0	C_e	(C_0-C_e)	
0.8500	0.113	0.083	0.075	0.090	100	24	76	±0.020
0.9000	0.108	0.070	0.049	0.076	100	20	80	±0.030
0.9500	0.117	0.055	0.095	0.089	100	24	76	±0.031
1.0000	0.138	0.088	0.098	0.108	100	25	75	±0.026

Appendix Table H3 Adsorption of phenol onto char from coconut shell by varies adsorbent dosage in range of 0.0500 – 1.000 g.

Adsorbent dosage (g)	Absorbance				Concentration of phenol (mg/L)			S.D.
	Repeat 1	Repeat 2	Repeat 3	Average	C_0	C_e	(C_0-C_e)	
0.0500	0.345	0.369	0.370	0.361	105	100	5	±0.0142
0.1000	0.343	0.362	0.352	0.352	105	98	7	±0.0095
0.1500	0.368	0.328	0.339	0.345	105	96	9	±0.0207
0.2000	0.357	0.338	0.339	0.345	105	95	9	±0.0107
0.2500	0.368	0.342	0.329	0.346	105	96	9	±0.0199
0.3000	0.350	0.355	0.354	0.353	105	98	7	±0.0026
0.3500	0.337	0.353	0.367	0.352	105	98	7	±0.0150
0.4000	0.336	0.345	0.320	0.334	105	92	12	±0.0127

Appendix Table H3 (Continued)

Adsorbent dosage	Absorbance				Concentration of phenol (mg/L)			S.D.
(g)	Repeat 1	Repeat 2	Repeat 3	Average	C_0	C_e	(C_0-C_e)	
0.4500	0.337	0.326	0.332	0.332	105	92	13	±0.0055
0.5000	0.316	0.322	0.284	0.307	105	85	20	±0.0204
0.5500	0.338	0.322	0.296	0.319	105	88	17	±0.0212
0.6000	0.326	0.305	0.293	0.308	105	85	20	±0.0167
0.6500	0.308	0.322	0.271	0.300	105	83	22	±0.0264
0.7000	0.328	0.310	0.280	0.306	105	85	20	±0.0242
0.7500	0.315	0.321	0.300	0.312	105	86	18	±0.0108
0.8000	0.317	0.318	0.311	0.315	105	87	18	±0.0038

Appendix Table H3 (Continued)

Adsorbent dosage	Absorbance				Concentration of phenol (mg/L)			S.D.
(g)	Repeat 1	Repeat 2	Repeat 3	Average	C_0	C_e	(C_0-C_e)	
0.8000	0.317	0.318	0.311	0.315	105	87	18	±0.0038
0.8500	0.329	0.253	0.294	0.292	105	81	24	±0.0380
0.9000	0.337	0.327	0.296	0.320	105	89	16	±0.0214
0.9500	0.338	0.339	0.303	0.327	105	90	14	±0.0205
1.0000	0.344	0.324	0.320	0.329	105	91	14	±0.0129

Appendix Table H4 Adsorption of phenol onto char from bamboo by varies concentration of phenol in range of 60 – 400 mg/L.

Concentration of phenol (mg/L)	Absorbance				Concentration of phenol (mg/L)			S.D.
	Repeat 1	Repeat 2	Repeat 3	Average	C_0	C_e	(C_0-C_e)	
60	0.126	0.124	0.131	0.127	60	29	31	±0.0036
100	0.195	0.185	0.183	0.188	100	43	57	±0.0064
150	0.117	0.134	0.137	0.129	165	74	91	±0.0108
200	0.187	0.186	0.189	0.187	218	109	110	±0.0015
250	0.192	0.247	0.252	0.230	271	134	137	±0.0333
300	0.290	0.208	0.215	0.238	305	138	167	±0.0455
350	0.339	0.301	0.360	0.333	367	194	172	±0.0299
400	0.418	0.404	0.397	0.406	419	237	182	±0.0107

Appendix Table H5 Adsorption of phenol onto char from oil palm shell by varies concentration of phenol in range of 60 – 400 mg/L.

Concentration of phenol (mg/L)	Absorbance				Concentration of phenol (mg/L)			S.D.
	Repeat 1	Repeat 2	Repeat 3	Average	C_0	C_e	(C_0-C_e)	
60	0.007	0.005	0.013	0.008	46	4	41	±0.004
100	0.011	0.007	0.012	0.010	104	6	99	±0.003
150	0.029	0.028	0.023	0.027	151	20	130	±0.003
200	0.045	0.045	0.043	0.044	226	36	190	±0.001
250	0.076	0.075	0.072	0.074	253	62	191	±0.002
300	0.103	0.100	0.098	0.100	297	85	213	±0.003
350	0.134	0.132	0.138	0.135	338	115	223	±0.003
400	0.239	0.183	0.173	0.198	395	170	225	±0.036

Appendix Table H6 Adsorption of phenol onto char from coconut shell by varies concentration of phenol in range of 60 – 1,000 mg/L.

Concentration of phenol (mg/L)	Absorbance				Concentration of phenol (mg/L)			S.D.
	Repeat 1	Repeat 2	Repeat 3	Average	C_0	C_e	(C_0-C_e)	
60	0.033	0.037	0.031	0.034	56	27	29	±0.0031
100	0.072	0.077	0.075	0.075	114	62	52	±0.0025
150	0.150	0.136	0.137	0.141	156	120	36	±0.0078
200	0.190	0.179	0.176	0.182	204	156	48	±0.0074
250	0.210	0.210	0.211	0.210	264	181	83	±0.0006
300	0.279	0.270	0.256	0.268	307	232	76	±0.0116
350	0.204	0.208	0.206	0.206	372	283	88	±0.0020
400	0.236	0.245	0.237	0.239	400	330	69	±0.0049
600	0.228	0.223	0.235	0.229	468	394	74	±0.0060

Appendix Table H6 (Continued)

Concentration of phenol (mg/L)	Absorbance				Concentration of phenol (mg/L)			S.D.
	Repeat 1	Repeat 2	Repeat 3	Average	C_0	C_e	(C_0-C_e)	
800	0.247	0.257	0.245	0.250	845	689	156	±0.0064
1,000	0.357	0.348	0.353	0.353	1,127	977	150	±0.0045

Appendix Table H7 Adsorption of phenol onto char from bamboo by varies contact time from 1 – 8 hours.

Contact time	Absorbance				Concentration of phenol (mg/L)			S.D.
(h.)	Repeat 1	Repeat 2	Repeat 3	Average	C_0	C_e	(C_0-C_e)	
1	0.349	0.361	0.359	0.356	347	309	38	±0.0064
2	0.291	0.361	0.359	0.337	347	292	55	±0.0398
3	0.277	0.301	0.286	0.288	347	249	98	±0.0121
4	0.202	0.213	0.231	0.215	347	185	162	±0.0146
5	0.243	0.238	0.245	0.242	347	209	138	±0.0036
6	0.261	0.274	0.249	0.261	347	226	121	±0.0125
7	0.247	0.273	0.264	0.261	347	226	121	±0.0132
8	0.258	0.239	0.227	0.241	347	208	139	±0.0156

Appendix Table H8 Adsorption of phenol onto char from oil palm shell by varies contact time from 1 – 8 hours.

Contact time	Absorbance				Concentration of phenol (mg/L)			S.D.
(h.)	Repeat 1	Repeat 2	Repeat 3	Average	C_0	C_e	(C_0-C_e)	
1	0.242	0.255	0.255	0.251	365	216	148	±0.008
2	0.193	0.226	0.217	0.212	365	182	182	±0.017
3	0.176	0.170	0.170	0.172	365	147	217	±0.003
4	0.174	0.178	0.181	0.178	365	152	212	±0.004
5	0.168	0.169	0.175	0.171	365	146	218	±0.004
6	0.148	0.148	0.147	0.148	365	126	238	±0.001
7	0.155	0.142	0.140	0.146	365	124	240	±0.008
8	0.140	0.146	0.151	0.146	365	124	240	±0.006

Appendix Table H9 Adsorption of phenol onto char from coconut shell by varies contact time from 1 – 8 hours.

Contact time	Absorbance				Concentration of phenol (mg/L)			S.D.
(h.)	Repeat 1	Repeat 2	Repeat 3	Average	C_0	C_e	(C_0-C_e)	
1	0.333	0.346	0.338	0.339	939	939	0	±0.0066
2	0.345	0.347	0.325	0.339	939	939	0	±0.0122
3	0.298	0.324	0.314	0.312	939	863	76	±0.0131
4	0.318	0.318	0.274	0.303	939	839	100	±0.0254
5	0.303	0.311	0.298	0.304	939	841	98	±0.0066
6	0.289	0.316	0.312	0.306	939	846	93	±0.0146
7	0.314	0.301	0.298	0.304	939	842	97	±0.0085
8	0.289	0.286	0.296	0.290	939	803	136	±0.0051

Appendix Table H10 Adsorption isotherm of phenol onto char from bamboo at room temperature (30±5°C).

Initial Concentration	Absorbance				Concentration of phenol (mg/L)			log C_e	q_e	log q_e	C_e/q_e	S.D.
(mg/L)	Repeat 1	Repeat 2	Repeat 3	Average	C_0	C_e	(C_0-C_e)					
300	0.168	0.157	0.155	0.160	321	219	102	2.341	5.361	1.584	38.356	±0.007
350	0.175	0.183	0.186	0.181	368	249	119	2.396	6.597	1.547	35.272	±0.006
400	0.201	0.186	0.188	0.192	414	263	150	2.421	7.413	1.580	38.057	±0.008
450	0.220	0.221	0.220	0.220	466	304	163	2.482	6.41	1.717	52.153	±0.001
500	0.254	0.255	0.253	0.254	520	351	170	2.545	6.184	1.800	63.037	±0.001

Appendix Table H11 Adsorption isotherm of phenol onto char from bamboo at temperature 40 C^{o}.

Initail Concentration	Absorbance				Concentration of phenol (mg/L)			log C_e	q_e	log C_e	C_e/q_e	S.D.
(mg/L)	Repeat 1	Repeat 2	Repeat 3	Average	C_0	C_e	(C_0-C_e)					
300	0.171	0.163	0.164	0.166	320	228	92	2.357	4.615	1.693	49.303	±0.004
350	0.186	0.190	0.190	0.189	373	259	114	2.414	5.688	1.659	45.582	±0.002
400	0.219	0.220	0.191	0.210	423	289	134	2.461	6.713	1.634	43.063	±0.016
450	0.225	0.226	0.229	0.227	481	312	168	2.495	8.415	1.57	37.125	±0.002
500	0.200	0.197	0.199	0.199	527	342	186	2.534	9.295	1.565	36.75	±0.001

Appendix Table H12 Adsorption isotherm of phenol onto char from bamboo at temperature 50 C^{o}.

Initail Concentration	Absorbance				Concentration of phenol (mg/L)			log C_e	q_e	log C_e	C_e/q_e	S.D.
(mg/L)	Repeat 1	Repeat 2	Repeat 3	Average	C_0	C_e	(C_0-C_e)					
300	0.101	0.110	0.112	0.108	320	146	174	2.164	8.695	1.225	16.788	±0.006
350	0.163	0.165	0.165	0.164	373	225	148	1.353	7.389	1.484	30.479	±0.001
400	0.209	0.199	0.195	0.201	423	277	147	2.442	7.343	1.576	37.657	±0.007
450	0.230	0.235	0.236	0.234	481	322	159	2.508	7.925	1.609	40.653	±0.003
500	0.214	0.216	0.195	0.208	527	358	169	2.554	8.45	1.628	42.421	±0.012

Appendix Table H13 Adsorption isotherm of phenol onto char from bamboo at temperature 60 C^{o}.

Initail Concentration	Absorbance				Concentration of phenol (mg/L)			Log C_e	q_e	Log C_e	C_e/q_e	S.D.
(mg/L)	Repeat 1	Repeat 2	Repeat 3	Average	C_0	C_e	(C_0-C_e)					
300	0.129	0.138	0.140	0.136	320	185	135	2.268	6.737	1.439	27.481	±0.006
350	0.173	0.175	0.168	0.172	373	236	137	2.373	6.853	1.537	34.429	±0.004
400	0.193	0.194	0.185	0.191	423	262	161	2.418	8.065	1.512	32.491	±0.005
450	0.218	0.212	0.201	0.210	443	290	153	2.462	7.669	1.577	37.757	±0.009
500	0.190	0.193	0.183	0.189	527	324	203	2.511	10.169	1.503	31.868	±0.005

Appendix Table H14 Adsorption isotherm of phenol onto char from oil palm shell at room temperature (30±5°C).

Initail Concentration	Absorbance				Concentration of phenol (mg/L)			log C_e	q_e	log q_e	C_e/q_e	S.D.
(mg/L)	Repeat 1	Repeat 2	Repeat 3	Average	C_0	C_e	(C_0-C_e)					
300	0.121	0.123	0.120	0.121	332	103	229	2.014	22.927	0.653	4.500	±0.002
350	0.144	0.143	0.138	0.142	366	121	245	2.083	24.506	0.693	4.935	±0.003
400	0.146	0.152	0.150	0.149	397	128	269	2.106	26.913	0.676	4.743	±0.003
450	0.175	0.176	0.180	0.177	421	152	269	2.181	26.872	0.752	5.65	±0.003
500	0.245	0.241	0.241	0.242	501	209	292	2.320	29.228	0.854	7.149	±0.002

Appendix Table H15 Adsorption isotherm of phenol onto char from oil palm shell at temperature 40 C^{o}.

Initail Concentration	Absorbance				Concentration of phenol (mg/L)			log C_e	q_e	log q_e	C_e/q_e	S.D.
(mg/L)	Repeat 1	Repeat 2	Repeat 3	Average	C_0	C_e	(C_0-C_e)					
300	0.054	0.063	0.021	0.046	320	60	260	1.776	26.014	0.361	2.296	±0.022
350	0.059	0.043	0.059	0.054	373	70	303	1.848	30.256	0.367	2.328	±0.010
400	0.087	0.098	0.074	0.086	423	116	307	2.065	30.723	0.5776	3.78	±0.012
450	0.110	0.128	0.098	0.112	470	190	280	2.279	27.972	0.832	6.794	±0.015
500	0.146	0.138	0.146	0.143	520	245	276	2.389	27.564	0.949	8.882	±0.046

Appendix Table H16 Adsorption isotherm of phenol onto char from oil palm shell at temperature 50 C^{o}.

Initail Concentration	Absorbance				Concentration of phenol (mg/L)			log C_e	q_e	log q_e	C_e/q_e	S.D.
(mg/L)	Repeat 1	Repeat 2	Repeat 3	Average	C_0	C_e	(C_0-C_e)					
300	0.062	0.064	0.097	0.074	320	99	221	1.997	22.051	0.654	4.505	±0.020
350	0.133	0.119	0.121	0.124	373	169	204	2.227	20.373	0.919	8.309	±0.008
400	0.086	0.098	0.099	0.094	423	159	264	2.202	26.421	0.78	6.024	±0.007
450	0.172	0.174	0.157	0.168	470	230	240	2.362	23.987	0.982	9.584	±0.010
500	0.111	0.113	0.124	0.116	499	197	302	2.295	30.245	0.814	6.515	±0.007

Appendix Table H17 Adsorption isotherm of phenol onto char from oil palm shell at temperature 60 C^{o}.

Initail Concentration	Absorbance				Concentration of phenol (mg/L)			log C_e	q_e	log q_e	C_e/q_e	S.D.
(mg/L)	Repeat 1	Repeat 2	Repeat 3	Average	C_0	C_e	(C_0-C_e)					
300	0.071	0.065	0.060	0.065	320	87	233	1.938	23.31	1.368	3.722	±0.006
350	0.094	0.083	0.080	0.086	373	115	258	2.061	25.781	1.411	4.468	±0.007
400	0.110	0.110	0.104	0.108	423	146	277	2.166	27.692	1.442	5.289	±0.004
450	0.147	0.166	0.157	0.157	470	214	255	2.331	25.526	1.407	8.403	±0.010
500	0.110	0.108	0.103	0.107	499	181	318	2.258	31.818	1.503	5.698	±0.004

Appendix Table H18 Adsorption isotherm of phenol onto char from coconut shell at room temperature (30±5°C).

Initail Concentration	Absorbance				Concentration of phenol (mg/L)			log C_e	q_e	log q_e	C_e/q_e	S.D.
(mg/L)	Repeat 1	Repeat 2	Repeat 3	Average	C_0	C_e	(C_0-C_e)					
800	0.245	0.240	0.237	0.241	810	664	146	2.822	7.319	1.958	90.713	±0.004
850	0.255	0.249	0.258	0.254	852	701	151	2.846	7.552	1.9678	92.852	±0.005
900	0.270	0.259	0.271	0.267	903	737	166	2.867	8.298	1.9483	88.775	±0.007
950	0.297	0.298	0.285	0.293	959	811	147	2.909	7.366	2.042	110.139	±0.007
1,000	0.309	0.309	0.300	0.306	992	847	145	2.928	7.273	2.066	116.423	±0.005

Appendix Table H19 Adsorption isotherm of phenol onto char from coconut shell at temperature 40 C^o.

Initail Concentration	Absorbance				Concentration of phenol (mg/L)			log C_e	q_e	log q_e	C_e/q_e	S.D.
(mg/L)	Repeat 1	Repeat 2	Repeat 3	Average	C_0	C_e	(C_0-C_e)					
800	0.260	0.262	0.275	0.266	805	734	71	2.866	3.543	2.316	207.132	±0.008
850	0.279	0.287	0.281	0.282	852	781	72	2.892	3.590	2.337	217.429	±0.004
900	0.311	0.306	0.298	0.305	928	844	84	2.926	4.196	2.305	201.133	±0.007
950	0.324	0.320	0.316	0.320	959	886	73	2.947	3.636	2.387	243.615	±0.004
1,000	0.351	0.350	0.349	0.350	1,006	970	36	2.987	1.808	2.730	536.480	±0.001

Appendix Table H20 Adsorption isotherm of phenol onto char from coconut shell at temperature 50 C^o.

Initail Concentration	Absorbance				Concentration of phenol (mg/L)			log C_e	q_e	log q_e	C_e/q_e	S.D.
(mg/L)	Repeat 1	Repeat 2	Repeat 3	Average	C_0	C_e	(C_0-C_e)					
800	0.211	0.206	0.228	0.215	805	592	213	2.772	10.629	1.746	55.710	±0.011
850	0.154	0.160	0.159	0.158	825	432	421	2.635	21.026	1.313	20.537	±0.003
900	0.170	0.177	0.175	0.174	911	477	434	2.679	21.678	1.343	22.026	±0.004
950	0.188	0.179	0.180	0.182	959	501	458	2.699	22.890	1.340	21.878	±0.005
1,000	0.207	0.210	0.187	0.201	1,027	554	473	2.743	23.649	1.370	23.423	±0.012

Appendix Table H21 Adsorption isotherm of phenol onto char from coconut shell at temperature 60 C^o.

Initail Concentration	Absorbance				Concentration of phenol (mg/L)			log C_e	q_e	log q_e	C_e/q_e	S.D.
(mg/L)	Repeat 1	Repeat 2	Repeat 3	Average	C_0	C_e	(C_0-C_e)					
800	0.165	0.172	0.161	0.166	805	455	350	2.658	17.483	1.416	26.032	±0.005
850	0.158	0.159	0.160	0.159	852	436	417	2.639	20.839	1.32	20.899	±0.001
900	0.142	0.135	0.130	0.136	911	370	541	2.567	27.04	1.136	13.693	±0.006
950	0.116	0.120	0.110	0.115	959	313	645	2.496	32.261	0.987	9.714	±0.005
1,000	0.077	0.065	0.073	0.072	1,027	239	788	2.379	39.394	0.783	6.068	±0.006

Appendix I

Raw data of chromium (VI) adsorption on chars and soil minerals and adsorption isotherm

Appendix Table I1 Adsorption of chromium (VI) onto char from bamboo by varies adsorbent dosage in range of 0.0500 – 1.0000 g.

Adsorbent dosage (g)	Absorbance				Concentration of phenol (mg/L)			% Remove	S.D.
	Repeat 1	Repeat 2	Repeat 3	Average	C_0	C_e	(C_0-C_e)		
0.0500	0.054	0.054	0.055	0.054	63	46	17	27	±0.0006
0.2500	0.039	0.039	0.040	0.039	63	33	30	48	±0.0006
0.5000	0.049	0.041	0.048	0.046	63	10	53	85	±0.0044
0.6000	0.032	0.033	0.032	0.032	63	7	57	89	±0.0006
0.7500	0.031	0.034	0.030	0.032	63	7	57	90	±0.0021
1.0000	0.030	0.030	0.031	0.030	63	6	57	90	±0.0006

Appendix Table I2 Adsorption of chromium (VI) onto char from bamboo by varies contact time in range from 30 -240 minute.

Contact time	Absorbance				Concentration of phenol (mg/L)			% Remove	S.D.
(min.)	Repeat 1	Repeat 2	Repeat 3	Average	C_0	C_e	(C_0-C_e)		
30	0.061	0.058	0.066	0.062	64	13	50	79	±0.0040
60	0.043	0.041	0.058	0.047	64	10	54	84	±0.0093
90	0.035	0.036	0.035	0.035	64	7	56	88	±0.0006
120	0.034	0.035	0.037	0.035	64	7	56	88	±0.0015
180	0.034	0.034	0.036	0.035	64	7	56	89	±0.0012
240	0.039	0.033	0.036	0.036	64	7	56	88	±0.0030

Appendix Table I3 Adsorption of chromium (VI) onto char from bamboo by varies pH in range of 2 - 5.

pH	Absorbance				Concentration of phenol (mg/L)			% Remove	S.D.
	Repeat 1	Repeat 2	Repeat 3	Average	C_0	C_e	(C_0-C_e)		
2	0.034	0.033	0.031	0.033	54	4	51	93	±0.0015
3	0.103	0.100	0.099	0.101	57	16	41	72	±0.0021
4	0.124	0.126	0.127	0.126	57	20	37	64	±0.0015
5	0.114	0.117	0.116	0.116	62	37	25	40	±0.0015

Appendix Table I4 Adsorption of chromium (VI) onto char from bamboo by varies concentration in range of 30 – 300 mg/L.

Concentration of chromium (mg/L)	Absorbance				Concentration of chromium (VI) (mg/L)			% Remove	S.D.
	Repeat 1	Repeat 2	Repeat 3	Average	C_0	C_e	(C_0-C_e)		
30	0.020	0.038	0.020	0.026	24	2	22	90	±0.0104
50	0.044	0.044	0.055	0.048	37	6	31	83	±0.0064
100	0.049	0.049	0.049	0.049	75	33	42	56	±0.0000
150	0.049	0.048	0.050	0.049	103	65	38	37	±0.0010
200	0.084	0.082	0.087	0.084	154	129	25	16	±0.0025
300	0.100	0.101	0.098	0.100	272	251	21	8	±0.0015

Appendix Table I5 Adsorption of chromium (VI) onto char from oil palm shell by varies adsorbent dosage in range of 0.0500 – 1.0000 g.

Adsorbent dosage	Absorbance				Concentration of phenol (mg/L)			% Remove	S.D.
(g)	Repeat 1	Repeat 2	Repeat 3	Average	C_0	C_e	(C_0-C_e)		
0.0500	0.018	0.018	0.017	0.018	69	67	1	2	±0.0006
0.2500	0.014	0.014	0.014	0.014	69	51	18	26	±0.0000
0.5000	0.010	0.010	0.011	0.010	69	34	34	50	±0.0006
0.6000	0.005	0.005	0.005	0.005	69	10	58	85	±0.0000
0.7500	0.008	0.008	0.009	0.008	69	25	43	63	±0.0006
1.0000	0.008	0.010	0.006	0.008	69	24	45	65	±0.0020

Appendix Table I6 Adsorption of chromium (VI) onto char from oil palm shell by varies contact time in range from 30 - 240 minute.

Contact time	Absorbance				Concentration of phenol (mg/L)			% Remove	S.D.
(min.)	Repeat 1	Repeat 2	Repeat 3	Average	C_0	C_e	(C_0-C_e)		
30	0.012	0.011	0.012	0.012	69	40	28	41	±0.0006
60	0.018	0.015	0.010	0.014	69	52	16	24	±0.0040
90	0.091	0.089	0.084	0.088	69	19	50	72	±0.0036
120	0.014	0.012	0.015	0.014	69	31	38	55	±0.0015
180	0.063	0.055	0.054	0.057	69	12	57	82	±0.0049
240	0.007	0.007	0.007	0.007	69	12	57	82	±0.0000

Appendix Table I7 Adsorption of chromium (VI) onto char from oil palm shell by varies pH in range of 2 - 5.

pH	Absorbance				Concentration of phenol (mg/L)			% Remove	S.D.
	Repeat 1	Repeat 2	Repeat 3	Average	C_0	C_e	(C_0-C_e)		
2	0.047	0.046	0.048	0.047	54	10	44	82	±0.0010
3	0.091	0.093	0.088	0.091	57	20	37	65	±0.0025
4	0.010	0.011	0.012	0.011	57	19	38	67	±0.0010
5	0.014	0.017	0.016	0.016	57	29	28	49	±0.0015

Appendix Table I8 Adsorption of chromium (VI) onto char from oil palm shell by varies concentration in range of 30 – 300 mg/L.

Concentration of chromium (mg/L)	Absorbance				Concentration of chromium (VI) (mg/L)			% Remove	S.D.
	Repeat 1	Repeat 2	Repeat 3	Average	C_0	C_e	(C_0-C_e)		
30	0.046	0.045	0.056	0.049	32	10	21	67	±0.0061
50	0.060	0.058	0.064	0.061	60	13	47	78	±0.0031
100	0.027	0.029	0.023	0.026	127	53	74	58	±0.0031
150	0.048	0.050	0.050	0.049	186	105	81	44	±0.0012
200	0.066	0.064	0.065	0.065	223	140	83	37	±0.0010
300	0.074	0.073	0.075	0.074	284	200	84	30	±0.0010

Appendix Table I9 Adsorption of chromium (VI) onto char from coconut shell by varies adsorbent dosage in range of 0.0500 – 1.6000 g.

Adsorbent dosage	Absorbance				Concentration of phenol (mg/L)			% Remove	S.D.
(g)	Repeat 1	Repeat 2	Repeat 3	Average	C_0	C_e	(C_0-C_e)		
0.0500	0.055	0.054	0.058	0.056	63	48	16	25	±0.0021
0.2500	0.056	0.055	0.053	0.055	63	47	17	26	±0.0015
0.5000	0.044	0.044	0.044	0.044	63	37	26	41	±0.0000
0.7500	0.137	0.136	0.134	0.136	63	30	33	53	±0.0015
1.0000	0.102	0.101	0.105	0.103	63	22	41	64	±0.0021
1.2000	0.084	0.084	0.082	0.083	63	18	45	71	±0.0012
1.4000	0.072	0.073	0.075	0.073	63	16	47	75	±0.0015
1.6000	0.071	0.081	0.079	0.077	58	17	41	71	±0.0053

Appendix Table I10 Adsorption of chromium (VI) onto char from coconut shell by varies contact time in range from 30 - 240 minute.

Contact time	Absorbance				Concentration of phenol (mg/L)			% Remove	S.D.
(min.)	Repeat 1	Repeat 2	Repeat 3	Average	C_0	C_e	(C_0-C_e)		
30	0.116	0.117	0.116	0.116	56	26	31	55	±0.0006
60	0.094	0.094	0.087	0.092	56	20	37	65	±0.0040
90	0.067	0.080	0.078	0.075	56	16	40	71	±0.0070
120	0.061	0.065	0.058	0.061	56	13	43	77	±0.0035
180	0.055	0.057	0.055	0.056	56	12	45	79	±0.0012
240	0.052	0.059	0.053	0.055	56	12	45	79	±0.0038

Appendix Table I11 Adsorption of chromium (VI) onto char from coconut shell by varies pH in range of 2 - 5.

pH	Absorbance				Concentration of phenol (mg/L)			% Remove	S.D.
	Repeat 1	Repeat 2	Repeat 3	Average	C_0	C_e	(C_0-C_e)		
2	0.054	0.060	0.056	0.057	54	8	46	85	±0.0031
3	0.105	0.106	0.110	0.107	57	17	40	70	±0.0026
4	0.136	0.141	0.138	0.138	57	23	34	60	±0.0025
5	0.138	0.139	0.136	0.138	62	45	17	27	±0.0015

Appendix Table I12 Adsorption of chromium (VI) onto char from coconut shell by varies concentration in range of 30 – 250 mg/L.

Concentration of chromium (mg/L)	Absorbance				Concentration of chromium (VI) (mg/L)			% Remove	S.D.
	Repeat 1	Repeat 2	Repeat 3	Average	C_0	C_e	(C_0-C_e)		
30	0.054	0.056	0.054	0.055	37	8	30	80	±0.0012
50	0.066	0.065	0.060	0.064	75	23	52	69	±0.0032
100	0.066	0.066	0.061	0.064	103	46	57	55	±0.0029
150	0.073	0.080	0.082	0.078	154	118	35	23	±0.0047
250	0.112	0.112	0.114	0.113	272	225	47	17	±0.0012

Appendix Table I13 Adsorption of chromium (VI) onto char from bentonite by varies adsorbent dosage in range of 0.0500 – 1.0000 g.

Adsorbent dosage	**Absorbance**				**Concentration of phenol (mg/L)**			**% Remove**	**S.D.**
(g)	Repeat 1	Repeat 2	Repeat 3	Average	C_0	C_e	(C_0-C_e)		
0.0500	0.0160	0.0160	0.0160	0.016	60	60	0	0	±0.0000
0.2500	0.0120	0.0130	0.0150	0.013	60	48	12	20	±0.0015
0.5000	0.0160	0.0130	0.0150	0.015	60	54	6	10	±0.0015
0.7500	0.0100	0.0140	0.0090	0.011	60	37	22	38	±0.0026
1.0000	0.0120	0.0120	0.0090	0.011	60	37	22	38	±0.0017

Appendix Table I14 Adsorption of chromium (VI) onto char from bentonite by varies contact time in range from 30 - 240 minute.

Contact time	Absorbance				Concentration of phenol (mg/L)			% Remove	S.D.
(min.)	Repeat 1	Repeat 2	Repeat 3	Average	C_0	C_e	(C_0-C_e)		
5	0.019	0.019	0.019	0.019	73	73	0	0	±0.0000
10	0.018	0.019	0.019	0.019	73	72	1	2	±0.0006
15	0.017	0.018	0.016	0.017	73	64	9	12	±0.0010
30	0.017	0.016	0.016	0.016	73	61	12	16	±0.0006
60	0.019	0.017	0.018	0.018	73	69	4	6	±0.0010
120	0.018	0.018	0.018	0.018	73	69	4	6	±0.0000

Appendix Table I15 Adsorption of chromium (VI) onto char from bentonite by varies pH in range of 2 - 5.

pH	Absorbance				Concentration of phenol (mg/L)			% Remove	S.D.
	Repeat 1	Repeat 2	Repeat 3	Average	C_0	C_e	(C_0-C_e)		
1.6	0.015	0.015	0.016	0.015	69	57	12	17	±0.0006
2	0.014	0.012	0.014	0.013	55	48	7	14	±0.0012
3	0.014	0.015	0.015	0.015	60	54	6	10	±0.0006
4	0.016	0.015	0.015	0.015	60	57	3	5	±0.0006

Appendix Table I16 Adsorption of chromium (VI) onto char from bentonite by varies concentration in range of 30 – 250 mg/L.

Concentration of chromium (mg/L)	Absorbance				Concentration of chromium (VI) (mg/L)			% Remove	S.D.
	Repeat 1	Repeat 2	Repeat 3	Average	C_0	C_e	(C_0-C_e)		
30	0.009	0.009	0.009	0.009	37	28	9	24	±0.0000
50	0.015	0.014	0.015	0.015	64	54	10	16	±0.0006
100	0.031	0.031	0.031	0.031	141	127	13	10	±0.0000
150	0.048	0.050	0.048	0.049	212	207	6	3	±0.0012

Appendix Table I17 Adsorption isotherm of chromium (VI) onto char from bamboo.

Initail Concentration	Absorbance				Concentration of phenol (mg/L)			log C_e	q_e	log q_e	C_e/q_e	S.D.
(mg/L)	Repeat 1	Repeat 2	Repeat 3	Average	C_0	C_e	(C_0-C_e)					
50	0.047	0.051	0.042	0.047	37	6	31	0.786	1.195	0.709	5.118	±0.005
100	0.053	0.051	0.053	0.052	75	36	39	1.552	1.513	1.372	23.582	±0.001
150	0.101	0.101	0.104	0.102	103	80	23	1.905	0.876	1.963	91.871	±0.002
200	0.072	0.072	0.073	0.072	154	134	19	2.128	0.746	2.255	179.981	±0.001
250	0.086	0.083	0.082	0.084	182	160	23	2.204	0.873	2.263	183.027	±0.002

Appendix Table I18 Adsorption isotherm of chromium (VI) onto char from oil palm shell.

Initail Concentration	Absorbance				Concentration of phenol (mg/L)			log C_e	q_e	log q_e	C_e/q_e	S.D.
(mg/L)	Repeat 1	Repeat 2	Repeat 3	Average	C_0	C_e	(C_0-C_e)					
200	0.044	0.048	0.046	0.046	185	75	110	1.875	4.580	1.214	16.374	±0.002
250	0.062	0.063	0.063	0.063	239	112	126	2.051	5.260	1.329	21.365	±0.001
300	0.075	0.077	0.078	0.077	307	144	163	2.158	6.800	1.326	21.166	±0.001
350	0.107	0.107	0.107	0.107	353	272	81	2.434	3.360	1.907	80.800	±0.000
400	0.128	0.128	0.129	0.128	416	333	83	2.523	3.440	1.986	96.782	±0.001

Appendix Table I19 Adsorption isotherm of chromium (VI) onto char from coconut shell.

Initail Concentration	Absorbance				Concentration of phenol (mg/L)			log C_e	q_e	log q_e	C_e/q_e	S.D.
(mg/L)	Repeat 1	Repeat 2	Repeat 3	Average	C_0	C_e	(C_0-C_e)					
100	0.166	0.153	0.156	0.158	83	26	57	1.419	2.371	1.044	11.068	±0.007
150	0.030	0.036	0.030	0.032	107	17	90	1.240	3.754	0.665	4.624	±0.003
200	0.045	0.045	0.045	0.043	136	55	81	1.742	3.381	1.212	16.308	±0.003
250	0.100	0.101	0.102	0.101	201	159	41	2.202	1.727	1.964	92.105	±0.001
300	0.065	0.061	0.060	0.062	217	178	40	2.250	1.652	2.031	107.500	±0.003

Appendix Table I20 Adsorption isotherm of chromium (VI) onto bentonite.

Initail Concentration	Absorbance				Concentration of phenol (mg/L)			log C_e	q_e	log q_e	C_e/q_e	S.D.
(mg/L)	Repeat 1	Repeat 2	Repeat 3	Average	C_0	C_e	(C_0-C_e)					
10	0.015	0.015	0.017	0.016	10	1	9	0.051	0.0001	3.907	8,082	±0.001
20	0.067	0.059	0.060	0.062	21	4	16	0.647	0.0002	4.265	18,416	±0.004
30	0.011	0.012	0.011	0.011	35	10	24	1.007	0.0004	4.443	27,731	±0.001
40	0.014	0.015	0.014	0.014	40	13	27	1.109	0.0004	4.496	31,338	±0.001
50	0.022	0.022	0.021	0.021	63	19	44	1.282	0.0007	4.467	29,329	±0.001

CURRICULUM VITAE

NEME **:** Mr. Ratchaponl Batmart

BIRTH DATE **:** October 5, 1986

BIRTH PLACE **:** Khonkean, THAILAND

EDUCATION **:**

YEAR	INSTITUTION	DEGREE/DIPLOMA
2009	King Mongut's Institute Ladkhabang	B.Sc. (Agricultural)

POSITION/TITLE **:** Postgraduates student

WORKPLACE **:** Faculty of science, Kasetsart University

SCHOLARSHIP **:** Center for Innovation in Chemistry: Postgraduates student and Research Program in Chemistry (PERCH-CIC)